DEVELOPMENT OF NOVEL SORBENTS FOR THE DETERMINATION OF MERCURY IN WATERS BY COLD VAPOR ATOMIC ABSORPTION SPECTROMETRY

A Thesis Submitted to the
Graduate School of Engineering and Sciences of
İzmir Institute of Technology
in Partial Fulfillment of the Requirements for the Degree of

DOCTOR OF PHILOSOPHY

in Chemistry

by
Arzu ERDEM

September 2011
İZMİR

We approve the thesis of **Arzu ERDEM**

Prof.Dr. Ahmet E. EROĞLU
Supervisor

Prof.Dr. Emür HENDEN
Committee Member

Prof.Dr. F. Nil ERTAŞ
Committee Member

Assoc.Prof.Dr. Durmuş ÖZDEMİR
Committee Member

Assist.Prof.Dr. Ali ÇAĞIR
Committee Member

19 September 2011

Prof.Dr. Serdar ÖZÇELİK
Head of the Department of Chemistry

Prof.Dr. Sedat AKKURT
Dean of the Graduate School of
Engineering and Sciences

ACKNOWLEDGEMENTS

ABSTRACT

DEVELOPMENT OF NOVEL SORBENTS FOR THE DETERMINATION OF MERCURY IN WATERS BY COLD VAPOR ATOMIC ABSORPTION SPECTROMETRY

Mercury is one of the most toxic heavy metal ions to all living organisms. A novel solid support with selective functional groups was developed for mercury sorption from waters prior to its determination by cold vapor atomic absorption spectrometry. The support was prepared by immobilization of several functional groups (amino, mercapto, etc.) on silica. Among the sorbents developed, 3-MPTMS-silica has been shown to be an efficient material for the sorption of mercury species due to its selectivity. Sorption experiments were performed to optimize the necessary parameters and conclusively, sorption pH of 7.0, reaction temperature of 25 $^{\circ}$C, sorbent amount of 10.0 mg and shaking time of 30 min were applied throughout the study. Various mineral acids, organic acids, oxidizing agents and sulfur- or nitrogen-containing ligands were tried for the elution of mercury species and 2.0 M TGA was found to offer the maximum desorption. The validity of the method was checked via spike sorption experiments with four different types of water; namely, ultra pure, bottled drinking, tap and sea water. The method worked efficiently (>95%) for all types of water. Permeable reactive barriers, such as zero-valent iron and zero-valent copper were also applied for the removal of mercury species. Similar optimization parameters with 3-MPTMS-silica were also obtained for both sorbents. The method validation was also performed and although sea water is a heavy matrix, high uptake results were achieved for both sorbents.

ÖZET

SULARDAKİ CIVANIN SOĞUK BUHAR ATOMİK ABSORPSİYON SPEKTROMETRİ İLE TAYİNİ İÇİN YENİ SORBENTLERİN GELİŞTİRİLMESİ

Cıva tüm canlılar için en toksik ağır metal iyonlarından biridir. Bu çalışmada, sulardaki cıvanın soğuk buhar atomik absorpsiyon spektrometri ile tayini öncesi sorpsiyonunda kullanılmak üzere seçici fonksiyonel gruplar içeren yeni katı destek materyali geliştirilmiştir. Amino, merkapto gibi çeşitli fonksiyonel gruplar içeren kimyasallar silika üzerine immobilize edilerek hazırlanmıştır. Cıva türlerinin sulfur gruplarına selektif davranmasından dolayı hazırlanan adsorban maddeler arasından (3-merkaptopropil) trimetoksi silan (3-MPTMS) ile modifiye edilmiş silika sorpsiyon amaçlı kullanılmıştır. Sorpsiyon deneyleri gerekli parametreleri optimize etmek için yapılmıştır. Bütün çalışmalar sırasında pH 7.0, reaksiyon sıcaklığı 25 ^{o}C, sorbent miktarı 10.0 mg ve 30 dakika çalkalama süresi kullanılmıştır. Cıva türlerini geri almak için çeşitli mineral asitler, organik asitler, yükseltgen maddeler ve sülfür ya da azot içeren ligandlar denenmiştir ve inorganik cıva (Hg^{2+}) 2.0 M TGA ile %92 oranında geri alınmıştır. Metodun validasyonu, çeşitli sulara (saf su, şişelenmiş içme suyu, musluk suyu ve deniz suyu) eklenen cıva turlerinin tutunma sonuçları ile gösterilmiştir. Metot, bütün su tipleri için iyi çalışmaktadır (>95%). Aynı zamanda sıfır değerlikli demir ve sıfır değerlikli bakır gibi geçirgen reaktif bariyerler de cıvanın uzaklaştırılmasında sorbent olarak uygulanmıştır. 3-MPTMS-silikaya benzer optimizasyon parametreleri elde edilmiştir. Metot validasyonu da bu iki sorbent içinde yapılmıştır ve deniz suyu ağır bir matriks olmasına rağmen yüksek tutunma yüzdeleri elde edilmiştir.

TABLE OF CONTENTS

LIST OF FIGURES

LIST OF TABLES

LIST OF ABBREVIATONS

CVAAS	Cold Vapor Atomic Absorption Spectrometry
CVAFS	Cold Vapor Atomic Fluorescence Spectrometry
FAAS	Flame Atomic Absorption Spectrometry
MCM-41	Mobil Compositon Matter No.41
ZVI	Zero-Valent Iron
nZVI	Nanoscaled Zero-Valent Iron
ZVC	Zero-Valent Copper
SEM	Scanning Electron Microscopy
EDX	Energy-Dispersive X-ray Spectroscopy
TGA	Thermo Gravimetric Analysis
BET	Brunauer-Emmett-Teller Surface Area
PXRD	Powder X-ray Diffraction
PZC	Point of Zero Charge
3-MPTMS-silica	silica modified with –SH
sol gel-3-MPTMS	sol-gel silica modified with –SH (after synthesis)
3-MPTMS-sol gel	-SH modified sol-gel silica (during synthesis)
3-APTES-silica	silica modified with $-NH_2$
3-APTES-3-MPTMS-silica	silica modified with both $-NH_2$ and -SH

CHAPTER 1

INTRODUCTION

1.1. Introduction to Heavy Metals

Heavy metals are important environmental pollutants that threaten the human health and natural ecosystems. They are defined as the metals or metalloids which are stable and have a density greater than 4.5 g/cm^3 (Unece.org 2011). They tend to accumulate in living systems, resulting serious diseases (Bailey et al. 1999). They have been used in many different areas for years and there are several sources of this pollution, which are the coal, natural gas, paper and chlor-alkali industries. Most heavy metals may enter and go through the food chain where they are accumulated into bio-organic substances through chemical and biological processes. These metals, such as Cd, Co, Cu, Cr, Fe, Hg, Mn, Ni, Pb, Sn and Zn occur primarily in trace (mgL^{-1}) or ultra trace (μgL^{-1}) quantities in natural waters. Since these metals are usually found at trace levels in environment, they may be called as trace elements. Thus, monitoring the concentration of heavy metals and their removal has become increasingly important in global systems (Castrogonzalez and Mendezarmenta 2008).

There are several treatment processes to remove heavy metals from water. These are: reverse osmosis, chemical precipitation and electrochemical techniques. However, these techniques have the disadvantages of cost of process, pH dependency or the difficulty in removing the heavy metal when several metal ions are presented in solution (Bailey et al. 1999). Thus, more sensitive techniques are required for their removal. Nowadays, one of the most popular methods used for removal is solid phase extraction. Here, the components of the sample are distributed between the sample phase and a sorbent material. The analyte becomes bound to the sorbent by several mechanisms, such as adsorption, ion exchange and complex formation etc. This method is simple and reduces contamination and loss of analyte from the matrix (Spivakov et al. 2006). Both batch and column methods can be used for preconcentration purposes. In the batch mode, a specific amount of the sorbent is added to the sample solution and the mixture is then shaken for a certain time. If the conditions are suitable, the analytes make an

interaction with the sorbent and then filtration was performed to separate the analyte from the sample solution. On the other hand, the sorbent is packed into a suitable column through which a volume of sample is passed in the column method (Camel 2003).

The determination of mercury and its removal from waters has received great attention in recent years due to its toxicity and damage to living organisms (Dabrowski et al. 2004). The preconcentration of mercury using solid sorbents is commonly used for its detection.

1.2. Mercury in Environment

Mercury is a natural component of ecosystem, although it is not necessary for human life. It is one of the most hazardous environmental pollutants and is the only metal that is a liquid at room temperature. It has high volatility and relatively low water solubility. Mercury can be found in air, water and soil and cycles in the environment as a result of natural and anthropogenic activities (Leermakers et al. 2005). Although it is not abundant in nature, it plays an important role in many industrial and agricultural applications (Watersources.htm 2011). It is produced by the mining and smelting of cinnabar ore. It utilizes in chloralkali plants, in paints as preservatives or pigments, in electrical switching equipment and batteries, in measuring and control equipment (thermometers, medical equipment) and in copper and silver amalgams in tooth-filling materials. It is also used in navigational devices, instruments that measure temperature and pressure. It may create ecological problems when released to the environment. It may cause serious health problems when inhaled as vapor or passed through the skin and into the blood stream (Keating et al. 1997).

Mercury can be found in three oxidation states; Hg^0 (metallic), Hg_2^{2+} (mercurous) and Hg^{2+} (mercuric). The oxidation state of mercury is very important since it affects the properties and behavior of mercury. The most environmentally interesting species are elemental mercury (Hg^0), inorganic mercury (Hg^{2+}), monomethyl mercury (CH_3Hg^+), monoethyl mercury ($C_2H_5Hg^+$) and dimethyl mercury (CH_3HgCH_3). In the biogeochemical cycle of mercury, these species may be transformed into each other and transported through the aquatic and atmospheric environmental media. The most relevant process in the environment is the transformation of Hg^{2+} into CH_3Hg^+ by

2

sulfate-reducing bacteria. Most of the mercury in water, soil, sediments, or biota (i.e., all environmental media except the atmosphere) is in the form of inorganic mercury salts and organic forms of mercury (Zizek et al. 2007).

All mercury compounds are volatile and decompose easily to the free metal due to its high vapor pressure. It forms alloys with almost all other metals. Mercury in different forms enters the environment from a variety of sources. A schematic diagram of mercury cycle in the environment is demonstrated in Figure 1.1.
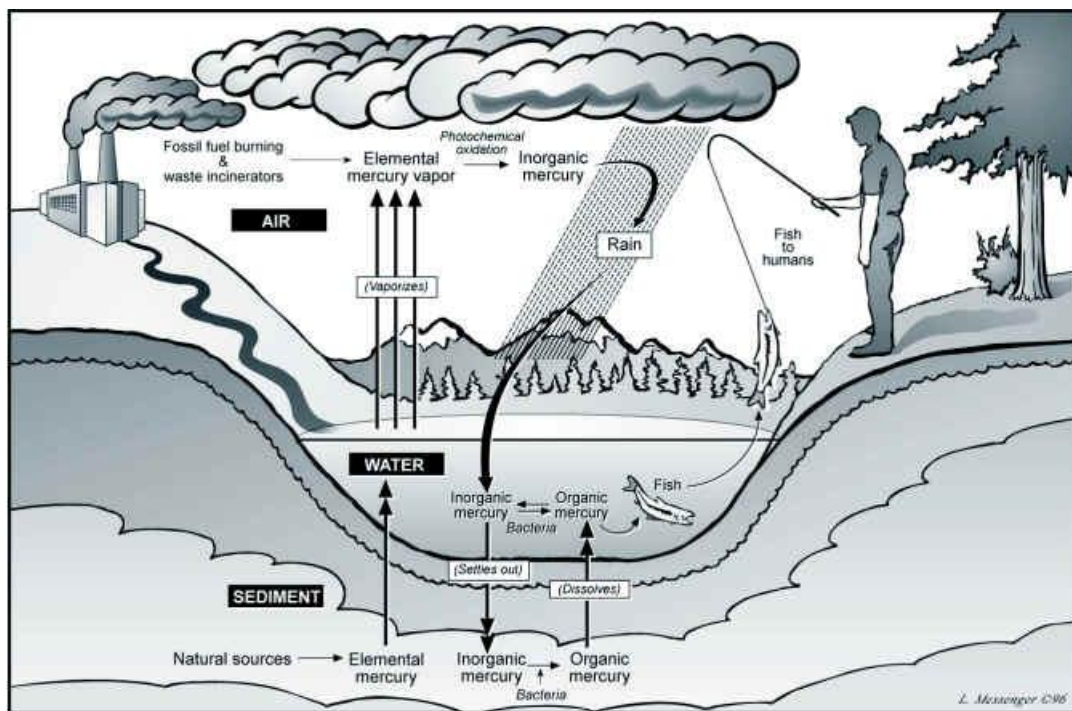
Figure 1.1. The mercury cycle in the environment.
(Source: Mercury.utah.gov 2011)

Mercury and its compounds are considered as pollutants of priority interest by the Environmental Protection Agency of the United States (USEPA) and according to the Agency, maximum contamination level goal (MCLG) and maximum contaminant level (MCL), are both 2 μgL^{-1} for the drinking water (Drinkingwater.htm 2011). The European Community also recommended a level of 1 μgL^{-1} mercury in drinking water.

Mercury has a high volatility among the other elements. This property causes the mercury to be moderately mobile in the environment. Two different forms of mercury are of human health concern. The first one, elemental mercury is very toxic in its vapor form. It vaporizes slowly at room temperature or quickly when heated. The natural sources of elemental mercury in the environment involve the release of mercury gases

from volcanic eruptions and the erosion of ores. It may be absorbed through the lungs when it is breathed as vapor. It may cause damage to human health such as insomnia, neuromuscular changes, headaches etc. (Wikipedia.org 2008). The other form is organic mercury which can be transformed from elemental and inorganic mercury salts by bacteria. Unlike elemental mercury, organic mercury can be readily absorbed by humans and the most likely source of organic mercury is contaminated fish. Its exposure can result in long term damage to the kidney, liver and central nervous system (Keating et al. 1997).

The generally recognized adverse effects attributed to the mercury exposure, are stomatitis, erethism and renal damage. Toxic responses, such as axial malformations, stunting, neurological deficits, decreased of weight and altered enzyme levels, are examples of chemically induced effects of mercury exposure (Leermakers et al. 2005).

1.3. Cold Vapor Generation

As mercury is one of the important harmful pollutants, its determination at trace levels is of great importance in environmental systems. Thus, powerful techniques are required for its detection. There are many methods for the determination of mercury in various samples including, potentiometry, flame and furnace atomic absorption spectrometry, cold vapor atomic absorption spectrometry, cold vapor atomic fluorescence spectrometry, inductively coupled plasma atomic emission spectrometry, fluorimetry, X-ray fluorescence and voltammetry. Several spectrophotometric methods are also applied for the trace determination of mercury using various reagents such as, p-nitrobenzoxosulfamate (Andac et al. 2003) besides the above mentioned techniques. As mercury exists at trace levels, flame atomic absorption spectrometry is not applicable due to its low sensitivity. Among the determination methods, cold vapor technique has widely applied for the mercury determination due to its simplicity, high sensitivity and relative freedom from interferences. The generation of volatile mercury species at room temperature has been shown to be an extremely effective introduction method for mercury.

The chemical properties of some elements are so distinct that specific techniques can be applied both to achieve its separation from the sample matrix before their introduction into the atomization/ionization unit and to generate its atomic vapor.

4

Mercury and those elements which form stable volatile covalent hydrides (As, Bi, Ge, Pb, Se, Sb, Sn, and Te) may be separated from the sample matrix by *vapor generation*.

Mercury is the only metallic element that has a vapor pressure as high as 0.0016 mbar at 20 ^{0}C, which corresponds to a concentration of approximately 14 mg/m^3 of mercury in the vapor phase. Thus, it is possible to analyze mercury directly by AAS without the use of an atomizer. The element must only be reduced to the metallic form and transferred to the vapor phase. This procedure is termed the *cold vapor technique* (Welz and Sperling 1999). Four main methods have been used to bring mercury into the vapor phase.

i) Reduction-aeration: This is the most common method applied to collect mercury into the vapor phase. Mercury in aqueous solution reacted with a reducing agent and then removed from the solution by passing a gas through it.

ii) Heating: The sample is decomposed and ignited at high temperatures.

iii) Electrolytic amalgamation: Mercury is covered with a thin layer of a copper cathode during electrolysis and then it is heated at high temperatures to release mercury.

iv) Direct amalgamation: Mercury is trapped on a silver or gold wire and released by heating (Ebdon et al. 1998).

There are two primary advantages of the cold vapor process. First, mercury is separated from the sample matrix, and consequently, matrix interferences are reduced. Second, an improvement is achieved in the detection limits due to the complete introduction of mercury sample into the atomizer within a few seconds.

Tin(II) chloride and sodium borohydride are widely used for the reduction of mercury in cold vapor technique. Tin(II) chloride, $SnCl_2$, requires the metallic mercury to be transported by an inert gas stream (argon or nitrogen) and purged through the solution to sweep out the mercury to the detector.

$$Sn^{2+} + Hg^{2+} \longrightarrow Sn^{4+} + Hg^0$$
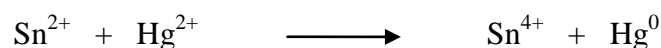
Nevertheless, sodium borohydride in an alkaline solution is becoming the preferred reagent; it requires no other reagents for reduction. Sodium borohydride is a stronger reducing agent than tin(II) chloride. In addition, hydrogen (H_2) is produced during reduction when sodium borohydride is applied as the reductant. (Anderson 2000).

$$BH_4^- + H^+ + 3\,H_2O \longrightarrow H_3BO_3 + 8\,H^\bullet$$

5

$$8\,H^{\bullet} \;+\; Hg^{2+} \;\longrightarrow\; Hg^{0} \;+\; 4\,H_2$$
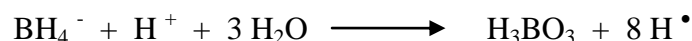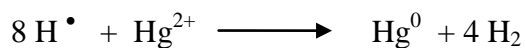
1.3.1. Cold Vapor Atomic Absorption Spectrometry (CVAAS)

Cold vapor atomic absorption spectrometry is a sensitive analytical technique that allows the determination of mercury at trace levels. In this technique, mercury is first reduced to the metallic element and vaporized. Then, the evolved mercury vapor is passed through an absorption cell, usually constructed of borosilicate glass with silica-end-windows and a transient absorption peak is obtained.

The 253.7 nm line is generally applied in mercury determination by AAS, but the transition is spin forbidden, and relatively insensitive. There is also one wavelength for mercury determination which is 184.9 nm is possibly 20-40 times more sensitive, however, at this wavelength most flame atmosphere gases absorb strongly (Ebdon et al. 1998).

1.3.2. Cold Vapor Atomic Fluorescence Spectrometry (CVAFS)

Mercury has also been determined by cold vapor AFS which utilizes the measurement of mercury vapor at room temperature. Mercury is first reduced to its elemental form with tin(II) chloride and the liberated vapor is swept out of the solution by a carrier gas (generally argon); then, it passes through the excitation cell. A mercury lamp is used for the excitation measurement and the fluorescence signal is detected by a photomultiplier at 253.7 nm. Since the fluorescence signal is measured at 90 ^{o}C to the optical path of the light source, fluorescence emission may be detected without any interference from any radiation received directly from the light source. This technique has the same advantages with CVAAS which has fewer spectral-chemical interferences, low detection limits and wide linear dynamic range. However, the fluorescence technique is generally considered to be more sensitive and has better linearity compared to the absorption methods (Ebdon et al. 1998).

1.4. Mercury Determination Methods

As mentioned before, the presence of mercury species is of great concern as it is well known that inorganic mercury (Hg^{2+}) is converted into highly toxic methylmercury ($MeHg^+$) by several processes. Due to the presence of mercury in environmental samples at low levels, its separation from other interfering elements present and the use of a preconcentration step prior to the determination is usually necessary.

There are many methods for the determination of mercury in various samples including chromatographic and non-chromatographic methods, with and without preconcentration or cold vapor generation, online and offline.

Several chromatographic techniques are used to determine the organomercuric compounds. In GC methods, the environmental sample must be extracted in order to obtain the organomercuric compounds. There are several procedures applied for the extraction of organomercury species from environmental samples. These are acid extraction (mostly combined with solvent extraction), distillation and alkaline extractions. The most crucial step is the extraction step for biota and sediments. Several problems may occur during the extraction procedures which are related with the extraction efficiency, conversion and destruction of the mercury species and moreover, a lack of selectivity may be achieved with the use of usual GC detectors for the speciation of Hg in environmental samples. In order to avoid these problems, a precolumn derivatization of Hg species has been developed. The non-polar derivatives can then be separated on non-polar packed or capillary columns. Iodation with acetic acid, hydration with $NaBH_4$, aqueous phase ethylation with $NaBEt_4$, chlorination and derivatization with a Grignard reagent, are the most widely applied methods (Nevado et al. 2005). The main drawback of the LC methods was the lack of sensitivity of the detectors. More sensitive detectors, such as a reductive amperometric electrochemical, ultraviolet (UV), ICP-AES, ICP-MS, AFS and AAS, has been developed for environmental studies. The main advantage of LC over a number of methods is the possibility of separating a great variety of organomercury compounds. Practically all HPLC methods for Hg speciation reported in the literature are based on reversed phase separations, involving the use of a silicabonded phase column and a mobile phase containing an organic modifier, a chelating or ion-pair reagent and, in some cases, a pH buffer (Houserov et al. 2006, Bramanti et al. 2005). Among the separation methods,

Capillary Electrophoresis (CE) is a relatively new and still developing technique, but has already shown a potential for various metal speciation. Rapid separation speed with high efficiency and a very small sample requirement are some of its principal virtues. Unlike in chromatographic methods, there is no interaction between the sample and the stationary phase in CE. By proper choice of a background electrolyte (BGE), the existing equilibrium among different species can be minimally affected and one of the possible sources of errors, arising from a shift in equilibrium because the stationary phase favors one species over another, is eliminated (Kuban et al. 2009).

Non-chromatographic methods have been also applied for the determination of mercury, such as potentiometry (Shamsipur et al. 2004), flame (Hinds 1998) and furnace atomic absorption spectrometry (Madden and Fitzgerald 2009), cold vapor atomic absorption spectrometry (Pourreza and Ghanemi 2009), atomic fluorescence spectrometry (Zhang et al. 2010), inductively coupled plasma atomic emission spectrometry (Wuilloud et al. 2002a), fluorimetry (Sandor et al. 1999), X-ray fluorescence (Bennun et al. 1999), and voltammetry (Guo et al. 1999). In addition to above mentioned methods several spectrophotometric methods are also reported for the trace determination of mercury using various reagents such as, p-nitrobenzoxosulfamate (Andac et al. 2003). Since mercury must mainly be determined in the trace range, flame atomic absorption spectrometry is not well-suited because of its low sensitivity. Among the determination methods, CVAAS has received great attention for the determination of mercury because of its simplicity, high sensitivity and relative freedom from interferences. Neto et al. (2000) have developed a flow injection system with a cation resin packed microcolumn for the determination of trace levels of mercury in agroindustrial samples by CVAAS where improved sensitivity and selectivity was achieved. Ma et al. (2007) have proposed a new method for the determination of trace amounts of mercury by CVAAS using dithizone-modified titanium dioxide as a solid phase extractor. Bendl et al. (2006) have suggested a mercury determination method by UV reduction. The reduction of mercury in acetic acid solution via UV radiation generates the mercury vapor. Detection limits have been improved within this technique.

1.5. Preparation of Solid Supports for Mercury Preconcentration

Since the mercury is an important environmental pollutant, the development of reliable methods for the determination of mercury at (ultra)trace levels in environmental and biological materials is of particular significance. Reduction, extraction and ion-exchange methods can be applied for the elimination of mercury from matrices.

There are many adsorptive compounds that can capture mercury ions from solution such as charcoal, zeolites and clays. However, these compounds have the disadvantages of low loading capacity and binding affinity on mercury. To overcome these limitations, the coupling of solid supports with chelating ligands (e.g. thiol, amine) is prepared (Mercier and Pinnavaia 1998). In recent years, modification of these surfaces with a specific functional group to make the surface available to form chelates with the metal ions has gained the attraction of the researchers. The donor atoms in forming chelates usually include oxygen, nitrogen, phosphorous, hydroxyl, ether, phosphoryl, carbonyl, carboxylic, hydroxyl, ether, phosphoryl, amine, nitro, nitroso, azo, diazo, nitrile, amide, thiol, thioether, thiocarbamate, bisulphite, etc. Hence, the adsorbing material is composed of a stable and insoluble porous matrix that contains appropriate active groups interacting with the metal ions. A variety of solid supports are available for use in laboratories and industrial applications such as organic polymers (e.g. agarose, dextran, etc.), cation or anion exchange resins, and inorganic substrates (silica, alumina, etc.). However, the selectivity of the surface with the immobilized functional groups towards metal ion(s) depends on factors like size of the modifier, activity of the loaded group and the characteristics of hard–soft acid–base.

1.5.1. The Sol-gel Method for Silica Synthesis

Sol-gel is a wet chemical method widely used recently in ceramic engineering and material science. It is based on hydrolysis and condensation of liquid precursors. This procedure gives sols, colloidal particles suspended in a liquid that proceed through a gelation process to form two interpenetrating networks which are known as the solid phase and the solvent phase (Brinker and Scherer 1990, Lev et al. 1995). Alkoxysilanes $Si(OR)_4$ are used as a precursor for silica synthesis which avoids the formation of salts

as side products that are major limitation of silica gel synthesis from sodium silicate (El-Nahhal and El-Ashgar 2007). It is a cheap and low-temperature technique that allows for the fine control of the product's chemical composition.

First step in sol-gel process is the hydrolysis reaction which occurs while alkoxide precursor is mixed with water in the presence of alcohol to achieve sufficient homogenization. Hydrolysis leads to the formation of silanol groups. Intermediates produced in the alcohol–water medium include silanols, ethoxy silanols and oligomers of low molecular weight which are formed at the first stages of the process. Hydrolysis reactions can be done either by acid or base catalysis. Two hydrolysis processes give different structures and morphology; acid catalysis form linear weakly cross-linked polymer, whereas base catalysis form more highly branched clusters as a result of rapid hydrolysis step (Brinker and Scherer 1990).

Second step of sol-gel synthesis is the polycondensation between the two silanol groups and condensation reaction between silanol and alkoxyde groups by releasing a water or alcohol unit, respectively. Further condensation results in SiO_2 network.

1.5.2. Preconcentration Using Silica Gel Modified with Various Functional Groups

Silica gel is a good solid support for trace element determinations due to its chemical inertness and its thermal, mechanical and chemical stability during the reaction process. It does not also swell or strain and can simply undergo heat treatment. Chelating agents can be easily loaded on silica gel with high stability, or be bound chemically to the support. In addition to these, the active sites are well dispersed on silica surface and these sites are ease of use for functionalization (Goswami and Singh 2002). The surface of silica gel is characterized by the presence of silanol groups, which are known to be weak ion-exchangers, causing low interaction, binding and extraction of ionic species (Kvitek et al. 1982). There are several methods for the synthesis of silica gel.

Mahmoud et al. (2000) have used silica gel phase-impregnated with dithizone for selective extraction and solid phase preconcentration of mercury(II) from aqueous and natural water samples.

The microspherical mesoporous silica has been synthesized by Bibby and Mercier (2002) via a one-step reaction between tetraethoxysilane (TEOS), 3-mercaptopropyl trimethoxysilane (MPTMS) and Triton-X-100. The resulting material is then characterized and used for mercury adsorption.

Antochshuk and Jaroniec (2002) have proposed a method for the synthesis and regeneration of mesoporous silica having high adsorption capacity towards mercury ions. MCM-41 silica having 5.0 nm pore size was used throughout the study. Aminopropyl silica was synthesized by the reaction between MCM-41, tetramethyl ammonium hydroxide (TMAOH) and cetyl trimethyl ammonium bromide (CTAB) under vigorous stirring. Finally, chemical modification of mesoporous MCM-41 with 1-allyl-3-propylthiourea was performed via the reaction between primary amine and allyl isothiocyanate. The modified mesoporous silica was then used for the sorption of mercury.

Two strategies (homogeneous and heterogeneous) have been followed by Perez-Quintanilla et al. (2006) for the modification of mesoporous silica with the organic ligands. First, the synthesis of mesoporous silica is done by using a poly(alkaline oxide) triblock copolymer surfactant. Afterwards, the immobilization of 2-mercaptothiazoline (MTZ) on silica surface was performed via one step reaction using the homogeneous method. Here, 3-chloropropylsilane reacted with MTZ to obtain the silylating agent and this compound was allowed to react with the silanol groups of activated silica. This method is known as homogeneous route. Nevertheless, a two step reaction was carried out for the modification of mesoporous silica surface. The first reaction involved the addition 3-chloropropylsilane ligand into the activated silica to have chlorinated silica and finally the chlorinated silica reacted with MTZ to obtain the desired solid support. Finally, the application of these materials was demonstrated for the adsorption of mercury from aqueous media (heterogeneous route).

The amorphous silica gel and ordered MCM-41 have been modified with 2-(3-(2-aminoethylthio)propyl)ethanamine by Puanngam and Unob (2008). Characterization of the sorbents was performed. Afterwards, the sorbents were used for Hg^{2+} removal from water.

1.5.3. Preconcentration Using Different Solid Supports Modified with Various Functional Groups

There are many other sorbents used for mercury determination apart from silica. Krishna et al. (2005) have employed polyaniline (PANI) for the preconcentration and speciation of Hg^{2+} and CH_3Hg^+ from aqueous solutions due to its good combination properties and stability of the adsorbent. The synthesis of PANI has been performed by the reaction between aniline and ammonium peroxydisulfate under continuous stirring. Hence, the batch and column experiments have been done for mercury determination.

Alumina membranes with controlled pore structures have been used for mercury sorption by Smuleac et al. (2005). A single-thiol (MPS or cysteine), a disulfide (cysteine) or a polythiol (PLC) have been immobilized on the membrane. Silylation has been applied for the chemical modification of alumina due to its simplicity and flexibility to the functional groups. The hydroxyl groups on the alumina membrane are appropriate in silane coupling. A single reaction between mercaptopropyl trimethoxysilane (MPS) and alumina occur in the formation of Si-O bonds at a single step. Nonetheless, intermediate steps are necessary for the immobilization of amine containing ligands (PLC, PLGA etc.). Hence, metal sorption capacity has been investigated for the synthesized solid support.

Ion imprinting polymer method (IIP) is another method used for the preconcentration of mercury (Fan 2006). The sol-gel method is applied for the preparation of Hg(II)-imprinted mesoporous sorbent since the sol-gel chemicals provide large surface area, good metal ion transfer kinetics, high metal adsorption capacity and high selectivity for ion-imprinted sorbent. The mesoporous sorbent has been synthesized by mixing CTAB, TEOS and NH_3H_2O under reflux for 10 hours. The solid support is then filtered by vacuum and washed with ethanol. For the synthesis of Hg(II)-imprinted mesoporous sorbent, a specific amount of mercury(II) nitrate in methanol is mixed with 3-mercaptopropyltrimethoxysilane (MPTMS) under reflux for 2 hours and mesoporous sorbent is added to this mixture. The resulting mixture is stirred for 10 hours and evaporated to dryness. Finally, the filtration and drying of the solid support is performed and used for the mercury preconcentration.

Cruz-Guzman et al. (2006) have modified two reference montmorillonites, Wyoming (SWy-2) and Arizona (SAz-1), with several natural organic cations containing different functional groups (L-carnitine, L-cysteine ethyl ester, L-cysteine

dimethyl ester and thiamine cations) and nonfunctionalized organic cations (hexadecyltrimethyl-ammonium (HDTMA) and phenyltrimethylammonium (PTMA)). The modified sorbents were then used for the adsorption of Hg^{2+} and Pb^{2+}.

The modification of chitosan via thiourea has been performed by Gavilan et al. (2009). During synthesis, a specific amount of chitosan is mixed with thiocyanate and thiourea and then heated at 130 ^oC for several hours. Finally, the cross-linking treatment was done with glutaraldehyde and used for mercury removal.

1.6. Permeable Reactive Barriers (PRBs)

In recent years, permeable reactive barriers have been developed and used in the removal of organic and inorganic pollutants from water samples. They are an in situ remediation technology where groundwater contamination is treated passively as it flows through a reactive medium. As the contaminants interact with the reactive barrier the contaminants are converted into less dangerous compounds. There is a growing interest for PRBs due to its long-term stability, excellent compatibility, low operating and maintenance costs.

The mechanism of PRBs is evaluated on the ability of their transformation or immobilization of the contaminants at an adequate rate and maintainance sufficient permeability and reactivity for a long time. Immobilization of the contaminant within the barrier may be done by sorption or precipitation. Hydrophobic interactions, electrostatic attraction or surface complexation occur during the sorption of the contaminant onto the surface of the barrier. Organic contaminants sorb via hydrophobic expulsion whereas the sorption of metals is due to electrostatic attraction, surface complexation reaction or reduction. Surfactant-modified zeolites (clay, zeolite, etc.), humic materials (peat and activated carbon), oxides (amorphous ferric oxide, goethite, hematite, hydrous titanium oxide, etc.), precipitation agents (hydrated lime and limestone) and chemical reaction barriers (zero-valent metals, bimetallic couples, minerals, etc.) are the most common materials used in reactive barriers (Blowes et al. 2000, Scherer et al. 2000, Ponder et al. 2001).

1.6.1. Zero-Valent Iron (ZVI)

Zero-valent iron (ZVI) is becoming a popular reactive material for the barriers due to its small particle size, large surface area and high in-situ reactivity. The nanoscale ZVI has a greater affinity to reduce/adsorb various toxic aqueous ions. Elemental iron itself has no known toxic effect since it is one of the most abundant element on earth crust (Üzüm et al. 2008).

Nanoscaled zero-valent iron can be synthesized by several methods. These methods can be classified into two groups: physical synthesis methods (inert gas condensation, severe plastic deformation, high energy ball milling and ultrasound shot peening) and chemical synthesis methods (reverse micelle, controlled chemical coprecipitation, chemical vapor condensation, pulse electrodeposition, liquid flame spray, liquid-phase reduction and gas phase reduction) (Sun et al. 2006, Nurmi et al. 2005, Li et al. 2006a). Among these methods, liquid-phase reduction utilizing sodium borohydride ($NaBH_4$) as the reducing agent is the most widely used methods used in nZVI (Wang and Zhang 1997, Wang et al. 2006). The proposed reaction is:

$$Fe^{2+} + 2BH_4^- + 6H_2O \rightarrow Fe^0 + 2B(OH)_3 + 7H_2 \uparrow$$
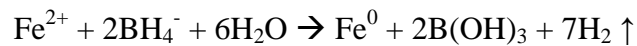
Synthesized zero-valent iron is unstable in atmospheric conditions and it tends to form oxides/hydroxides in the forms of Fe_2O_3, Fe_3O_4 and $FeOOH$ (Noubactep et al. 2005). In recent years, nZVI is synthesized in open air in the presence of ethanol to prevent massive oxidation (Liu, et al. 2005a, Liu et al. 2005b).

Since iron has a low reduction potential, ZVI has been preferred as an efficient and environmentally friendly sorbent for the removal of toxic metals.

$$Fe^{3+} + 3e^- \rightarrow Fe^0 \qquad E^0 = -0.037 \text{ V}$$
$$Fe^{2+} + 2e^- \rightarrow Fe^0 \qquad E^0 = -0.410 \text{ V}$$
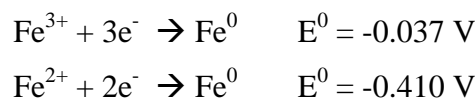
Figure 1.2 shows the core-shell structure of nZVI suggested by Li and Zhang (2007). The authors studied nZVI structure before and after contacting with various metal ions and proposed three possible mechanisms on nZVI surface:

i- only physical sorption occurs for cations having standard reduction potential, E^0, smaller than that of Fe,

ii- both sorption and chemical reduction arises for cations having E^0 slightly more positive than that of Fe,

iii- only chemical reduction occurs for cations with E^0 higher than that of Fe.
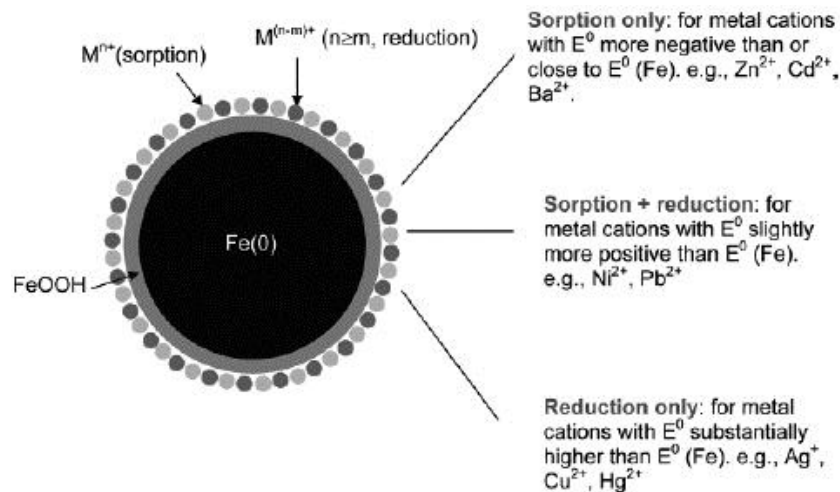
Figure 1.2. A model for core-shell structure of nZVI and metal uptake mechanisms.
(Source: Li and Zhang 2007)

Despite its high chemical sorption capacity, there are some restrictions on the use of nZVI in environmental applications. Iron nanoparticles have positive surface charges within the natural pH range and they tend to repel each other strongly. Therefore, it is very hard to keep the particles stable in the permeable reactive barrier. In addition, nZVI cannot be used at pH values smaller than 4.0 during sorption due to dissolution. To overcome these problems, iron nanoparticles can be modified, supported or mixed with filling materials.

1.6.2. Zero-Valent Copper (ZVC)

Apart from ZVI, zero-valent copper is also capable of reducing many environmental contaminants. ZVC are widely used in electronics, ceramics, films, polymers, inks, lubricant oil and coatings. ZVC has been also employed in osteoporosis-treatment drugs, additives in livestock and antibacterial materials (Rispoli et al. 2010).

Liquid-phase reduction utilizing sodium borohydride (NaBH$_4$) as the reducing agent can also be applied in the synthesis of ZVC.

As the reduction potential of copper is not so high and ZVC may be also preferred as an efficient and environmentally friendly sorbent for the removal of toxic metals.

$$Cu^{2+} + 2e^- \rightarrow Cu^0 \quad E^0 = 0.34 \text{ V}$$
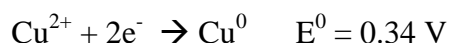
The possible reaction mechanisms occur after contacting with the metals is similar to ZVI as explained in section 1.6.1.

1.7. Characterization of the Solid Surfaces

1.7.1. Scanning Electron Microscopy (SEM)

Scanning Electron Microscopy is a powerful technique applied in micro-imaging of a variety of surfaces. It was invented in the early 1960's. Although SEM has some disadvantages as limited resolution, damaging polymer surfaces by electron beam, this technique is easy to use and involve easy sample preparation. SEM enables to explore the surface structure to determine particle size and texture on that surface. Prior to SEM analysis, the solid samples are sprinkled onto adhesive aluminum/carbon taps supported on metallic disks. Samples are then introduced to the instrument operating under vacuum and microimages, obtained by using electron beams, are recorded. In order to generate demagnified image of electron source lenses are utilized. Specimen is across scanned with this probe of electrons; signals are created as a result of sample-electron interaction. Then, these signals are detected, amplified and utilized to modulate intensity of image tube. The surface of a solid sample is scanned in a raster pattern with a beam of energetic electrons. Several types of signals are produced from a surface in this process, including backscattered, secondary, and Auger electrons; X-ray fluorescence photons; and other photons of various energies. All of these signals have been used for surface studies, but the two most common are backscattered-secondary electrons, which serve as the basis of SEM, and X-ray emission, which is utilized in electron microprobe analysis (Skoog and West 1971). When the sample is bombarded

with electrons, many different interactions occur between them. Electrons are reflected from the sample and collected by a detector in which they are converted into a small electrical signal. This signal includes a variety of information about a single point on the surface of sample. In order to obtain an image of the sample a large number of points over an area of sample is needed. The beam is moved point-by-point along a line and the reflected electron signal is collected. A line of 1000 points is completed, then the beam is moved quickly back to the start of that line. The beam is then shifted down one line width and repeats its scan. A complete scan includes 1000 lines in which they are 1000 points (Lawes 1998). There are two main types of sample/electron interactions: unscattered electrons and elastically scattered electrons. Elastically scattered electrons change direction but preserve almost all of their energy with < 1 eV loss. The angle through which the electron is deflected depends on how much energy it has, and how close it passes to the nuclei. Elastic scattering is more likely to be seen in samples of high atomic number, and with low accelerating voltage beams. Through inelastic scattering incident electrons transfer a large proportion of their kinetic energy to the target atoms. Inelastic scattering is more likely to be seen in the lighter elements and gives useful information about the surface of sample and elemental composition of sample.

SEM is near-surface sensitive technique. The primary electron beam causes ionization of atoms on its path which in turn cause ejection of secondary electrons from the solid surface having 0 - 20 eV and they are attracted to positively charged detector. Secondary electron images can be acquired about to 100 nm. Primary electron beam has the depth of penetration of 0.5 - 5 μm depending upon the density of the solid.

1.7.2. Energy-Dispersive X-ray Spectroscopy (EDX)

In addition to SEM, EDX is a complementary technique that can be applied in the identification of elemental composition of surfaces. This technique has enabled X-rays to be emitted by elements within the surface that are initially excited by bombarding electrons. X-rays are produced by the incident probe in a volume which is similar with these of backscattered electrons and consequently, the elements in a sample within that volume can be recognized by comparing the peaks with the characteristic

energies of the elements. Internal corrections for the cross sections of different elements is automatically performed, thus the concentrations of the elements can be calculated.

The dimension of the interaction volume depends on the mean atomic number and the density of the material, the beam energy, and the emitted X-ray energy. The sampling depth in EDS is approximately 1 μm and diameters are ranging from 0.03 μm to several μm. Hence, conventional EDS will not reveal compositional changes owing to surface separation. It is possible, however, by analyzing a point at several different beam energies, to determine the thickness and composition of this surface layers.

1.7.3. Elemental Analysis

Elemental analysis identifies the elemental composition and sometimes isotopic composition in a sample of material (soil, waste, minerals, chemical compounds, etc.). Elemental analysis can be qualitative and quantitative. The elemental analysis refers to CHNX analysis, the determination of the percentage weights of carbon, hydrogen, nitrogen, and heteroatoms (X) (halogens, sulfur) of a sample. This information is important to help determine the structure of an unknown compound, as well as to help ascertain the structure and purity of a synthesized compound. This technique depends on the high temperature oxidation of the organic compounds where the element of interest is determined in gaseous form. In this technique, a sample is burned in an excess of oxygen under static conditions and a gaseous mixture of carbon dioxide, carbon monoxide, water, elemental nitrogen and oxides of nitrogen are produced. Finally, these products are transported into a mixing chamber to be kept at a constant temperature and then, the resulting mixture is analyzed by thermal conductivity detectors. The weights of these combustion products can be used to calculate the composition of the unknown sample (Skoog et al. 1998).

1.7.4. Thermo Gravimetric Analysis (TGA)

Thermo gravimetric analysis is a technique in which the mass of a substance in a controlled atmosphere is monitored as a function temperature. A plot of mass or mass percent as a function of time is known as *thermogram*. TGA has some limitations in

decomposition and oxidation reactions because a temperature variation brings a change in mass of analyte. This method has a growing interest in quality control and research applications on industrial products, such as polymers, clays, minerals, metals and alloys. In TGA, the solid samples are heated from 25 ^{o}C to 650 ^{o}C in 10 minute intervals under N_2 atmosphere (Skoog et al. 1998).

1.7.5. Brunauer-Emmett-Teller (BET) Surface Area Analysis

BET describes the physical sorption (both adsorption and desorption) of gas molecules on the surface of dry solid powders, solids, granules and determines the specific surface area of these materials. The BET surface area measurement is important in understanding the behaviour of a material, as the material reacts with its surrounding via its surface. A higher surface area material is more likely to react faster, dissolve faster and adsorp more gas than a similar material with a low surface area. In a gas sorption method, firstly the material is heated and degassed to remove previously adsorbed molecules. Then known doses of an inert gas, such as nitrogen, are introduced and the gas is adsorbed (or desorbed). The sample material is placed in a vacuum chamber at a constant and very low temperature, and the pressure upon is varied in a wide range to obtain adsorption and desorption isotherms. Various amounts of gas molecules will be adsorbed or desorbed at different doses of the gas. Since the area occupied by one gas molecule is known, an appropriate adsorption model can be used to determine the total surface area of the sample. The most well known isotherm equation for multilayer adsorption is the equation derived by Brunauer, Emmett, and Teller in 1938.

1.7.6. Powder X-ray Diffraction (PXRD)

X-rays are high energy radiations with wavelengths around 1 Å (10^{-10} m). In electromagnetic spectrum, X-rays are placed between gamma-ray region and the ultraviolet region. Since wavelengths of X-rays are nearly in atomic scale, crystalline structures at the atomic level can be determined using this type of radiation. X-ray diffraction method can be used for the fingerprint characterization of crystalline

materials and the determination of their structure. Each crystalline solid has its unique characteristic X-ray powder patterns and these patterns can be used as fingerprints for further comparison. Using databases, material can be identified and using X-ray crystallography packing of the atoms in crystalline structure, interatomic distances and angles can be determined.

X-ray diffraction is one of the most important characterization tools used in industry and science since its discovery in 1912. This method can be used to gather qualitative and quantitative information about the compounds in the sample (Skoog et. al 1998).

1.7.7. Zeta-Meter

Zeta potential controls collodial suspensions. Colloidal suspensions can be as thick as paste or as dilute as the turbidity particles in water. The double layer is formed in order to neutralize the charged colloid and causes an electrokinetic potential between the surface of the colloid and any point in the mass of the suspending liquid. Each colloidal microscopic particle in a suspension, having a surface charge, produces a difference in electrical potential between its surface and the bulk of the suspension. This difference, in millivolts, is called the zeta potential. Zeta potential, ξ, can be easily determined because when the suspension is subjected to a direct current (DC) between two ends, a charged particle moves with a fixed velocity in a voltage field. This phenomenon is called "electrophoresis". The particle's mobility is related to the dielectric constant and viscosity of the suspending liquid and to the electrical potential at the boundary between the moving particle and the liquid. Determination of zeta potential is important to more fully understand the bulk properties of many suspensions because the key for many bulk-scale processes is again the control of individual colloids.

1.7.8. Particle Size Measurements

Particle size analysis is an analytical technique by which the distribution of sizes in a sample of particulate material is measured. Laser Particle Size Analysis consists in

measuring the size of particles (powders, suspensions and emulsions) using the diffraction and diffusion of a laser beam. During the laser diffraction measurement, particles are passed through a focused laser beam. These particles scatter light at an angle that is inversely proportional to their size. The angular intensity of the scattered light is then measured by a series of photosensitive detectors. The map of scattering intensity versus angle is the primary source of information used to calculate the particle size.

1.8. The Aim of this Work

The purpose of this study is to prepare novel solid substrates for the determination of trace mercury in environmental samples. For this purpose, the synthesis of solid sorbents was performed and the surface modification of the sorbents was carried out. Finally, the selectivity of newly prepared sorbents towards Hg^{2+} and CH_3Hg^+ was examined.

The newly synthesized materials were characterized using X-ray Diffraction (XRD), Scanning Electron Microscopy-Energy Dispersive X-ray Spectroscopy (SEM/EDX), Brunauer-Emmett-Teller (BET) surface area analysis, in addition to elemental analysis to reveal the C and N contents.

The efficiency of the sorbent will be studied as a preconcentration agent and then will be examined by recovery studies. The samples prepared using the mentioned methodology was analyzed by cold vapor atomic absorption spectrometry (CVAAS).

CHAPTER 2

EXPERIMENTAL

2.1. Chemicals and Reagents

All chemicals were of analytical reagent grade. Ultra pure water (18MΩ) was used throughout the study. Glassware and plastic ware were cleaned by soaking in 10% (v/v) nitric acid and rinsed with distilled water prior to use.

i. Standard Hg^{2+} stock solution (100 mgL^{-1}): Prepared from 1000 mgL^{-1} Hg^{2+} stock solution (Merck, Germany) in 250 mL ultra pure water and acidified with concentrated HNO_3 (Merck, Germany) to have a final acid concentration of 0.14 M.

ii. Standard CH_3Hg^+ stock solution (100 mgL^{-1}): Prepared by dissolving 0.0125 g methyl mercury chloride (CH_3HgCl) (Merck, Germany) in acetone (Merck, Germany), diluted to 100 mL ultra pure water and acidified with concentrated HNO_3 (Merck, Germany) to have a final acid concentration of 0.14 M.

iii. Calibration standards: Lower concentration standards were prepared daily from mercury stock standards. Each solution contained 0.14 M HNO_3.

iv. Potassium persulfate ($K_2S_2O_8$) solution (3% m/v): Prepared daily from its solid (Merck, Germany) in ultra pure water for the oxidation of CH_3Hg^+ to Hg^{2+}.

v. Tin(II) chloride solution (5% m/v): Prepared daily from its stock solution ($SnCl_2.2H_2O$) (Merck, Germany) in 0.96 M HCl (Merck, Germany) for the reasons of solubility and stability.

vi. Tetraethylortosilicate (TEOS) (Merck, Germany), 3-mercaptopropyl trimethoxysilane (3-MPTMS) (Fluka, Germany), 3-aminopropyl triethoxysilane (3-APTES) (Merck, Germany) were used as received.

vii. Potassium persulfate ($K_2S_2O_8$) solution (3% m/v): Prepared daily from its solid (Merck, Germany) in ultra pure water for the oxidation of CH_3Hg^+.

viii. pH adjustment: Various concentrations of HNO_3 and NH_3 solutions were used.

2.2. Instrumentation and Apparatus

Mercury determinations were performed with CVAAS using an atomic absorption spectrometer; Thermo Elemental Solaar M6 Series was used for the measurements. A mercury hollow cathode lamp at the wavelength of 253.6 nm and a deuterium lamp were employed as the source line and for background correction, respectively. The monochromator slit was kept at 0.5 mm. A 15 cm long (8 mm i.d., 10 mm i.d.) glass absorption cell with quartz windows mounted on the standard air-acetylene burner head was used for the determination of mercury by the cold vapor technique (the details of the system are outlined in the following section). In sorption studies with batch process, GFL 1083 water bath shaker (Burgwedel, Germany) equipped with microprocessor thermostat was utilized to provide efficient mixing. The elemental composition of silica was determined by LECO-CHNS-932 elemental analyzer (Mönchengladbach, Germany). Crystallographic properties were obtained with Philips X'Pert Pro X-ray Diffractometer (Eindhoven, The Netherland). Images of sorbents were taken with Phillips XL-30S FEG (Eindhoven, The Netherland) and FEI Quanta250 FEG (Eindhoven, The Netherland). Thermal properties of sorbents were analyzed with Perkin Elmer Pyris Diamond TG/DTA (Boston, MA, USA). Surface area measurements were performed with Micromeritics-Gemini V (Norcross, USA). The pH measurements were performed by using Denver pH/ion meter with a combination pH electrode. Zeta potential measurements were done with Malvern Zetasizer Nanoseries Nano-ZS (Worcestershire, United Kingdom).

2.2.1. CVAAS for Hg

Using the parameters given in Table 2.1, samples/standards were placed in the 50-mL reaction vessel. After the addition of 500 μL 5% (m/v) $SnCl_2$ with a micropipette, the vessel was closed immediately and then the solution was mixed by a magnetic stirrer. Hg^{2+} was also converted to elemental mercury during 60 seconds reaction/equilibration time (optimized) and then separated from the liquid phase as an atomic vapor. An inert gas (N_2) was passed through the reaction vessel to transport the atomic mercury into the glass absorption cell with quartz windows at both ends, placed

on top of the burner head of the atomic absorption spectrometer. The cold vapor system used in mercury determination is shown in Figure 2.1.

Table 2.1. Operating parameters of the CVAAS system used

Carrier gas (N_2) flow rate (mL min^{-1})	700
$SnCl_2$ concentration (m/v)	5.0
$SnCl_2$ volume (µL)	500
Reaction time (sec)	60
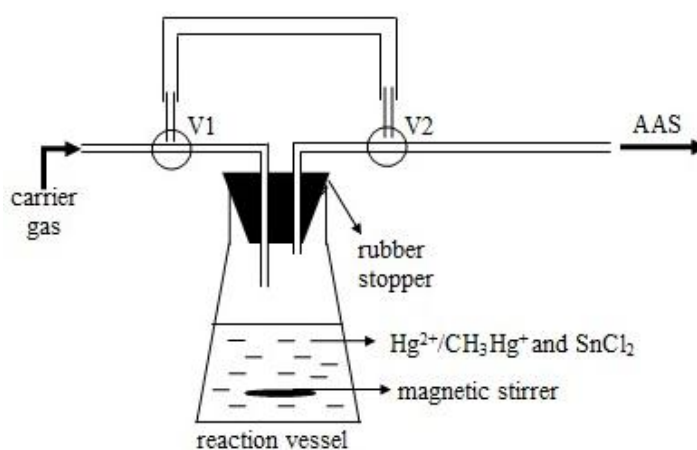
Function	Positions of the 3-way valve	
	V1	V2
Carrier gas flow between measurement cycles	⊕	⊕
Cold vapor Hg generation	⊖	⊖

Figure 2.1. Cold Vapor Atomic Absorption Spectrometry (CVAAS) system (positions of the 3-way valves, V1 and V2 indicate the flow directions during various steps).

2.3. Aqueous Calibration Plot

Standard solutions from 0.005 mgL^{-1} to 0.100 mgL^{-1} were prepared from 100.0 mgL^{-1} Hg^{2+} and CH_3Hg^+, respectively with simple dilution. All standards contained 5.0% (v/v) HNO_3 corresponding to a HNO_3 concentration of 1.1 M and measured with CVAAS. In addition, the limit of detection (LOD) based on 3s (3 times the standard deviation above the blank value) were also evaluated.

2.4. Synthesis of Sorbents

The novel sorbents for the determination of mercury species were synthesized as outlined in the proceeding subsections. Silica gel was chosen as the solid support matrix due to its high specific area, good resistance to organic solvents and high thermal resistance. To follow the text easily, the synthesized sorbents were abbreviated as given in Table 2.2.

Table 2.2. The abbreviation of the synthesized sorbents

Sorbent	Abbreviation
commercial silica	silica
commercial silica modified with –SH	3-MPTMS-silica
silica prepared by sol-gel method	sol-gel silica
sol-gel silica modified with -SH	sol gel-3-MPTMS
-SH modified sol-gel silica (during synthesis)	3-MPTMS-sol gel
commercial silica modified with –NH$_2$	3-APTES-silica
commercial silica modified with both –NH$_2$ and -SH	3-APTES-3-MPTMS-silica

2.4.1. Synthesis of Silica Gel by Sol-Gel Method

Synthesis of silica gel via sol-gel method was carried out as described by Eroğlu (1996). In this method, 25 mL of TEOS, 8 mL of water and 27 mL of C_2H_5OH were mixed instantly in a beaker. The pH of the mixture was adjusted to 4.5 with $2x10^{-4}$ M HCl and stirred for 30 minutes. After that it was allowed to gel at room temperature for 3 days in a closed container and dried for one week at 60 °C. Finally the obtained silica gel (sol-gel) was crushed in a porcelain cup.

2.4.2. Synthesis of (3-Mercaptopropyl) Trimethoxysilane (MPTMS)- Modified Silica Gel

MPTMS-modified silica gel was prepared by the method reported by Göktürk et al. (2000). Firstly, 5 grams of silica gel was rinsed with 100 mL of 0.01 M acetic acid solution under vacuum for 10 minutes. Then, it was filtered using a vacuum pump and

transferred to a round bottomed flask containing 25 mL of toluene. After that the dropwise addition of 3.0 mL of (3-mercaptopropyl)trimethoxysilane (MPTMS) was done under constant stirring to prevent self polymerization. Later 0.15 mL of acetic acid was added drop by drop and the mixture was stirred overnight. A second volume of 0.15 mL acetic acid was added before refluxing the solution at 60 °C for 2 h by vigorous stirring. Finally, the mercapto-functionalized silica gel was filtered using a vacuum pump and washed well with toluene before being left overnight in an oven at 80 °C. The proposed functionalization reaction is illustrated in Figure 2.2.
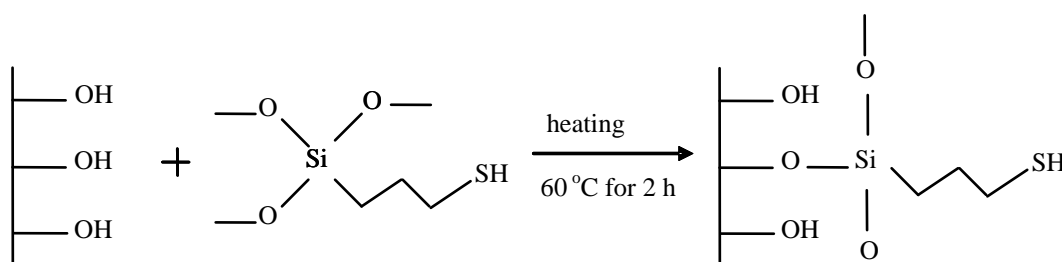
Figure 2.2. MPTMS modification of silica

2.4.3. Synthesis of (3-Mercaptopropyl) Trimethoxysilane (MPTMS)-Modified Silica Gel Prepared by Sol-Gel Method

Synthesis of MPTMS-modified silica gel (prepared by sol-gel method) was similar to the procedure described in Section 2.4.2. The only difference was the use of sol-gel silica instead of commercial silica gel.

2.4.4. Synthesis of (3-Mercaptopropyl) Trimethoxysilane (MPTMS)-Sol-Gel Resin

Silica gel was modified with MPTMS during sol-gel synthesis as reported by Eroğlu (1996) with a small difference. MPTMS was used instead of APTES in this procedure. TEOS, (25 mL), water (8 mL) and C_2H_5OH (27 mL) were taken and mixed immediately. The pH of the mixture was adjusted to 4.5 with $2x10^{-4}$ M HCl. Then 2.75 mL of MPTMS was added drop by drop with vigorous stirring and continued stirring for an additional 30 minutes. The mixture then was allowed to gel at room

temperature for 3 days in a closed container and dried for one a week at 60 °C. Finally, the glass was crushed in a porcelain cup after drying.

2.4.5. Synthesis of (3-Aminopropyl) Triethoxysilane (APTES)-Modified Silica Gel

For the synthesis of amino-functionalized silica (3-aminopropyl)triethoxysilane (APTES) was used as the organic source. Prior to silanization, a pretreatment step was carried out to activate the silica gel. For this purpose, 20.0 grams of silica gel was mixed with 100.0 mL of 0.01 M acetic acid solution for 1.0 hour. Then it was filtered using a vacuum pump and washed with distilled water until pH 6.0. Afterwards, it was transferred to a round bottomed flask containing 50.0 mL of toluene and 12.0 mL of APTES. The mixture was then stirred for 24.0 h under reflux at 110.0 °C under N_2 atmosphere. The resulting product was filtered off and washed with ethanol. After removal of the traces of solvent, the resulting product was further dried at 50.0°C at for 24.0 h.
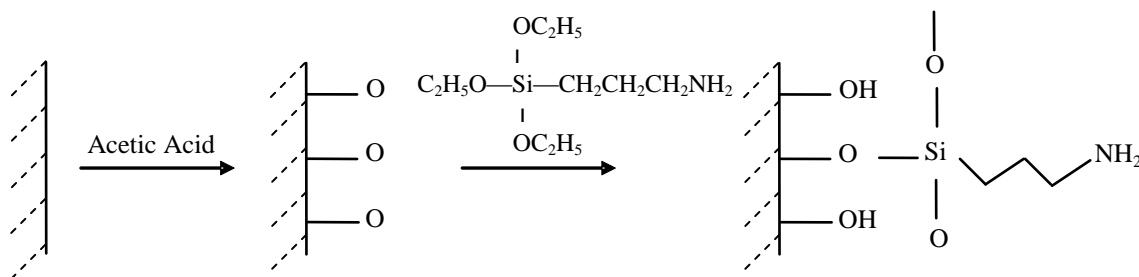
Figure 2.3. APTES modification of silica

2.4.6. Synthesis of (3-Aminopropyl) Triethoxysilane (APTES)-(3-Mercaptopropyl) Trimethoxysilane (MPTMS)-Modified Silica Gel

A similar procedure explained in Section 2.4.5 was applied for the synthesis of silica-amino-mercapto sorbent. Two functional groups (-SH or -NH$_2$) were attached to the silica surface at the same time, so a bifunctional resin was prepared. First the activation of silica was performed and then it was mixed with 9 mL of APTES and

9 mL of MPTMS in 30 mL toluene for 24.0 h under reflux at 110.0 °C under N_2 atmosphere. After filtration, the resulting product was washed with 20 mL acetone and 10 mL toluene. Finally, the synthesized sorbent was further dried at 50.0°C at for 24.0 h.

2.4.7. Synthesis of Nanoscaled Zero-Valent Iron (nZVI)

Nanoscaled zero-valent iron (nZVI) was synthesized using the method of liquid-phase reduction, utilizing sodium borohydride ($NaBH_4$) as the reducing agent (Wang and Zhang 1997, Wang et al. 2006) and iron(III) chloride tetrahydrate ($FeCl_3. 6H_2O$) as the ion source. The proposed reaction is:

$$4Fe^{3+} + 3BH_4^- + 9H_2O \rightarrow 4Fe^0 + 3H_2BO_3^- + 12H^+ + 6H_2 \uparrow$$
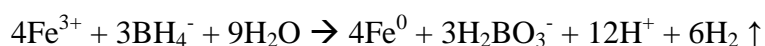
In a typical synthesis procedure, 7.25 g $FeCl_3.6H_2O$ was dissolved in a 4:1 (v/v) ethanol/water mixture (20 mL ethanol + 5 mL ultra pure water) and stirred on a magnetic stirrer. On the other hand, 3.50 g $NaBH_4$ was dissolved in 100 mL of ultra pure water. The final BH_4^-/Fe^{3+} ratio is adjusted to 3, since excess borohydride is needed for better growth of nanoparticles. $NaBH_4$ solution, from a burette, was added dropwise to the iron(III) solution, while still stirring on magnetic stirrer. Black solid particles immediately appeared after introducing the first drop of $NaBH_4$ solution. After adding the whole borohydride solution, the mixture was left for another 10 minutes of stirring. To separate the black iron nanoparticles from the liquid phase, vacuum filtration was applied. At this point, solid particles were washed at least three times with 25 mL portions of absolute ethanol to remove all traces of water. This washing process is probably the key step of synthesis since it prevents the rapid oxidation of zero-valent iron nanoparticles. Synthesized nanoparticles were finally dried in oven at 50 °C overnight. Drying in evacuated ovens must be avoided because this would cause Fe nanoparticles to spontaneously ignite upon exposure to air.

2.4.8. Modification of Ion Exchange Resins with nZVI

5.0 g cation or anion exhange resin was treated with 50 mL of 1.0 M FeCl$_3$.6H$_2$O for 24 hour. The mixture was filtered under vacuum, washed with absolute ethanol to remove all the water and dried in oven at 50 ^{o}C. After drying step, the Fe^{3+}-loaded resin was taken into a beaker and was treated with 3.5 % (m/v) NaBH$_4$ added dropwise from a burette. The mixture was filtered under vacuum; the resin was washed with absolute ethanol and dried in oven at 50 ^{o}C overnight; hence the ZVI-modified resin was obtained. The washing (with ethanol) process is thought to be the key step of modification to prevent the rapid oxidation of ZVI. The ion exchange resins used in this study are given in Table 2.3.

Table 2.3. Ion exchange resins used in this study

Ion exchange resin	Type	Functional Groups	Matrix
Diaion SK 116	strong cation exchanger	Sulfonic acid	Polystyrene gel
Amberlite IRC 50	weak cation exchanger	Carboxylic acid	Acrylic polymer
Amberlite IRA 400	strong anion exchanger	Quaternary ammonium	Polystyrene gel
Amberlite IRA 458	strong anion exchanger	Quaternary ammonium	Polyacrylic gel
Amberlite IRA 67	weak anion exhanger	Polyamine	Acrylic gel

2.4.9. Modification of Inorganic Substrates with nZVI

Alumina (Al$_2$O$_3$), silica (SiO$_2$) or titania (TiO$_2$) (2.8 g each) was treated with 50 mL of 1.0 M FeCl$_3$.6H$_2$O for 24 hour. The inorganic substrate/Fe^{3+} ratio is adjusted to 1 during modification. The mixture was filtered under vacuum and the Fe^{3+}-loaded inorganic substrate was taken into a beaker and then was treated with 3.5 % (m/v) NaBH$_4$ added dropwise from a burette. The mixture was filtered under vacuum; the substrate was washed with absolute ethanol as explained in the previous section and dried in oven at 50 ^{o}C overnight; hence the ZVI-modified substrate was obtained.

2.4.10. Synthesis of Zero-Valent Copper (ZVC)

A similar procedure explained in Section 2.4.7 was applied for the synthesis of zero-valent copper. The only difference was the use of 4.27 g of $CuCl_2.2H_2O$ instead of 7.25 g $FeCl_3.6H_2O$. The proposed reaction is:

$$Cu^{2+} + 2BH_4^- + 6H_2O \rightarrow Cu^0 + 2B(OH)_3 + 7H_2 \uparrow$$
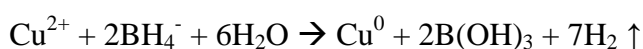
2.4.11. Modification of Inorganic Substrates/Ion Exchange Resins with ZVC

Synthesis of ZVC-modified inorganic substrates/ion exchange resins was same with the procedure described in Section 2.4.8 and Section 2.4.9. The modified sorbents used in this part are alumina, Amberlite IRA 458, Amberlite IRA 67, Diaion SK 116 and Amberlite IRC 50.

2.5. Characterization of the Synthesized Sorbents

Characterization is very important to enlighten the structure and properties of the synthesized sorbents. The structural details may also help to understand the possible sorption mechanism between the mercury species and the solid sorbents. Thus, a number of characterization experiments were performed to understand whether the functional groups were attached to the support material. Characterization of the sorbents was performed using techniques such as, Brunauer-Emmett-Teller (BET), X-ray diffraction (PXRD), surface area analysis and elemental analysis. Images of newly synthesized materials were taken with scanning electron microscopy (SEM) while their thermal degradation behaviors were investigated through TGA measurements.

2.6. Silver Capacity Measurement of 3-MPTMS-Silica

Several strategies have been used to determine the uptake capacity of the sorbents. One of the methods applied is the silver uptake capacity since the –SH functional group has a strong affinity towards Ag^+ ions. For this purpose, 0.100 g of 3-MPTMS-silica was added into 10.0 mL of 0.05 M $AgNO_3$ solution, the mixture was acidified with 0.5 mL of 14.3 M HNO_3 and shaken for one hour in a dark atmosphere at room temperature. After shaking, the solution was filtered and washed well with water to remove all remaining Ag^+ cations. Afterwards, a few drops of 0.1 M ferric ammonium sulfate, $(NH_4)Fe(SO_4)_2.6H_2O$, were added to the filtrate and titrated with 0.1 M NH_4SCN according to Volhard method. NH_4SCN was standardized with $AgNO_3$ prior to titration. For a blank, the same procedure was applied with silica gel.

2.7. Effect of pH on the Stability of ZVI- or ZVC-Modified sorbents

It is known from our previous experience that the solubility of nZVI increases with the increasing acidity of solutions. In order to investigate this in a more systematic way, modified sorbents were placed in solutions having different pHs. For this purpose, 10.0 mL of ultra pure water was taken and its pH was adjusted to 1.0, 2.0, 3.0, 4.0 and 6.0. After the addition of 10.0 mg of the sorbents into each, the mixture was shaken manually for 1-2 minutes and then placed on the shaker for 30 minutes. The contents were filtered through quantitative (blue band) filter paper and the filtrates were analyzed by FAAS for their iron or copper concentrations. The same procedure was also applied for the unmodified sorbents.

2.7. Sorption Studies

In order to understand the chemical behavior of Hg^{2+} and CH_3Hg^+ in aqueous solutions, several ion exchange resins, nano-scaled zero-valent iron (nZVI), zero-valent copper (ZVC), nZVI/ZVC-modified sorbents, alumina, titania, silica and the functionalized silicas were investigated.

In order to find the most suitable sorbent among the synthesized materials, for mercury species, 500 μgL^{-1} or 1.0 mgL^{-1} separate standard solutions of Hg^{2+} and CH$_3$Hg$^+$ were prepared at different pHs adjusted with various concentrations of HNO$_3$ and NH$_3$. From each of these solutions 10.0 mL were taken into which 10.0 mg of the tested sorbent were added. The resulting mixture was shaken manually for 1-2 minutes and then for a further 30 minutes on a shaker at room temperature. At the end of the shaking period, the mixture was filtered and the filtrate was analyzed for its mercury content by CVAAS.

The sorption percentage of mercury was calculated using Equation 2.1, where C_i is the initial and C_f is the final concentration in the solution.

$$Sorption \, \% = \frac{C_i - C_f}{C_i} \times 100 \qquad (2.1)$$

For the studies with 3-MPTMS modified silica, nZVI and ZVC the effect of the sorbent amount, shaking time, solution pH, reaction temperature and desorption was also investigated. In all these experiments, batch sorption was followed by the filtration of the mixture through blue-band filter paper and analysis of the filtrate for the determination of the mercury concentration by CVAAS.

2.7.1. Studies Utilizing 3-MPTMS-Silica

2.7.1.1. Effect of pH

Solution pH is one of the most important factors to understand the interaction between the forms of mercury and the functional groups on the sorbents. In order to investigate the effect of solution pH on the sorption of Hg^{2+} and CH$_3$Hg$^+$, 500.0 μgL^{-1} standard solutions were prepared at different pHs from 1.0 to 10.0 adjusted with various concentrations of HNO$_3$ and NH$_3$. From each of these solutions, 10.0 mL were taken into which 10.0 mg of 3-MPTMS-modified silica was added. The mixture was first shaken for 1-2 min manually and then for 30.0 min on a shaker at 25 ^{o}C. The contents were filtered through quantitative (blue band) filter paper and the samples were analyzed by CVAAS.

2.7.1.2. Effect of Sorbent Amount (Solid/Liquid Ratio)

Determination of sorbent amount is an important factor for quantitative sorption of the analyte from the solution and this was investigated through batch studies. Different amounts of sorbents, from 5.0 mg to 200.0 mg, were added to 10.0 mL of 500.0 μgL^{-1} Hg^{2+} and CH_3Hg^+ at pH 7.0 and shaken 1-2 min manually; then for 30 min on a shaker. After filtration the Hg concentration in the filtrates were determined by CVAAS.

2.7.1.3. Effect of Shaking Time

In order to obtain efficient sorption, the effect of contact time was investigated. For this purpose, 10.0 mL of 500.0 μgL^{-1} Hg^{2+} and CH_3Hg^+ at pH 7.0 containing 10.0 mg of 3-MPTMS-modified silica were shaken at 25.0 ^oC for time intervals of 1, 2, 5, 10, 15, 30, 45, 60 and 90 min. After filtration, the resulting solutions were analyzed by CVAAS and percent sorption was calculated.

2.7.1.4. Effect of Temperature

Effect of reaction temperature on the sorption of mercury ions by 3-MPTMS-modified silica was investigated at 25.0 and 60.0 ^oC. During the experiments, Hg^{2+} and CH_3Hg^+ concentrations, solution volume, shaking time, solution pH and sorbent amount were 500.0 μgL^{-1}, 10.0 mL, 30 minutes, pH=7.0, and 10.0 mg, respectively.

2.7.1.5. Desorption from the Sorbent

After deposition of Hg^{2+}/CH_3Hg^+ on the 3-MPTMS-modified silica, its release was examined using several eluents. For this purpose, 10.0 mg of sorbent was added to 10.0 mL of 500.0 μgL^{-1} Hg^{2+}/CH_3Hg^+ solutions at pH 7.0. After shaking for 30 min, the mixture was filtered and the sorbent was taken into the eluent. The new mixture was

shaken once again for 30 min. At the end of this period, the solution was filtered and the eluate was analyzed for its mercury content using CVAAS.

2.7.1.6. Sorption Capacity of 3-MPTMS-Silica

The sorption ability of 3-MPTMS-modified silica gel was also investigated for Hg^{2+} concentrations from 50.0, 100.0, 200.0, 500.0, 1000.0 mgL^{-1} since the removal of mercury from the aqueous solution may depend on the concentration. For this purpose, 5.0 mL of these solutions (at pH=7) were taken and 5.0 mg of sorbent was added to each of them. Then, the mixtures were shaken for 30 min on the shaker at 25 ^{o}C. After filtration, the filtrates were analyzed with CVAAS.

2.7.1.7. Application to Real Samples

The sorption performance of 3-MPTMS-modified silica and unmodified silica was first investigated using the spiked samples of ultrapure, bottled drinking, tap, sea and geothermal water. The spike concentration was 1.0 mgL^{-1} and the other parameters were as follows; solution pH 7.0, shaking time of 30 min, solution volume of 10.0 mL, reaction temperature of 25.0 ^{o}C. Batch process was applied for sorption and the concentration of mercury in water samples was determined by CVAAS.

2.7.2. Studies Utilizing nZVI

2.7.2.1. Effect of pH

The sorption behavior of nZVI towards Hg^{2+} and CH_3Hg^+ was examined using batch process. For this purpose, 1.0 mgL^{-1} of each Hg standard was prepared separately in different pH solutions, 5.0, 7.0 and 10.0, respectively, using various concentrations of HNO_3 and NH_3. From each of these solutions, 10.0 mL were taken into which 10.0 mg of nZVI were added. The mixture was shaken manually for a minute and then placed on the shaker for 30 min. The contents were filtered through quantitative (blue band) filter

paper and the filtrates prepared were analyzed by CVAAS for Hg concentration. The filtrates were also analyzed by FAAS to determine Fe concentrations dissolved and therefore released from the substrate.

2.7.2.2. Effect of Sorbent Amount (Solid/Liquid Ratio)

The optimum sorbent amount is determined in order to find the quantitative sorption of the analyte from the solution and this was investigated through batch studies. Different amounts of sorbents, from 5.0 mg to 200.0 mg, were added to 10.0 mL of 1.0 mgL^{-1} Hg^{2+} (and CH$_3$Hg$^+$) at pH 7.0 and shaken for a minute manually; then for 30 min on a shaker. After filtration the Hg concentration in the filtrates was determined by CVAAS. The Fe content of the filtrates was also determined using FAAS.

2.7.2.3. Effect of Shaking Time

The effect of contact time on the efficiency of sorption was investigated. For this purpose, 10.0 mL of 1.0 mgL^{-1} Hg^{2+} (and CH$_3$Hg$^+$) at pH 7.0 containing 10.0 mg of nZVI were shaken at 25.0 ^{o}C for time intervals of 1, 2, 5, 15, 30, 60 and 120 min. After filtration, the resulting solutions were analyzed by CVAAS and percent sorption was calculated. The filtrates were also analyzed by FAAS for their Fe content.

2.7.2.4. Effect of Temperature

The sorption efficiency of nZVI towards Hg^{2+} and CH$_3$Hg$^+$ was examined at three temperatures (25 ^{o}C, 50 ^{o}C and 75 ^{o}C) by keeping the other parameters constant (10.0 mL of sample volume, pH of 7.0, 10.0 mg of sorbent and 30 min of shaking time). After sorption, mercury species were determined by CVAAS whereas the Fe content of the filtrates was detected by FAAS.

2.7.2.5. Desorption from the Sorbent

After collection of mercury species by nZVI, their release was investigated using several eluents (HNO_3, HCl, thiourea, etc.). For this purpose, 10.0 mL of 1.0 mgL^{-1} mercury was prepared and 10.0 mg of nZVI was added to it. After shaking for 30 min, the mixture was filtered and the sorbent was taken into the desorbing solution (10.0 mL). The new mixture was shaken once again for 30 min. Finally, the resulting solution was filtered and the filtrate was analyzed for its mercury content by CVAAS. The Fe content was also determined in the following solutions by FAAS.

2.7.2.6. Sorption Capacity of nZVI

The sorption ability of nZVI was also examined for Hg^{2+} concentrations from 50.0, 100.0, 200.0, 500.0, 1000.0 mgL^{-1}. For this purpose, 5.0 mL of these solutions at pH=7 were prepared and 5.0 mg of nZVI was added to each of them. Then, the mixtures were shaken for 30 min on the shaker at 25 ^{o}C. After filtration, the filtrates were analyzed with CVAAS and FAAS for mercury and iron content, respectively.

2.7.2.7. Application to Real Samples

The performance of the proposed methodology with the use of nZVI and ZVI-modified silica was investigated using the spiked samples of ultrapure, bottled drinking, tap and sea water. The spike concentration was 1.0 mgL^{-1} and the other parameters were as follows; solution pH 7.0, shaking time of 30 min, solution volume of 10.0 mL, reaction temperature of 25.0 ^{o}C. Batch process was applied for sorption and the concentration of mercury in water samples was determined by CVAAS while the Fe concentration in the filtrates was measured with FAAS.

2.7.3. Studies Utilizing ZVC

2.7.3.1. Effect of pH

To understand the uptake behavior of ZVC, separate solutions of mercury (Hg^{2+} at 1.0 mgL^{-1} concentration were prepared at pH's 5.0, 7.0 and 10.0. These pH ranges were chosen since ZVC dissolved at pH values lower than 5.0. The sorbent (10.0 mg) was added immediately to these solutions. The mixtures were shaken manually for 1-2 min and then placed on the shaker for 30 min at room temperature. The contents were collected on filter papers. The resultant solutions were determined by CVAAS using the optimum conditions for Hg content. The filtrates were also analyzed by FAAS to determine Cu concentrations dissolved and therefore released from the substrate.

2.7.3.2. Effect of Sorbent Amount (Solid/Liquid Ratio)

The amount of sorbent is an important factor for quantitative sorption of the analytes from a given solution. For this purpose, 10.0 mL of 1.0 mgL^{-1} Hg^{2+} at pH 7.0 were shaken with varying amounts of ZVC, from 5.0 mg to 200.0 mg, for 30 min. After filtration the Hg concentration in the filtrates was determined by CVAAS where the Cu content of the filtrates was also determined using FAAS.

2.7.3.3. Effect of Shaking Time

Samples were shaken for 1, 2, 5, 15, 30, 60 and 120 min to understand the effect of shaking time on sorption. Other parameters were kept constant at 1.0 mgL^{-1} Hg^{2+} concentration, 10.0 mL sample volume, 10.0 mg sorbent amount and 25.0 ^{o}C sorption temperature. Sorption experiments were carried out at pH 7.0. After filtration, the resulting solutions were analyzed by CVAAS and percent sorption was calculated. The filtrates were also analyzed by FAAS for their Cu content.

2.7.3.4. Effect of Temperature

Effect of sorption temperature on the sorption of Hg^{2+} was examined at three temperatures (25 ^{o}C, 50 ^{o}C and 75 ^{o}C) by keeping the other parameters constant (10.0 mL of sample volume, pH of 7.0, 10.0 mg of sorbent and 30 min shaking time). After sorption, mercury species were determined by CVAAS whereas the Cu content of the filtrates was detected by FAAS.

2.7.3.5. Desorption from the Sorbent

After deposition of Hg^{2+} on the ZVC, its release was examined using several eluents. For this purpose, 10.0 mg of sorbent was added to 10.0 mL of 1.0 mgL^{-1} Hg^{2+} solutions at pH 7.0. After shaking for 30 min, the mixture was filtered and the sorbent was taken into the eluent. The new mixture was shaken once again for 30 min. At the end of this period, the solution was filtered and the eluate was analyzed for its mercury content using CVAAS. The Cu content of the eluates was also determined by FAAS.

2.7.3.6. Application to Real Samples

The performance of the proposed methodology with the use of ZVC and ZVC-modified alumina was investigated using the spiked samples of ultrapure, bottled drinking, tap and sea water. The spike concentration was 1.0 mgL^{-1} and the other parameters were as follows; solution pH 7.0, shaking time of 30 min, solution volume of 10.0 mL, reaction temperature of 25.0 ^{o}C. Batch process was applied for sorption and the concentration of mercury in water samples was determined by CVAAS while the Cu concentration in the filtrates was measured with FAAS.

CHAPTER 3

RESULTS AND DISCUSSION

3.1. Characterization

3.1.1. Characterization of Silica-Based Sorbents

3.1.1.1. Scanning Electron Microscopy (SEM)/Energy-Dispersive X-ray Spectroscopy (EDX)

SEM/EDX characterization was performed using a Philips XL-30S FEG type instrument. Prior to analysis, a small amount of sample from the sorbents was taken and sprinkled onto adhesive carbon tapes which were supported on metallic disks. Images of the sample surfaces were recorded at different magnifications. EDX analysis was carried out on randomly selected points on the solid surfaces and back-scatter electron (BSE) detector was utilized during SEM analysis. The back-scatter electron detector allows materials with different compositions to be imaged as different (grey scale/atomic) contrast and it is used for the elements having a large atomic number difference between each other.

The typical SEM images of the silica-based sorbents are shown in Figure 3.1. The presence of -SH and -NH$_2$ functional groups on the sorbent surface was followed by the S and N signals obtained. As can be seen from the figure, when functional groups were attached onto the surface of commercial/sol-gel silica, the morphology changed. The change in the morphology can be attributed to the vigorous reaction conditions during the synthesis rather than the attachment of the functional groups onto the surface.
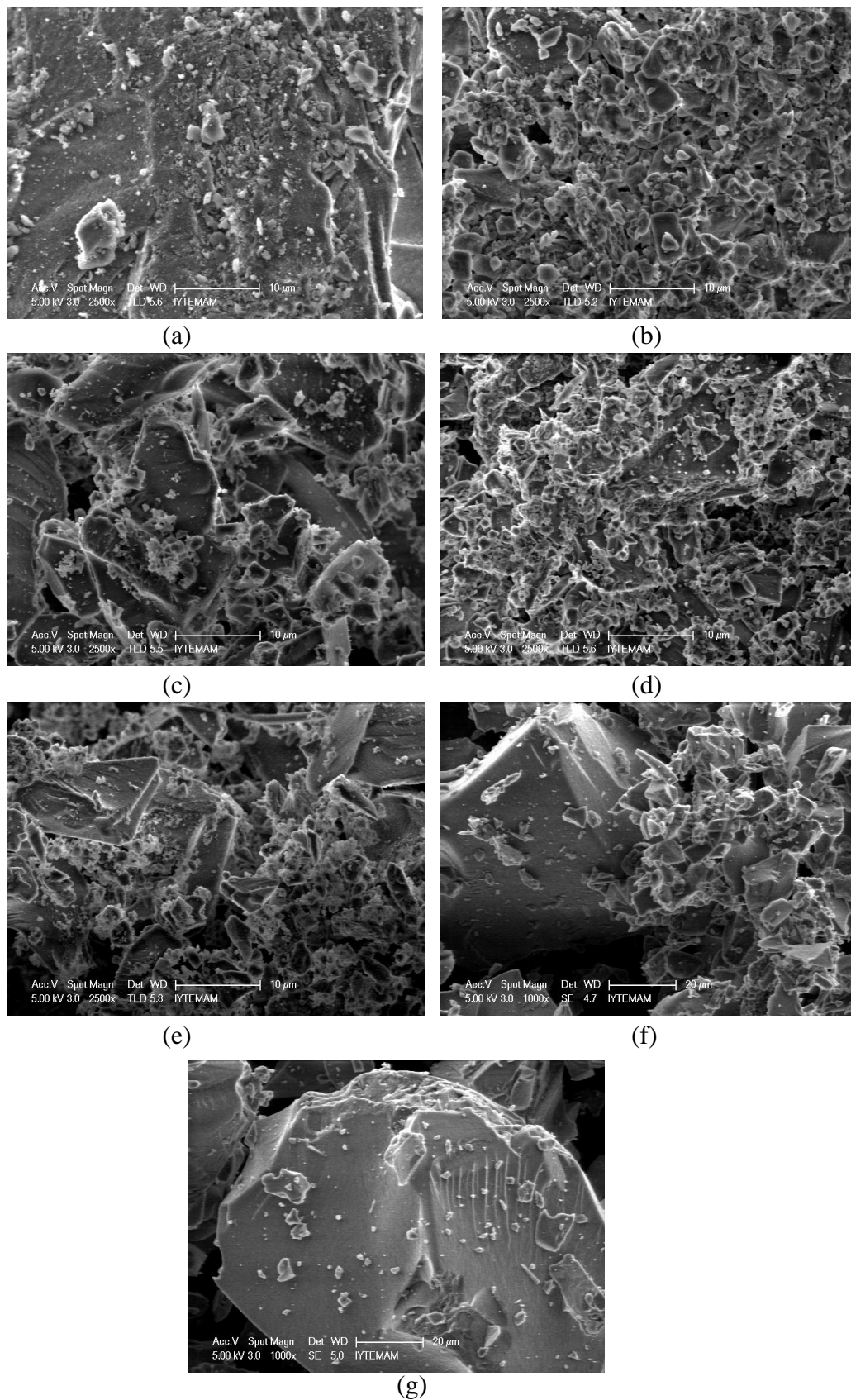
Figure 3.1. Typical SEM images of modified/unmodified silica. (a) unmodified silica, (b) 3-MPTMS-silica, (c) unmodified sol-gel silica, (d) sol gel-3-MPTMS, (e) 3-MPTMS-sol gel, (f) 3-APTES-silica and (g) 3-APTES-3-MPTMS-silica.

EDX results for silica-based sorbents are shown in Table 3.1. The sorbents contain mainly carbon, silicon, oxygen and small quantities of sulfur and/or nitrogen depending on the functional groups attached. The percentage values given in the tables must be evaluated very carefully not be considered precise as quantitative results cannot be obtained in EDX for low concentrations. According to Table 3.1, the percentage of S was nearly 5% and the relatively high percentage of S in 3-MPTMS-silica demonstrated the successful attachment of -SH functional group onto the surface.

EDX data obtained for the modified sol-gel sorbents are also demonstrated in the same table (Table 3.1) and the S content varies between 3-5%. The attachment of -SH group during sol-gel synthesis appears to be more successful compared to sol gel-3-MPTMS. However, the percent sorption of Hg^{2+}/CH_3Hg^+ with both sorbents was higher than 95% indicating that the small difference in S content of the two sorbents did not result in big difference in sorption percentage under the employed reaction conditions although the S content in 3-MPTMS-sol gel was greater.

EDX results of silica, 3-APTES-silica and 3-APTES-3-MPTMS-silica are also given in Table 3.1. It can be concluded that the presence of $-NH_2$ and -SH functional groups on silica surface showed the achievement of modification. The percentages of S and N on bifunctional silica decrease compared to modifications with -SH and $-NH_2$ alone. However, the sum of the percentages of S and N (5.79%) are between the percentages of S and N alone in the sorbent (4.51% for S and 6.20% N, respectively).

Table 3.1. EDX results for unmodified and modified sorbents used.

Element	silica Wt (%)	At (%)	sol gel silica Wt (%)	At (%)	3-MPTMS-silica Wt (%)	At (%)	sol gel-3-MPTMS Wt (%)	At (%)	3-MPTMS-sol gel Wt (%)	At (%)	3-APTES-silica Wt (%)	At (%)	3-APTES-3-MPTMS-silica Wt (%)	At (%)
C K	1.0	1.6	-	-	11.7	19.3	18.0	28.3	17.9	27.6	10.5	16.6	9.7	15.9
O K	54.4	67.0	53.1	66.5	36.2	44.7	33.7	39.7	38.7	44.5	38.3	45.6	35.7	44.0
Si K	44.6	31.4	46.9	33.5	44.7	31.5	42.6	28.6	34.9	23.0	46.6	31.6	48.8	34.3
S K	-	-	-	-	7.4	4.5	5.7	3.4	8.5	4.9	-	-	2.9	1.8
N K	-	-	-	-	-	-	-	-	-	-	4.6	6.2	2.8	3.9

3.1.1.2. Elemental Analysis

Modified silica and sol-gel silica with different functional groups (-SH, -NH$_2$, or both) were also investigated using elemental analysis. The results of elemental analysis are shown in Table 3.2. The percentages of S and N of modified silicas demonstrate that the functional groups are bonded onto the silica surface. This is also confirmed by the increase in the percentages of C and H indicating the attachment of 3-MPTMS and 3-APTES onto silica. It can also be said that 3-MPTMS-sol gel have been functionalized to a greater extent among the sorbents with –SH groups. This could have been resulted from the differences in accessible silanol groups of silica materials. The sorbent containing both -SH and –NH$_2$ groups has lower sulfur and nitrogen content compared to the other sorbents.

Table 3.2. Elemental analysis results of the novel sorbents.

Sorbent	C %	H %	N %	S %
silica	0.16	0.88	-	-
3-MPTMS-silica	8.34	1.96	-	7.60
sol-gel silica	0.99	2.05	-	-
sol gel-3-MPTMS	8.29	2.48	-	7.41
3-MPTMS-sol gel	9.47	3.01	-	8.95
3-APTES-silica	6.16	1.85	2.17	-
3-APTES-3-MPTMS-silica	4.62	1.38	0.81	1.83

3.1.1.3. Thermo Gravimetric Analysis (TGA) of 3-MPTMS-Silica

TGA is one of the methods that is applied for the characterization of unmodified/modified silica. It allows the determination of the degree of surface modification through comparison of the percent weight loss as a function of temperature.

In the present study, TGA was applied in order to see the effect of heat on the structure of the synthesized sorbents. The analyzer was a Perkin Elmer Diamond TG/DTA instrument and the solid samples were heated from 50 °C to 800 °C by a heating rate of 10 °C/min under N$_2$ atmosphere. The results are provided in Figure 3.2

for unmodified (as purchased) and modified (with 3-MPTMS) silica gel. When the TGA curve of silica gel is considered (Figure 3.2a) 3-4% weight loss at ~110 ^{o}C can be seen due to the loss of residual water from silica structure. Increasing the temperature induces condensation between silanol groups, resulting in the release of water, which is then vaporized, and decreasing the sample weight. After 200 ^{o}C weight decreases gradually and only 3% weight loss is observed. When silica gel modified with 3-MPTMS (Figure 3.2b) was heated to 800 ^{o}C the total loss from the sample was about 15-20%. Approximately 10-12% difference in the weight loss compared to that of the unmodified silica is attributed to the loss of organic functional groups on the modified silica. This is another indication of the success of the modification process.
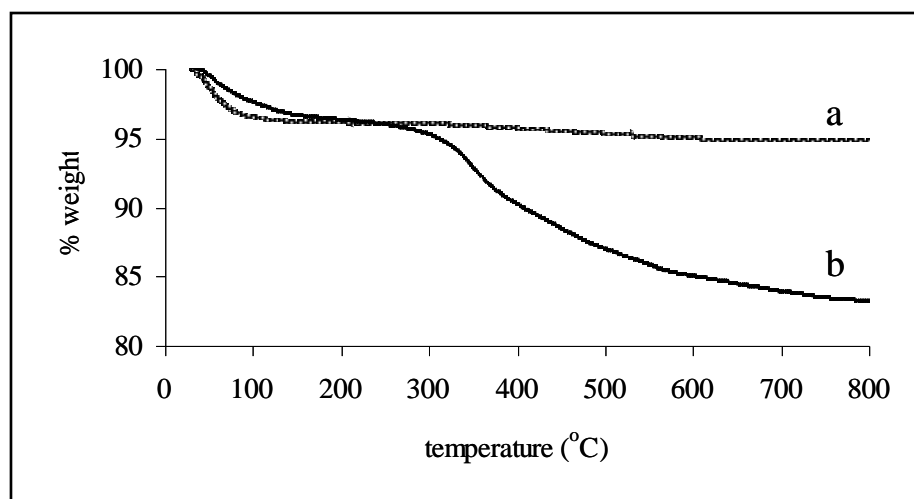
Figure 3.2. TGA curves of (a) unmodified (b) 3-MPTMS-modified silica.

3.1.1.4. Bruner-Emmett-Teller (BET) Surface Area Analysis of 3-MPTMS-Silica

Three fundamental parameters, (i) specific surface area (m^2g^{-1}), (ii) specific pore volume; distribution of pore size or pore area and (iii) particle size can be used for physical characterization of the silica surface. Nitrogen sorption isotherm is an efficient way for providing information about the pore system of materials. Specific surface area of silica gel is determined to express concentration of reactive surface species and provides an idea about surface loading, which is directly related to steric hindrance. Pore size distribution gives a deeper insight in availability of reactive silanol groups towards the reacting molecule. It also explains the sorption characteristics of silica. As

44

the organic fragments enter the channels, the isotherms are expected to have gradual changes at each stage of modification. Table 3.3 indicates that modified silica have lower surface area and smaller pore widths than silica. The reason for this result must be the coverage of the silica with -SH functional group through the formation of bonds between silanol groups on the surface and the functional silanes.

Table 3.3. BET analysis results of silica and 3-MPTMS-modified silica.

Sorbent	Surface area[a] (m^2g^{-1})	Average pore width[b] (A^o)	Pore volume[c] (cm^3g^{-1})
silica	302.9	19.4	0.147
3-MPTMS-silica	112.8	13.8	0.039

[a]BET surface area
[b]Pore diameter according to the maximum of the BJH pore size distribution
[c]Single point total pore volume

3.1.1.5. Zeta Potential Measurements of 3-MPTMS-Silica

The magnitude of electrostatic interaction between the modified surfaces and the metal ions is explained in terms of zeta potential. The pH_{PZC} (Point of Zero Charge) of an oxide is the value of pH at which the net surface charge is zero. There is a relationship between pH_{PZC} and uptake mechanism of a sorbent. In electrostatic sorption, cations are adsorbed at pH values higher than the pH_{PZC} while anion adsorption is favored at pH values lower than the pH_{PZC}. Figure 3.3 demonstrates the zeta potentials of unmodified/modified silica as a function of pH. In the case of silica (Figure 3.3a) the zeta potential approaches zero at pH 2.8. This is due to surface silanol (Si-OH) groups losing a proton. On the other hand, the chemical modification of silica surface with 3-MPTMS reduced the pH_{PZC} of silica and presented negative values within the pH range tested. This is due to its increased negative charge contribution to the sorbent surface. Therefore, 3-MPTMS-silica is more advantageous to adsorb metal cations.
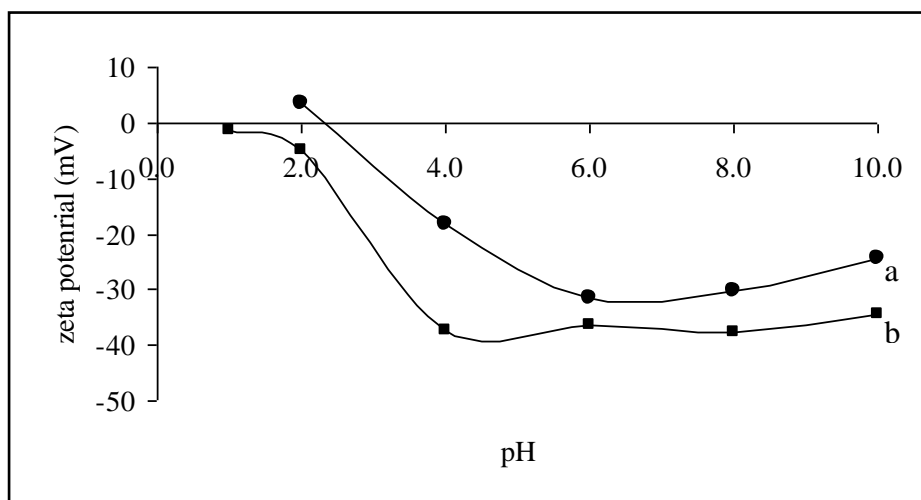
Figure 3.3. Effect of pH on zeta potential of (a) silica and (b) 3-MPTMS-modified silica

3.1.1.6. Particle Size Measurements of 3-MPTMS-Silica

Particle size measurements are also required for physical characterization of the solids. Table 3.4 indicates the particle size distribution of the unmodified and modified silicas. As can be seen from the table, as the surface is modified with -SH functional group, smaller silica particles are obtained. This is probably due to the effect of mechanical stirring applied through the modification process.

Table 3.4. Particle size of silica and 3-MPTMS-modified silica.

sorbent	size (nm)
silica	5277
3-MPTMS-silica	3742

3.1.1.7. Silver Capacity Measurement of 3-MPTMS-Silica

The capacity of 3-MPTMS-silica was measured by the batch type extraction of Ag^+ by the sorbent as explained in Section 2.6. The silica gel itself is able to form complexes with many metal ions due to its silicic –OH groups and silica gel was found to have a silver capacity of 0.09 ± 0.02 mmol g^{-1} (Ag^+/sorbent). Hence, in order to find

the capacity of the mercapto functional group on 3-MPTMS-silica, this value was assumed as blank and subtracted from the silver capacity of 3-MPTMS-silica. Finally, the silver capacity of 3-MPTMS-silica was found as 0.63 ± 0.14 mmol g^{-1} and this capacity value is very sufficient for the removal of mercury species from environmental samples.

3.1.2. Characterization of nZVI and ZVI-Modified/Unmodified Sorbents

3.1.2.1. Scanning Electron Microscopy (SEM)/Energy-Dispersive X-ray (EDX) Spectroscopy

Scanning electron microscopy (SEM) was used for the characterization of nZVI and ZVI-modified ion-exchange resins or inorganic substrates.

3.1.2.1.1. SEM/EDX of nZVI and ZVI-Modified Ion Exchange Resins

The SEM images of nZVI and ZVI-modified ion exchange resins are demonstrated in Figure 3.4 and 3.5. As seen from Figure 3.4a, nZVI has a chain-like structure. The SEM images of ZVI-modified/unmodified Diaion SK116 and Amberlite IRC50 are also shown in the same figure. According to the figure, the surface morphology did not change much after processing but spots were observed on the surface. However, the modified particles develop a dark brown color after modification process due to the presence of iron.

A similar analysis was also performed for ZVI-modified/unmodified Amberlite IRA400, Amberlite IRA458 and Amberlite IRA67 and the SEM images are demonstrated in Figure 3.5. The surface morphology appeared to be similar after the modification process despite a color change was observed on the resin surface indicating the success of modification.
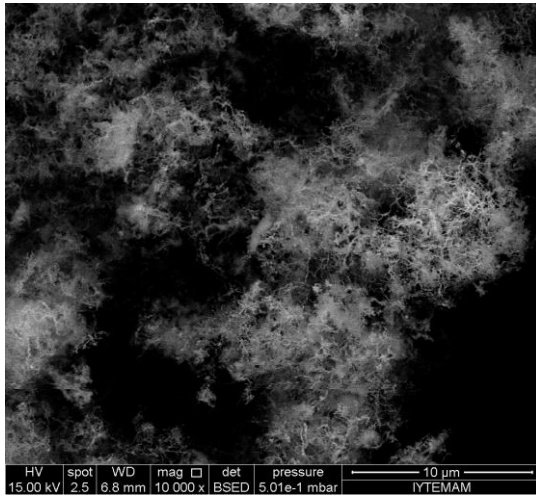
(a)
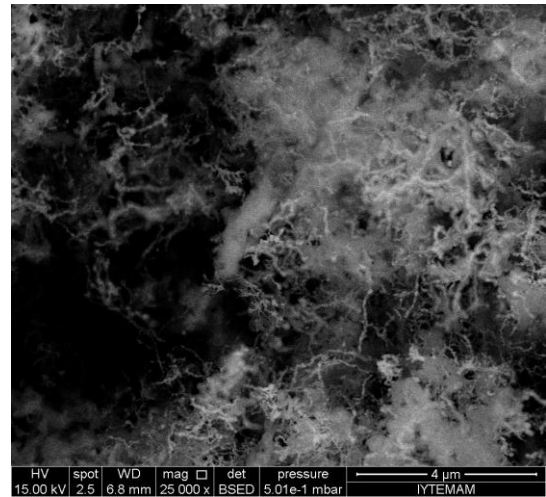
(b)
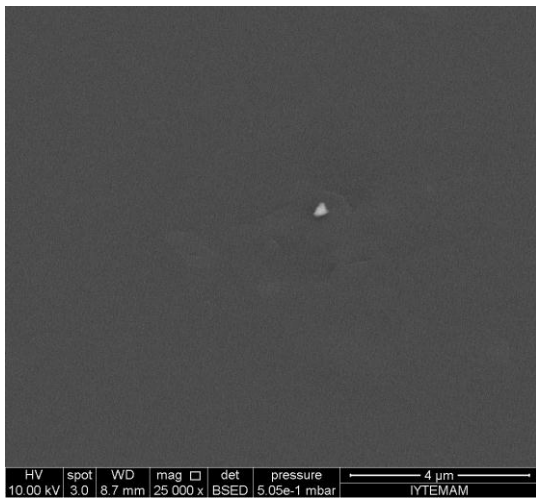
(c)
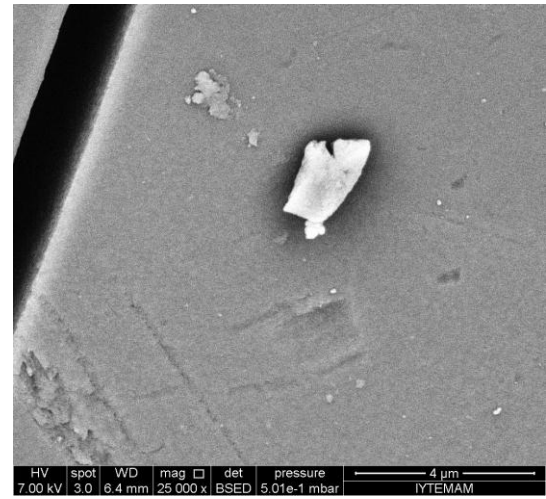
(d)
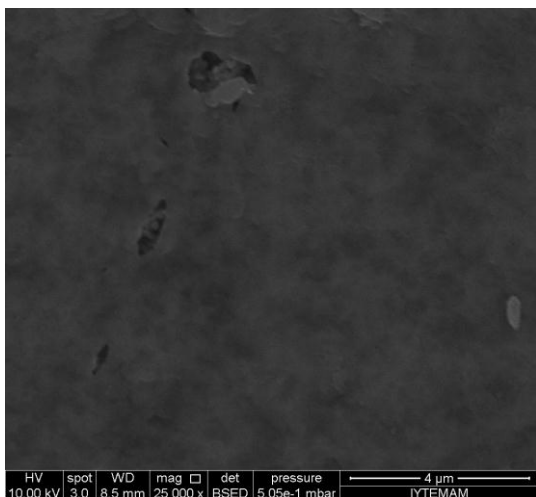
(e)
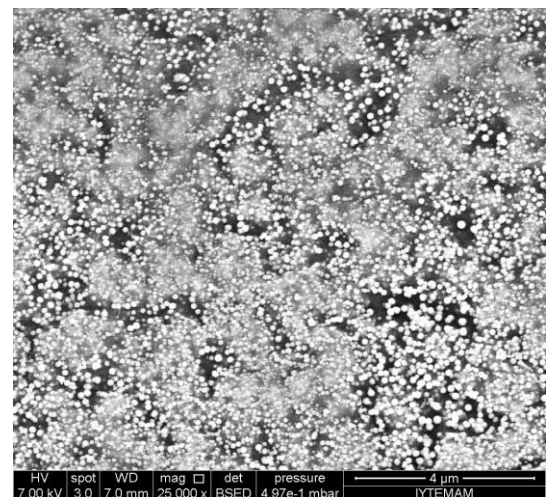
(f)

Figure 3.4. Typical SEM images of (a) nZVI (10000x), (b) nZVI (25000x), (c) Diaion SK116, (d) ZVI-modified Diaion SK116, (e) Amberlite IRC50 and (f) ZVI-modified Amberlite IRC50 at 25000x magnification.
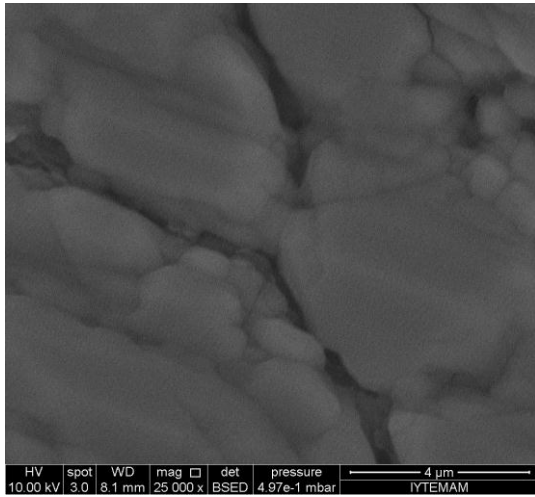
(a)
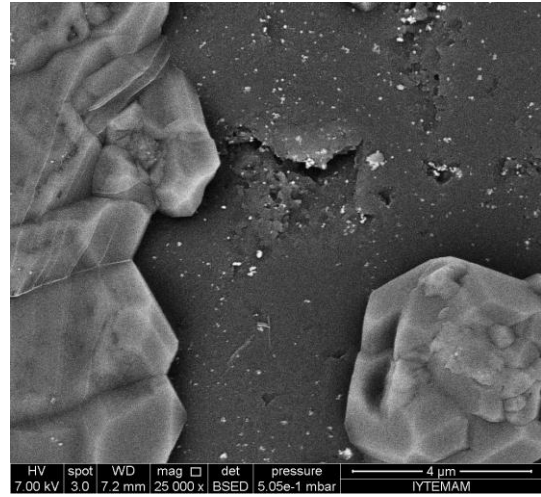
(b)
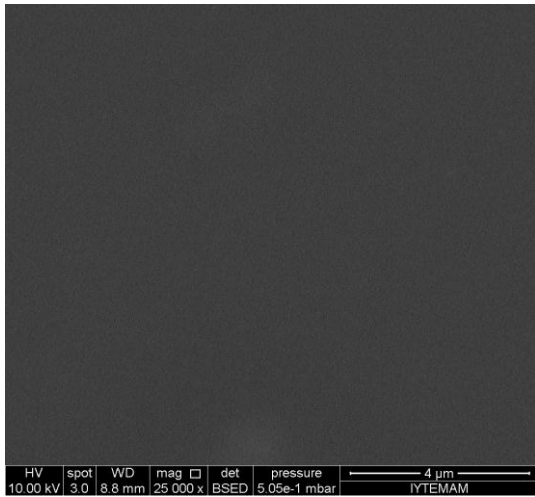
(c)
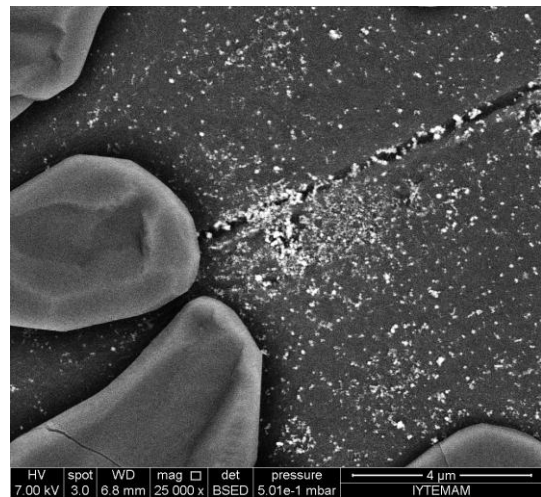
(d)
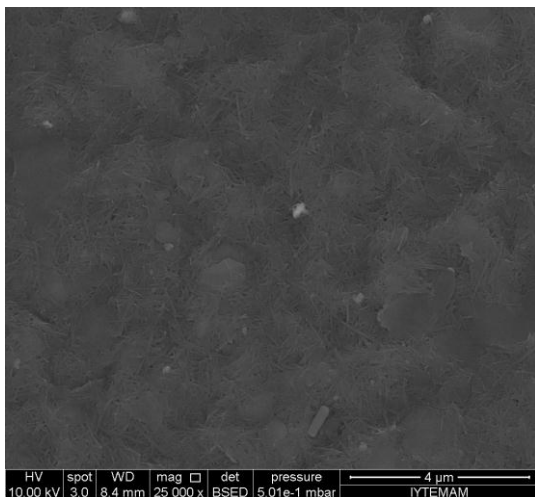
(e)
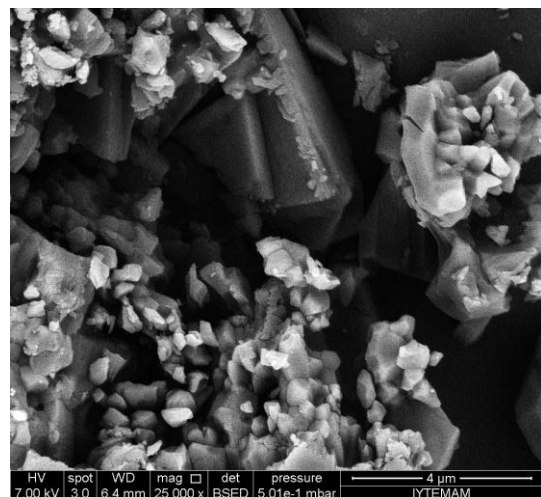
(f)

Figure 3.5. Typical SEM images of (a) Amberlite IRA400, (b) ZVI-modified Amberlite IRA400, (c) Amberlite IRA458, (d) ZVI-modified Amberlite IRA458, (e) Amberlite IRA67 and (f) ZVI-modified Amberlite IRA67 at 25000x magnification.

The nZVI and ZVI-modified/unmodified samples were also analyzed with EDX by randomly selected three regions on the solid surface. The average weight percent of elements formed during the synthesis are shown in Table 3.5 and 3.6. In terms of the table, the presence of C in EDX results could be due to the scattering of nZVI on carbon tapes. The presence of ZVI on the sorbent surface was followed by the Fe signals obtained.

Table 3.5 exhibits the EDX results of ZVI-modified/unmodified Diaion SK116 and Amberlite IRC50. In spite of the fact that the EDX results at low concentrations should be appreciated very carefully, it can be said that the resins Diaion SK116 and Amberlite IRC50 were successfully modified with Fe. The presence of Na and B is due to the use of $NaBH_4$ in the reduction of Fe(III). A typical EDX spectrum is shown in Figure 3.6.

(a)   (b)
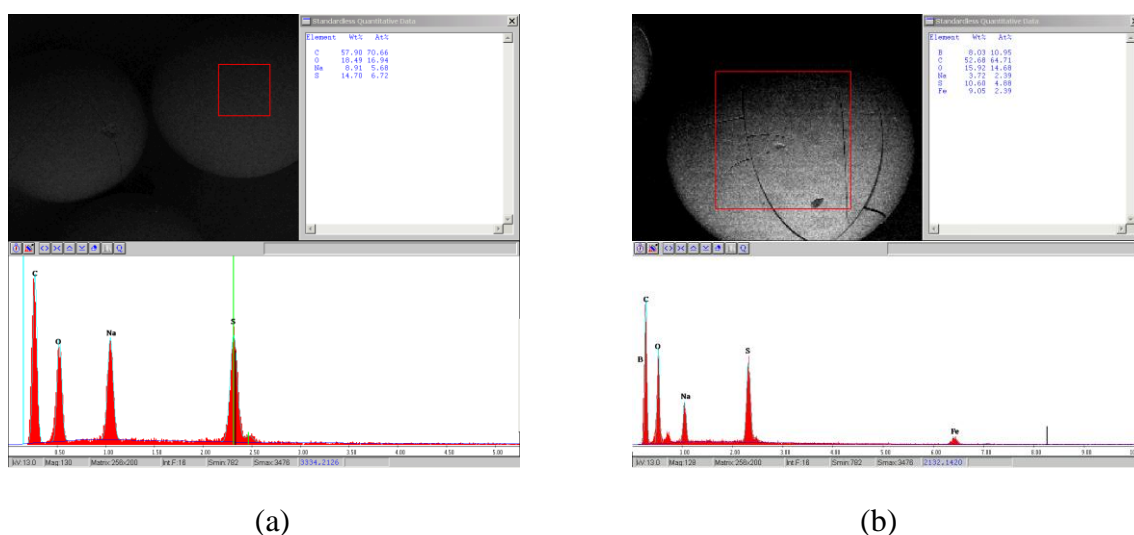
Figure 3.6. EDX spectra of (a) Diaion SK116 and (b) ZVI-modified Diaion SK116.

EDX results for ZVI-modified/unmodified Amberlite IRA400, Amberlite IRA458 and Amberlite IRA67 are shown in Table 3.6. EDX analysis showed the sorbent materials consisting small quantities of iron in addition to the matrix elements such as carbon and oxygen. The Fe content of the sorbents was again assumed to be the indication of successful modification of the resin surface.

Table 3.5. The average weight percent of elements obtained with EDX from the surface of nZVI and ZVI-modified/unmodified cation exchange resins (M: modified).

	nZVI		SK116		SK116 M		IRC50		IRC50 M	
Element	Wt (%)	At (%)	Wt (%)	At (%)	Wt (%)	At (%)	Wt (%)	At (%)	Wt (%)	At (%)
C K	22.3	41.5	57.9	70.7	52.7	64.7	74.7	79.4	61.8	69.7
O K	26.0	36.3	18.5	16.9	15.9	14.7	25.4	20.3	19.6	16.6
Na K	2.4	2.3	8.9	5.7	3.7	2.4	-	-	7.8	4.6
Cl K	0.8	0.6	-	-	-	-	-	-	-	-
S K	-	-	14.7	6.7	10.6	4.9	-	-	-	-
B K	-	-	-	-	8.0	10.9	-	-	6.4	8.1
Fe K	48.5	19.4	-	-	9.1	2.4	-	-	4.5	1.1

Table 3.6. The average weight percent of elements obtained with EDX from the surface of ZVI-modified/unmodified anion exchange resins (M: modified).

	IRA400		IRA400 M		IRA458		IRA458 M		IRA 67		IRA67 M	
Element	Wt (%)	At (%)	Wt (%)	At (%)	Wt (%)	At (%)	Wt (%)	At (%)	Wt (%)	At (%)	Wt (%)	At (%)
B K	-	-	8.8	11.8	-	-	9.0	13.4	-	-	8.3	12.0
C K	84.0	92.1	32.4	39.2	75.39	83.79	9.2	12.3	30.5	38.8	24.4	32.5
O K	4.6	3.7	47.3	42.9	15.17	12.66	60.2	60.7	51.6	49.3	52.7	50.0
Na K	-	-	7.8	4.9	-	-	17.7	12.4	17.9	11.9	13.5	9.2
Cl K	11.4	4.2	1.7	0.7	9.44	3.56	0.9	0.4	-	-	-	-
Fe K	-	-	2.1	0.6	-	-	2.9	0.9	-	-	1.1	0.3

The surface modification of ion exchange resins was also performed with NaOH which was supposed to precipitate iron as $Fe(OH)_3$ and FeOOH. The iron loading on the resin surface was not successful and also Fe^0 in the surface was not stable on the surface due to oxidation. Hence, NaOH was not used in the further experiments.

3.1.2.1.2. SEM/EDX of nZVI and ZVI-Modified Inorganic Substrates

Figure 3.7 demonstrates the SEM images of unmodified silica, alumina, titania and their ZVI-modified forms. As can be seen from the figure, some changes occurred in the surface morphology of silica and titania after modification with nZVI. A chain-like structure was obtained on both of the inorganic substrates. On the other hand, no chain-like can be seen on the surface of alumina after ZVI modification, instead ZVI particles were formed on the surface. This behavior demonstrates the efficiency of alumina in distributing the individual ZVI particles on the surface. In all substrates, the modified particles developed a gray color after modification process due to the presence of black iron particles.

The EDX results of ZVI-modified/unmodified inorganic substrates are displayed in Table 3.7. Although the EDX results at low concentrations should be evaluated very carefully, it can be said that the inorganic substrates (silica, alumina and titania) were successfully modified with Fe.
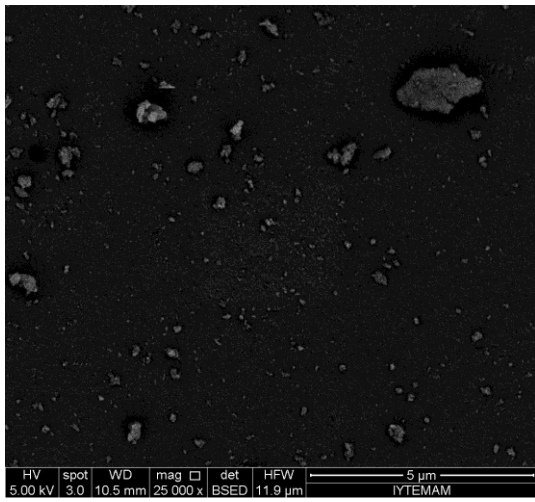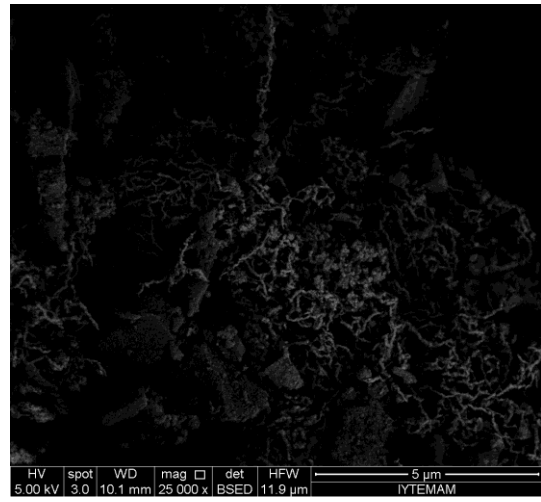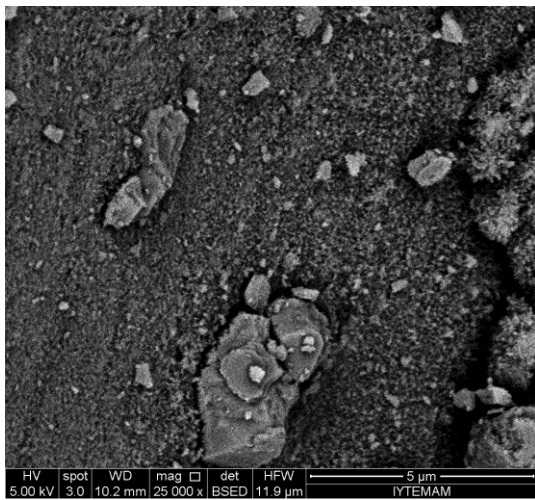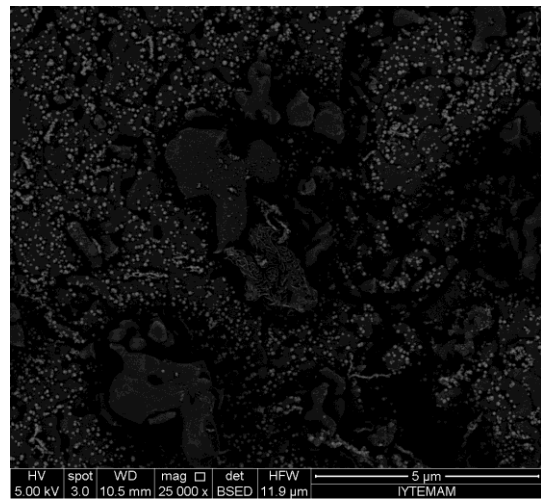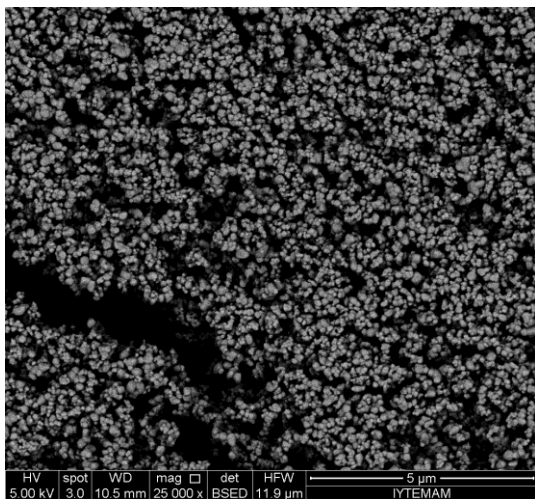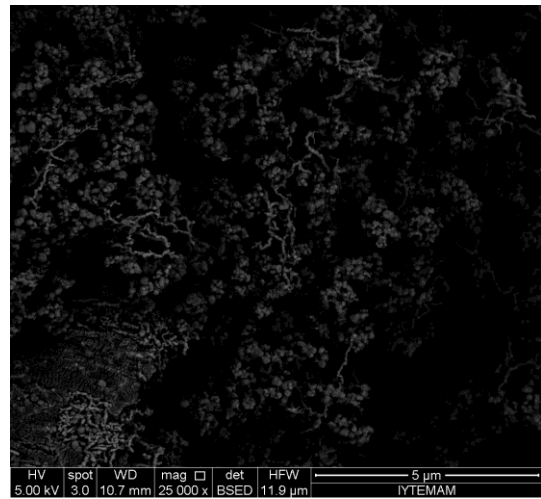
Figure 3.7. Typical SEM images of (a) unmodified silica, (b) ZVI-modified silica, (c) unmodified alumina, (d) ZVI-modified alumina, (e) unmodified titania and (f) ZVI-modified titania at 25000x magnification.

Table 3.7. The average weight percent of elements obtained with EDX from the surface of the ZVI-modified/unmodified inorganic substrates.

Element	silica		ZVI-modified silica		alumina		ZVI-modified alumina		titania		ZVI-modified titania	
	Wt (%)	At (%)	Wt (%)	At (%)	Wt (%)	At (%)	Wt (%)	At (%)	Wt (%)	At (%)	Wt (%)	At (%)
B K	-	-	3.2	7.1	-	-	1.4	2.7	-	-	1.6	5.0
C K	1.0	1.6	16.3	32.0	5.1	8.5	8.1	13.7	2.7	6.3	2.0	5.4
O K	52.4	67.0	19.0	28.1	41.5	51.8	34.8	44.0	31.4	55.9	17.9	37.0
Na K	-	-	0.3	0.3	0.8	0.7	0.6	0.5	-	-	0.2	0.3
Si K	44.6	29.4	16.1	13.5	-	-	-	-	-	-	-	-
Al K	-	-	-	-	52.6	39.0	49.2	37.0	-	-	-	-
Ti K	-	-	-	-	-	-	-	-	65.9	37.8	60.6	41.9
Fe K	-	-	45.1	19.1	-	-	5.9	2.1	-	-	17.7	10.5

3.1.2.2. Thermo Gravimetric Analysis (TGA) of nZVI

Thermo gravimetric analysis measures the amount and rate of change in the weight of a material as a function of temperature or time in a controlled atmosphere. Measurements are performed in order to determine the composition of materials and to understand their thermal stability at high temperatures. In the present study, TGA was applied in order to see the effect of heat on the structure of the nZVI. TGA analysis of nZVI is presented in Figure 3.8 and the results demonstrated a 7% weight loss at 190 ^{o}C due to the loss of residual water from nZVI whereas a ~5% weight gain was observed after 400 ^{o}C which can be attributed to the oxidation of nZVI.
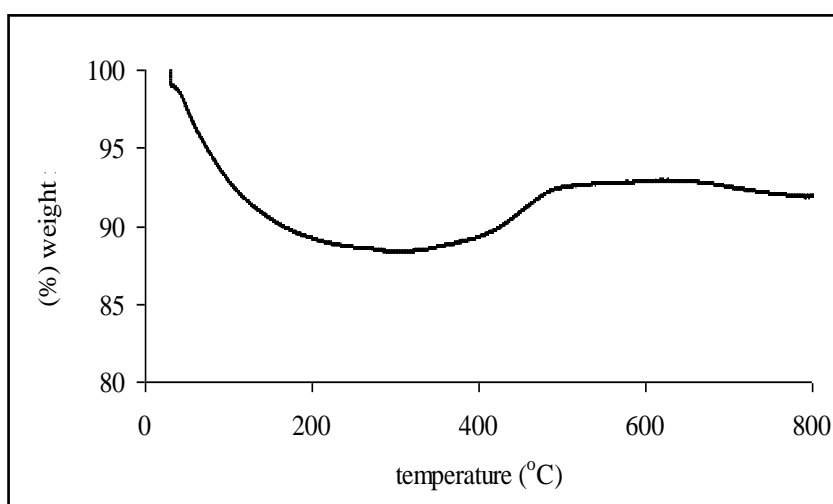
Figure 3.8. TGA curve of nZVI

3.1.2.3. X-ray Diffraction of nZVI

The XRD pattern of nZVI under ambient conditions is presented in Figure 3.9. According to the figure, iron is mainly present in its Fe^{0} state showing its characteristic diffraction line at a 2-theta value of 44.9^{o}.
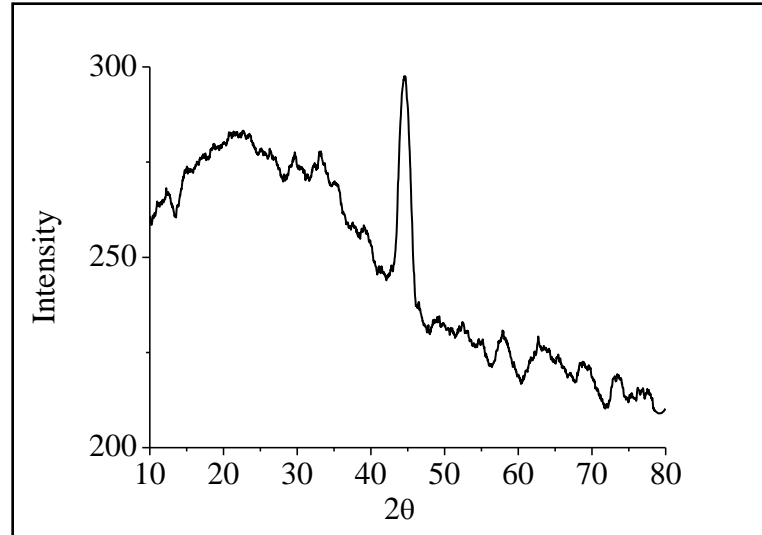
Figure 3.9. XRD pattern of nZVI

3.1.2.4. Brunauer-Emmett-Teller (BET) Surface Area Analysis of nZVI

The specific surface area of nZVI was measured by BET-N_2 method. The BET surface area, average pore width and pore volume of nZVI were 31.1 m^2g^{-1}, 35.9 ^oA and 0.028 cm^3g^{-1}, respectively. This finding is compatible with the literature (Choe et al. (2000) and Kanel et al. (2005)).

3.1.2.5. Zeta Potential Measurements of nZVI

In order to identify the point of zero charge (PZC) of nZVI, the zeta potential was measured for a series of suspensions in the pH range 6.0 and 10.0. The measurements were performed using Malvern Zetasizer Nanoseries Nano-ZS instrument. The results, given in Figure 3.10, indicate that the PZC occurred within the pH value of 6.8.
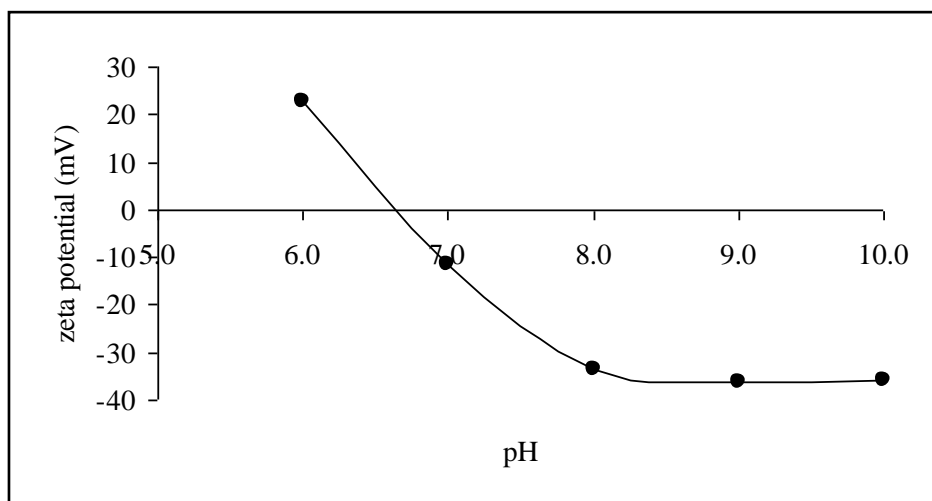
Figure 3.10. Effect of pH on zeta potential of nZVI

3.1.2.6. Particle Size Measurements of nZVI

In addition to the characterization techniques aforementioned, the particle size of nZVI was also measured with a particle size analyzer and the particle size of nZVI was found as 84.5 nm. This finding shows that the synthesized zero-valent iron is in the range of nano size.

3.1.3. Characterization of ZVC and ZVC-modified/unmodified Sorbents

3.1.3.1. Scanning Electron Microscopy (SEM)/ Energy Dispersive X-ray Spectroscopy (EDX)

ZVC and ZVC-modified sorbents were first characterized with SEM/EDX. The SEM images of ZVC and ZVC-modified sorbents are illustrated in Figure 3.11 and 3.12. As seen from Figure 3.11a, ZVC particles seem to be in an agglomerated form. The SEM images of ZVC-modified/unmodified Diaion SK116 and Amberlite IRC50 are also displayed in the same figure. According to the figure, the surface morphology seemed to change much after modification for both of the modified resins and spots were observed on the surface of ZVC-modified Diaion SK116 (Figure 3.11d) whereas agglomeration of ZVC was observed on the surface of ZVC-modified Amberlite IRC50

(Figure 3.11f). In addition, the modified particles develop a black color after processing due to the presence of copper.

ZVC-modified/unmodified Amberlite IRA458, Amberlite IRA67 and alumina were also characterized with SEM and the SEM images are shown in Figure 3.12. The surface morphology changed again after the modification process. A similar behavior with Diaion SK116 was observed for Amberlite IRA458 representing spots on the resin surface (Figure 3.12b). Nevertheless, ZVC-modified Amberlite IRA67 or alumina coagulated (Figure 3.12d and 3.12f). A color change was also observed on the surface indicating the success of modification.
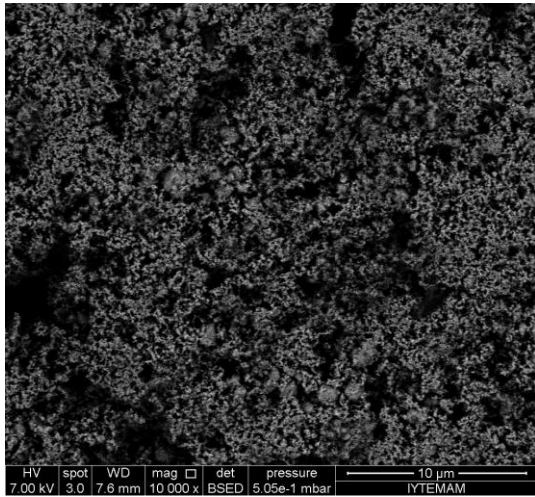
(a)
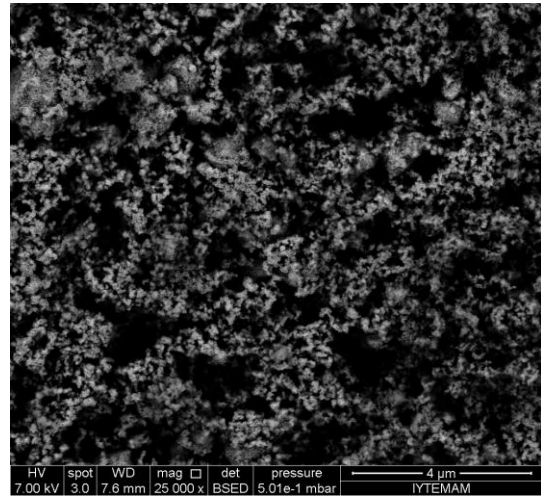
(b)
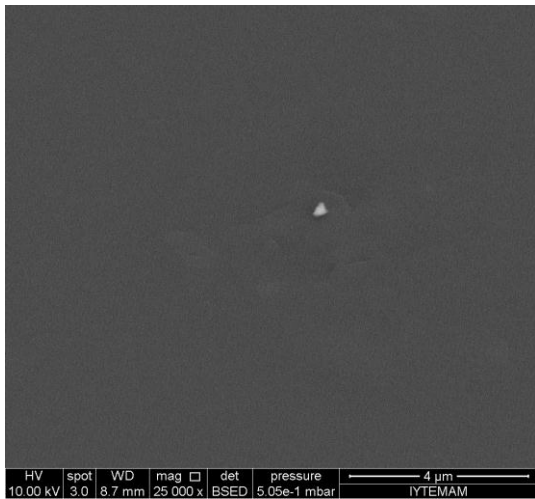
(c)
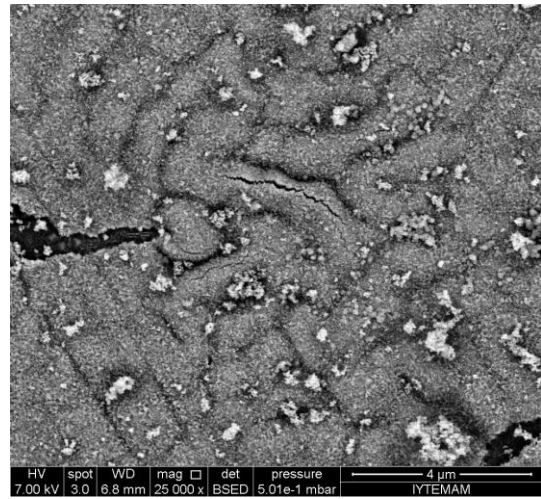
(d)
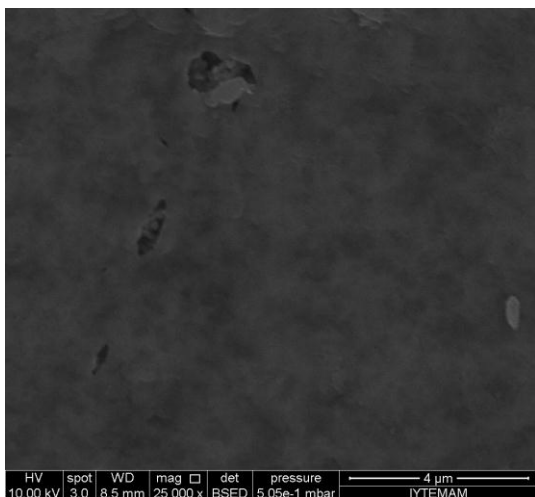
(e)
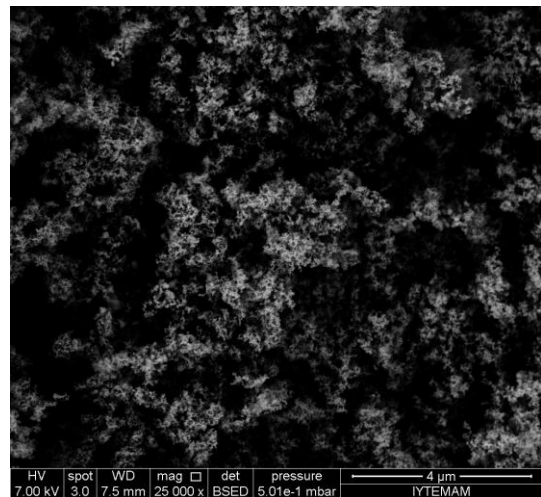
(f)

Figure 3.11. Typical SEM images of (a) ZVC (10000x), (b) ZVC (25000x), (c) Diaion SK116, (d) ZVC-modified Diaion SK116, (e) Amberlite IRC50 and (f) ZVC-modified Amberlite IRC50 at 25000x magnification.
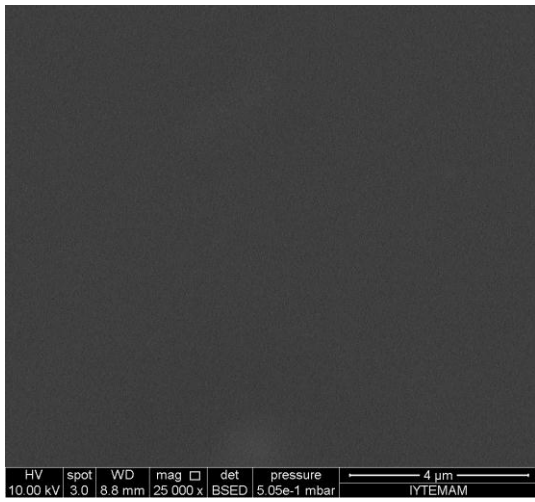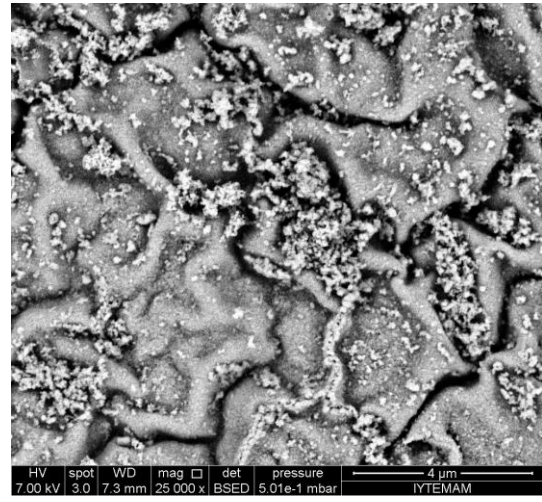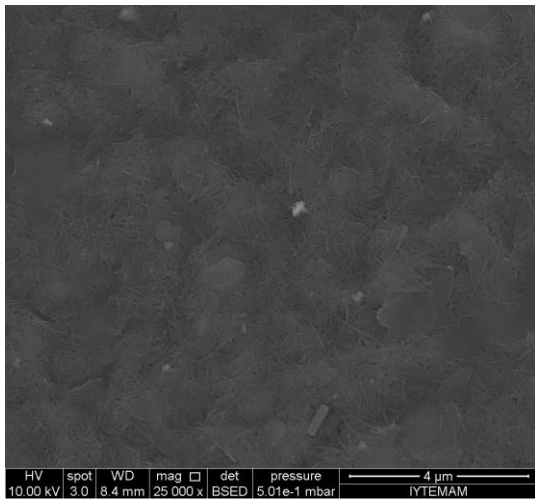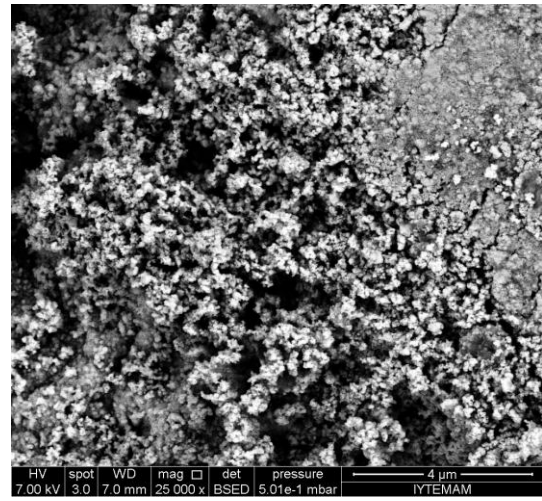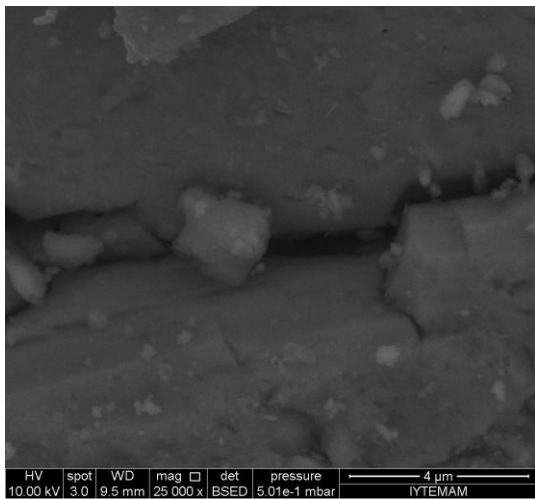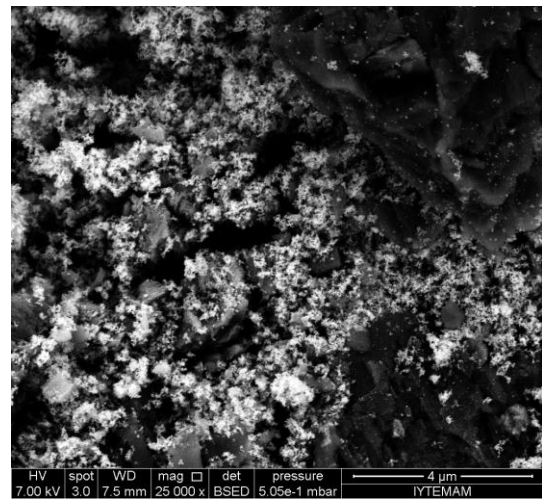
Figure 3.12. Typical SEM images of (a) Amberlite IRA458, (b) ZVC-modified Amberlite IRA458, (c) Amberlite IRA67, (d) ZVC-modified Amberlite IRA67, (e) alumina and (f) ZVC-modified alumina at 25000x magnification.

EDX analysis was also performed for ZVC and ZVC-modified/unmodified samples by randomly selected three regions on the solid surface. The average weight percent of elements formed during the synthesis are demonstrated in Table 3.8 and 3.9. The presence of ZVC on the sorbent surface was followed by the Cu signals obtained. It is demonstrated in Table 3.8 that ZVC was successfully synthesized by liquid-phase reduction method although quantitative results cannot be achieved with EDX.

The EDX results of ZVC-modified/unmodified Diaion SK116 and Amberlite IRC50 are also demonstrated in Table 3.8. Although the EDX results at low concentrations should be evaluated very carefully, it can be said that the modification of Diaion SK116 and Amberlite IRC50 with ZVC were successfully performed. The presence of Na and B is due to the use of $NaBH_4$ in the reduction of Cu(II).

The average weight percent of ZVC-modified/unmodified Amberlite IRA458, Amberlite IRA67 and alumina is presented in Table 3.9. It is clearly seen that the modification of alumina with ZVC was successfully performed with ZVC.

Table 3.8. The average weight percent of elements obtained with EDX from the surface of the ZVC and ZVC-modified/unmodified cation exchange resins (M: modified).

	ZVC		SK116		SK116 M		IRC50		IRC50 M	
Element	Wt (%)	At (%)	Wt (%)	At (%)	Wt (%)	At (%)	Wt (%)	At (%)	Wt (%)	At (%)
B K	1.1	5.4	-	-	3.1	10.3	-	-	13.3	17.1
C K	-	-	57.9	70.7	6.0	18.1	74.7	79.4	56.4	65.1
O K	3.2	10.9	18.5	16.9	8.4	19.1	25.3	20.6	11.9	10.2
Na K	1.3	3.0	8.9	5.6	3.7	5.7	-	-	9.1	5.5
Cl K	0.03	0.05	14.7	6.7	4.4	4.4	-	-	-	-
Cu K	94.4	80.7	-	-	74.5	42.4	-	-	9.4	2.1

Table 3.9. The average weight percent of elements obtained with EDX from the surface of the ZVC-modified/unmodified anion exchange resins and alumina (M: modified).

	IRA458		IRA458 M		IRA67		IRA67 M		Alumina		Alumina M	
Element	Wt (%)	At (%)	Wt (%)	At (%)	Wt (%)	At (%)	Wt (%)	At (%)	Wt (%)	At (%)	Wt (%)	At (%)
Al K	-	-	-	-	-	-	-	-	52.6	39.0	43.7	41.2
B K	-	-	-	-	-	-	0.9	4.3	-	-	1.6	3.8
C K	75.4	83.8	2.9	10.4	30.5	38.8	1.7	6.9	5.1	8.5	-	-
O K	15.2	12.7	9.5	25.1	51.6	49.3	3.3	10.3	41.5	51.8	27.0	42.9
Na K	-	-	5.2	9.6	17.9	11.9	3.5	7.5	0.8	0.7	1.3	1.5
Cl K	9.4	3.6	0.4	0.5	-	-	0.3	0.4	-	-	-	-
Cu K	-	-	81.9	54.5	-	-	90.3	70.6	-	-	26.4	10.6

3.1.3.2. X-ray Diffraction of ZVC

Characterization of ZVC is also performed with X-ray diffractometer and the XRD pattern of ZVC under ambient conditions is demonstrated in Figure 3.13. According to the figure, three main peaks (43°, 50° and 75°) indicating Cu^0 (its characteristic diffraction line at a 2-theta value) were observed whereas the weak XRD peaks detected between 35° and 40° represented the presence of thin layers of copper oxides.
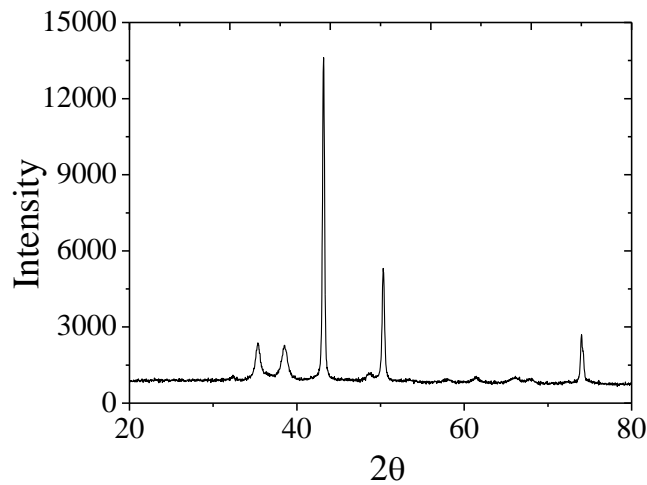
Figure 3.13. XRD pattern of ZVC

3.1.3.3. Zeta Potential Measurements of ZVC

To demonstrate if the surface charge of ZVC is changed with pH, zeta potential is measured. Figure 3.14 illustrates the variation of surface charge of ZVC with pH and the PZC thus obtained is at 7.3.
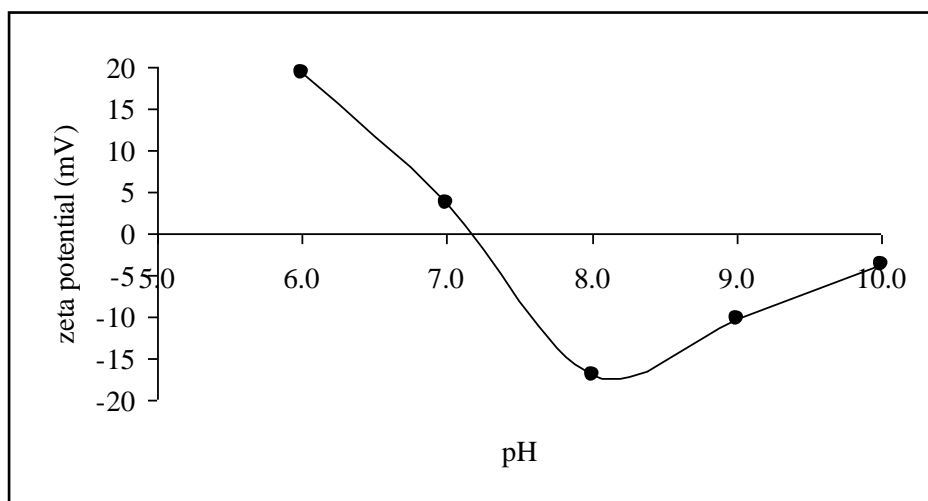
Figure 3.14. Effect of pH on zeta potential of ZVC

3.1.3.4. Particle Size Measurements of ZVC

The particle size of ZVC was also determined by using Malvern Zetasizer Nanoseries particle size analyzer and the particle size of ZVC was found as 375.4 nm. This finding shows that the synthesized zero-valent copper is in the range of micron size.

3.2. Determination of Mercury Species

Mercury occurs principally in two different forms in environmental samples: inorganic mercury (Hg^{2+}) and organic mercury (CH_3Hg^+). Among these two forms, CH_3Hg^+ is more toxic than Hg^{2+}. Therefore, it is of great importance to monitor mercury species separately instead of total mercury.

3.2.1. Calibration Plot for Hg^{2+}

Absorbance versus concentration plot was obtained for Hg^{2+} as shown in Figure 3.15. The calibration curve was linear at least up to 100 μgL^{-1}. The limit of detection

(LOD) based on 3s (3 times the standard deviation above the blank value) was found as 0.20 μgL^{-1}.
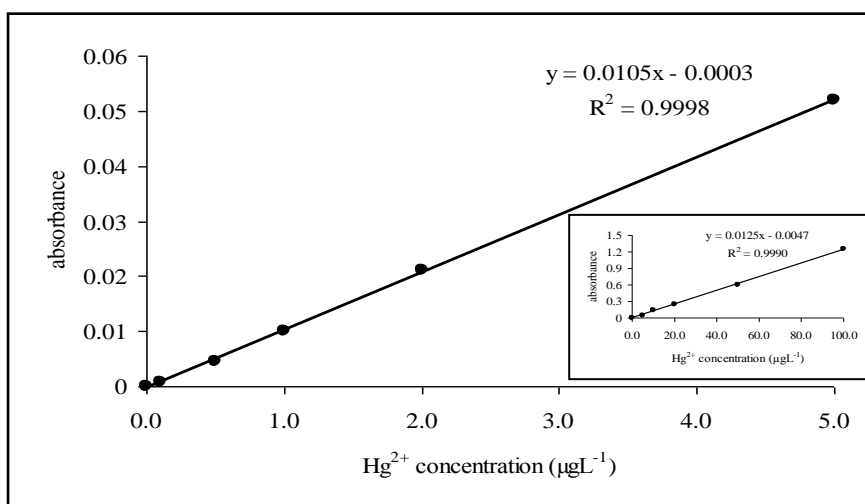
Figure 3.15. Calibration curve of Hg^{2+}, (y=0.0105x-0.0003, R^2= 0.9998), (inset: concentration range: 5- 100 μgL^{-1}, y= 0.0125x-0.0047, R^2= 0.9990) (500 μL of 5% (m/v) $SnCl_2$, 5.0 mL sample volume).

3.2.2. Calibration Plot for CH_3Hg^+

An oxidation step is necessary for CH_3Hg^+ determination since it cannot be measured directly by CVAAS. Two oxidizing agents/solutions namely, potassium persulfate ($K_2S_2O_8$) (Hintelmann and Wilken 1993, Wuilloud et. al 2002b, Burguera et. al 1999), potassium bromate ($KBrO_3$)/bromide mixture (Bloxham et. al 1996, Ramalhosa et. al 2001), UV radiation as well (Falter and Schöler 1994, Krishna et. al 2005) have been used for the oxidation of methyl mercury. In this work, a mixture of KBr-KBrO$_3$ (0.5%- 0.14% (m/v), respectively) in 2 M HCl was firstly tried and no signal was obtained for CH_3Hg^+ determination. High amounts of bromine (Br_2) gas were also formed during the analysis. $K_2S_2O_8$ (3% (m/v)) was then used for determination and the calibration curve obtained is shown in Figure 3.16. The signals were nearly the same with Hg^{2+} signals and the calibration curve was again linear at least up to 100 μgL^{-1}. The limit of detection (LOD) based on 3s (3 times the standard deviation above the blank value) was found as 0.20 μgL^{-1}.
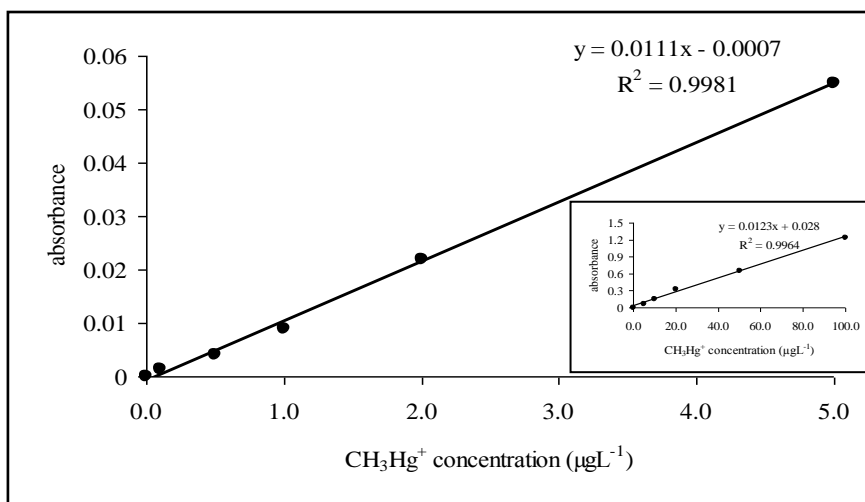
Figure 3.16. Calibration curve of CH_3Hg^+, (y=0.0111x-0.0007, R^2= 0.9981), (inset: concentration range: 5-100 μgL^{-1}, y= 0.0123x+0.028, R^2= 0.9964) (500 μL of 5% (m/v) $SnCl_2$, 5.0 mL sample volume).

In order to see the matrix effect of $K_2S_2O_8$ on Hg^{2+} signal, standards were prepared from 0.2 μgL^{-1} to 5.0 μgL^{-1} in 2.8 M HNO_3 and analyzed by CVAAS. As seen from Figure 3.17, Hg^{2+} signal did not change with the addition of $K_2S_2O_8$ and very similar signals were obtained for both species.
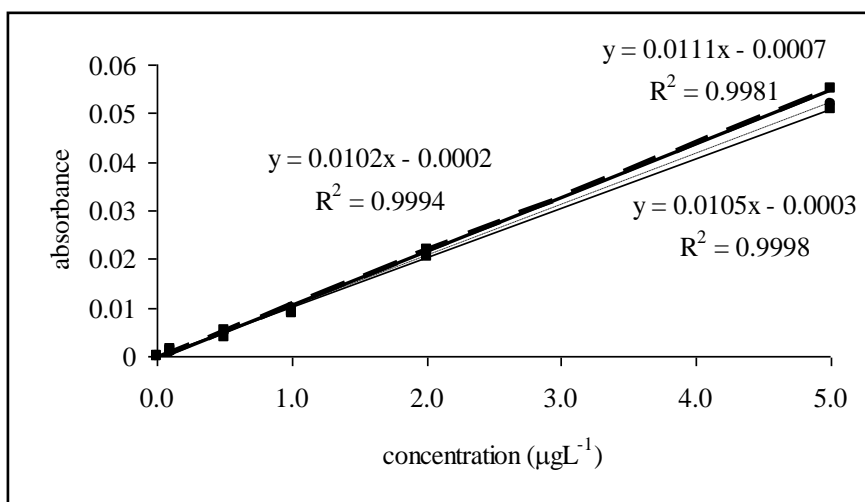
Figure 3.17. Calibration curve of (■) CH_3Hg^+, (y=0.0111x-0.0007, R^2= 0.9981), (●) Hg^{2+} (y=0.0105x-0.0003, R^2= 0.9998), and (▲) Hg^{2+} in 3% (m/v) $K_2S_2O_8$ (y=0.0102x-0.0002, R^2= 0.9994) (500 μL of 5% (m/v) $SnCl_2$, 5.0 mL sample volume).

3.3. Sorption Studies with Synthesized Sorbents

The form of mercury is sensitive to redox conditions and pH of the natural matrices. Depending also on the presence of other ions in the solution, mercury can be found in different forms. The chemical speciation analysis of aqueous mercury ions under different pH conditions was performed using visual MINTEQ software. The input conditions such as temperature, pH, ionic strength etc. were adjusted at suitable conditions and the chemical speciation diagram is given in Figure 3.18. According to the figure, up to pH 3, the dominant chemical form of Hg in aqueous media is Hg^{2+}. Around pH 3, $HgOH^+$ can also be found at appreciable concentrations in addition to Hg^{2+} and $Hg(OH)_2$ and above pH 3, $Hg(OH)_2$ is the dominant form.
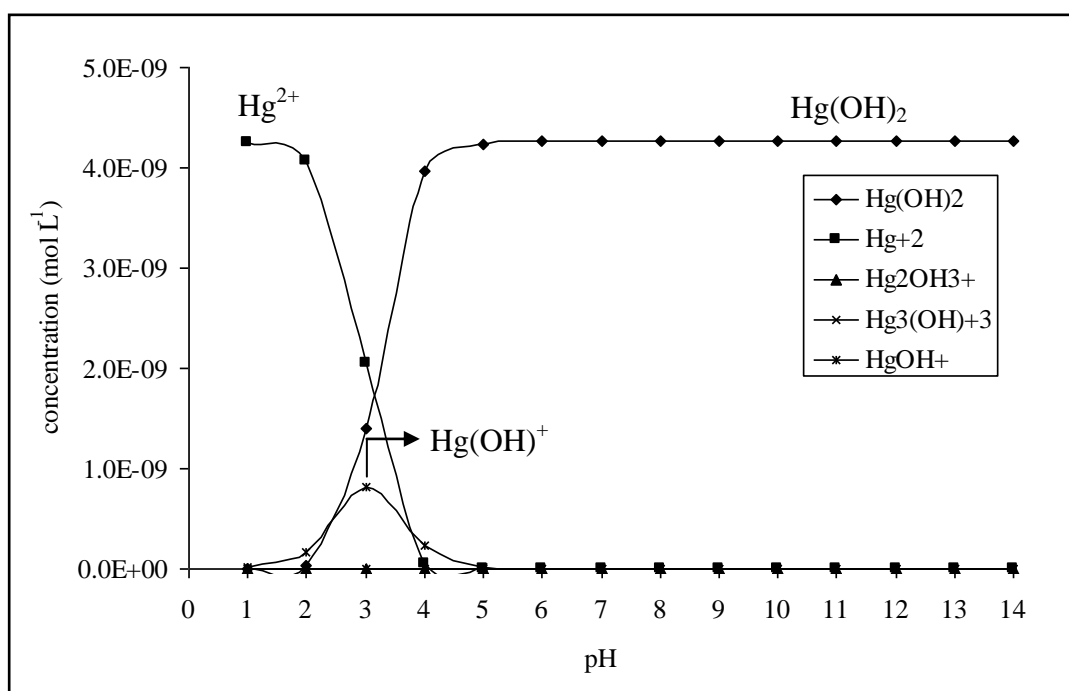
Figure 3.18. Hg^{2+} speciation diagram by using MINTEQ program for Hg(II).

3.3.1. Sorption with Silica-Based Sorbents

3.3.1.1. Effect of Solution pH

3.3.1.1.1. Effect of pH with 3-MPTMS-Silica and Silica

Sorption characteristics of Hg^{2+} and CH_3Hg^+ by silica, sol-gel silica, 3-MPTMS-silica, sol gel-3-MPTMS, 3-MPTMS-sol gel, 3-APTES-silica and 3-APTES-3-MPTMS-silica are given in Figures 3.19- 3.26.

Sorption capacity of the sorbents was examined at different solution pHs since sample acidity plays an important role in sorption. It affects the electrostatic attraction between the analyte and the functional groups on the surface, the complexation reaction between the metal ions in solution and ligands immobilized on the surface, etc. For this purpose, the initial experiments focused on the investigation of sorption pH with each sorbent. In order to evaluate the effect of pH on sorption, the pH of solutions were adjusted between 1.0 and 10.0.

As can be seen from Figure 3.19, silica exhibited a low affinity in acidic conditions; only about 45% of Hg^{2+} was retained onto silica. To the contrary, a quantitative sorption (>95%) was found for Hg^{2+} at pH's 5.0, 7.0 and 10.0.

The capacity of modified sorbents to remove metal ions from various media depends greatly also on the choice of ligand. Sulfur donor atoms covalently attached onto the silica surface show a particularly high selectivity for mercury atoms. At low pH values, the strong sulfur atoms were the only available adsorption sites which increased mercury complexation. In Figure 3.19, it was observed that Hg^{2+} accumulation on 3-MPTMS-silica was >98% and the sorption of Hg^{2+} on 3-MPTMS-silica was independent of pH.
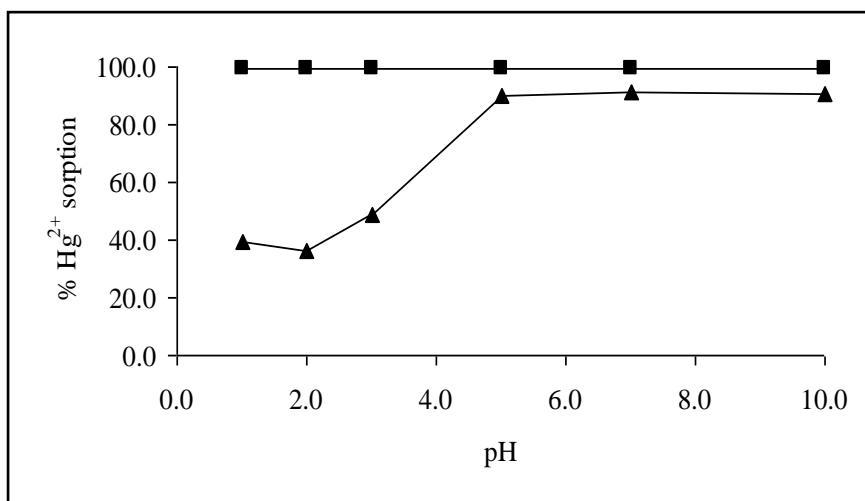
Figure 3.19. Hg^{2+} sorption as a function of pH on (▲) unmodified silica (reference) and (■) 3-MPTMS-silica (10.0 mL of 500.0 μgL^{-1} solution, sorbent amount: 10.0 mg, shaking time: 30 min, n=3).

A similar trend was also observed for CH$_3$Hg$^+$. As shown in Figure 3.20, at lower pH values CH$_3$Hg$^+$ uptake onto silica was low whereas the retention of CH$_3$Hg$^+$ increased at pH 7.0 and 10.0. However, when -SH functional group was attached onto silica surface, the removal of CH$_3$Hg$^+$ was again independent of pH and quantitative at all values.
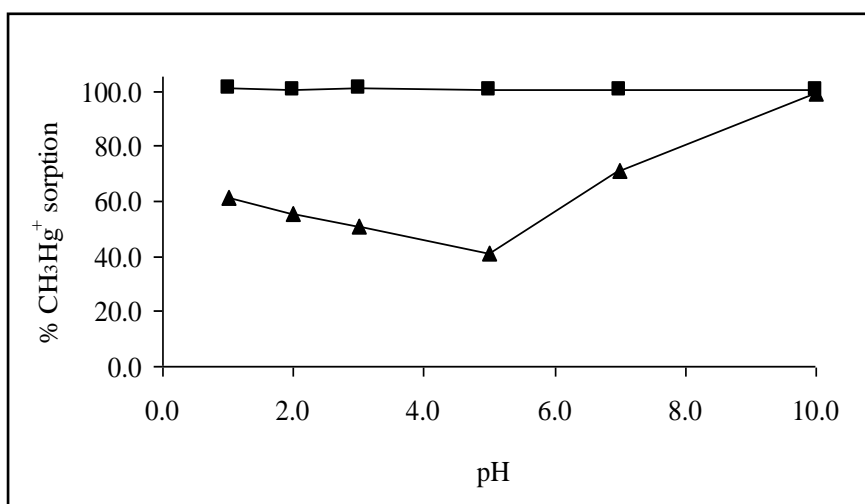
Figure 3.20. CH$_3$Hg$^+$ sorption as a function of pH on (▲) unmodified silica (reference) and (■) 3-MPTMS-silica (10.0 mL of 500.0 μgL^{-1} solution, sorbent amount: 10.0 mg, shaking time: 30 min, n=3).

3.3.1.1.2. Effect of pH with Sol-Gel Silica, 3-MPTMS-Sol Gel and 3-MPTMS-Sol Gel

The modification thiol group via sol-gel synthesis was performed in two different ways. In the first method, MPTMS was added into the silica prepared through sol-gel synthesis and named as sol gel-3-MPTMS. In the second method, the addition of this reagent was performed during the sol-gel synthesis and was known as 3-MPTMS-sol gel. As seen from Figure 3.21, Hg^{2+} uptake on sol-gel silica was again less at low pH's but it increased to ~90% at higher pH values. The removal of Hg^{2+} with mercapto resins was again high at all pH values.
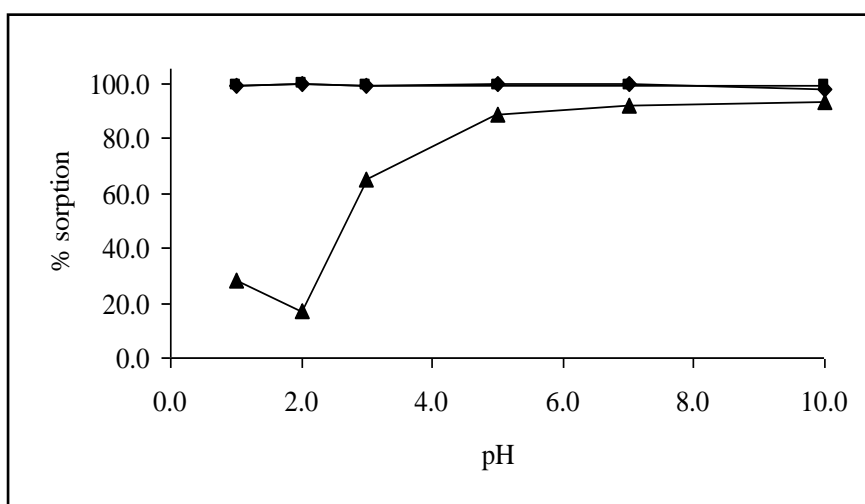
Figure 3.21. Hg^{2+} sorption as a function of pH on (▲) sol-gel silica (reference), (■) sol gel-3-MPTMS and (♦) 3-MPTMS-sol gel (10.0 mL of 500.0 μgL^{-1} solution, sorbent amount: 10.0 mg, shaking time: 30 min, n=3).

The retention of CH_3Hg^+ on sol-gel silica, sol gel-3-MPTMS and 3-MPTMS-sol gel is demonstrated in Figure 3.22. According to the figure, the efficiency of CH_3Hg^+ sorption was quantitative (>99%) at all pH values when sol gel-3-MPTMS or 3-MPTMS-sol gel resin was used as sorbent for removal. However, the removal of CH_3Hg^+ on sol-gel silica was lower than 80% at pH 1.0 to 3.0, but it increased to higher values at pH >5.0.
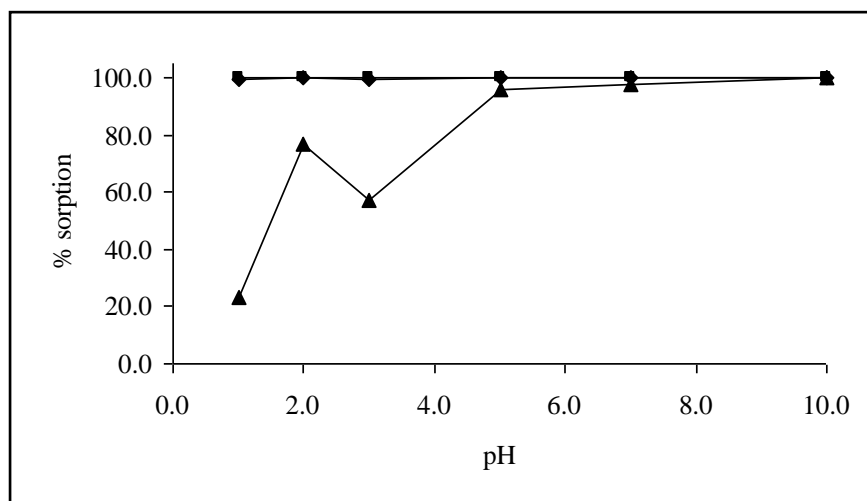
Figure 3.22. CH_3Hg^+ sorption as a function of pH on (▲) unmodifed sol-gel silica (reference), (■) sol gel-3-MPTMS and (♦) 3-MPTMS-sol gel (10.0 mL of 500.0 μgL^{-1} solution, sorbent amount: 10.0 mg, shaking time: 30 min, n=3).

3.3.1.1.3. Effect of pH with Silica and 3-APTES-Silica

Figure 3.23 demonstrates the sorption behavior of silica and 3-APTES-silica towards Hg^{2+}. Lower sorption was obtained for 3-APTES-silica at pH 1.0 and 2.0 which could be due to the protonation of the nitrogen donor atom and this could inhibit its binding to Hg^{2+} ion. At pH values lower than 3.0, the major species of Hg(II) ions are Hg^{2+} cations, while $Hg(OH)_2$ species dominate at pH values higher than 3.0. The binding ability of the protonated ligand with Hg^{2+} cations is lower than that of non-protonated molecule with $Hg(OH)_2$ at pH values higher than 3.0. As can be concluded from the figure, when the amine group on silica surface was protonated, $-NH_2$ acted as an electrostatic barrier inside the silica thus causing an electrostatic repulsion with the entering proton and finally, a low sorption was obtained for Hg^{2+}. This effect is less pronounced in unmodified silica because the positive charge is randomly distributed which results less electrostatic repulsion.

The sorption percentage of CH_3Hg^+ on silica and 3-APTES-silica is shown in Figure 3.24. It was observed that sorption was low at pH up to 10.0 for both sorbents and ~99% adsorption was obtained when the pH was adjusted to 10.0. As this and the previous figure demonstrate $-NH_2$ is not as selective as $-SH$ groups towards Hg^{2+} and CH_3Hg^+.

71
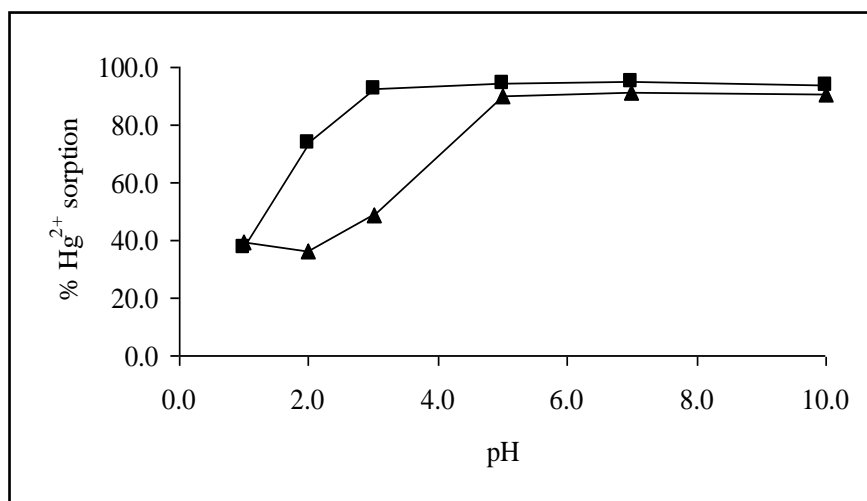
Figure 3.23. Hg^{2+} sorption as a function of pH on (▲) unmodified silica (reference) and (■) 3-APTES-silica (10.0 mL of 500.0 μgL^{-1} solution, sorbent amount: 10.0 mg, shaking time: 30 min, n=3).
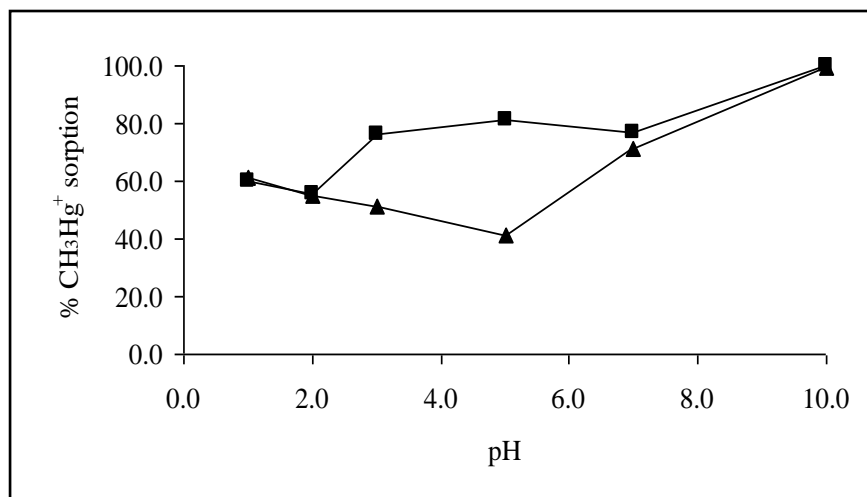
Figure 3.24. CH_3Hg^+ sorption as a function of pH on (▲) unmodified silica (reference) and (■) 3-APTES-silica (10.0 mL of 500.0 μgL^{-1} solution, sorbent amount: 10.0 mg, shaking time: 30 min, n=3).

3.3.1.1.4. Effect of pH with Silica and 3-APTES-3-MPTMS-Silica

In addition to the modification of silica only with –SH or –NH$_2$ group, silica gel was also modified with both of these groups as explained in Section 2.4.6. The results of the sorption experiments are shown in Figure 3.25. The sorption behavior of mixed sorbent prepared physically with –SH modified and –NH$_2$ modified silicas is also demonstrated in the following figure. It can be concluded from the figure that the

sorption of Hg^{2+} on modified silica was quantitative (>99%) for both sorbents and independent of pH.
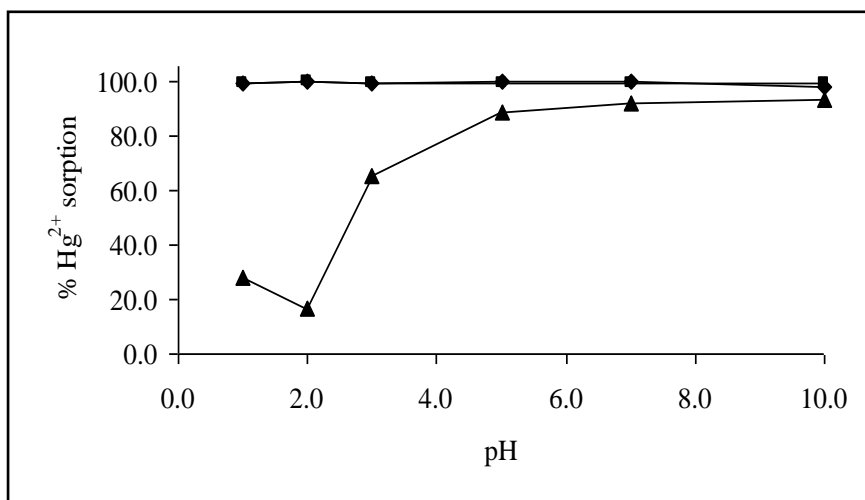
Figure 3.25. Hg^{2+} sorption as a function of pH on (▲) unmodified silica (reference), (■) 3-APTES-3-MPTMS-silica and (♦) 3-APTES-3-MPTMS-silica (physically mixed) (10.0 mL of 500.0 μgL^{-1} solution, sorbent amount: 10.0 mg, shaking time: 30 min, n=3).

A similar trend was also observed for CH_3Hg^+ removal. As can be seen from Figure 3.26, CH_3Hg^+ sorption was >99% at all pH's and independent of pH.
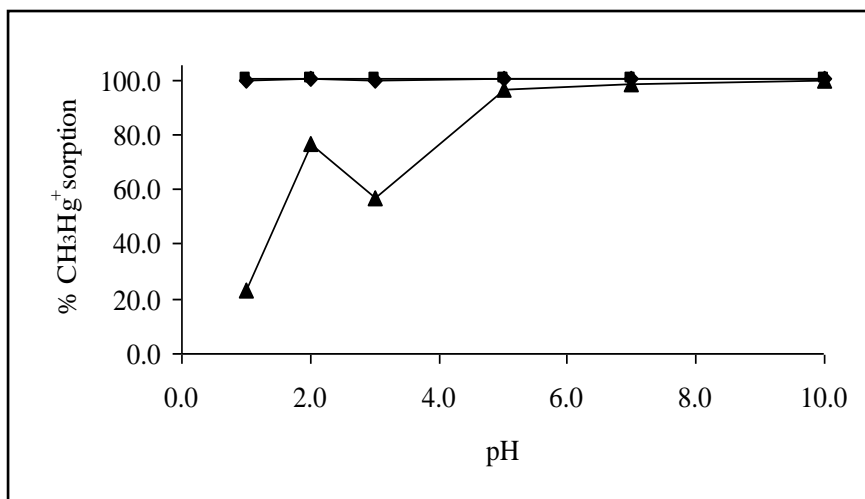
Figure 3.26. CH_3Hg^+ sorption as a function of pH on (▲) silica (reference), (■) 3-APTES-3-MPTMS-silica and (♦) 3-APTES-3-MPTMS-silica (physically mixed) (10.0 mL of 500.0 μgL^{-1} solution, sorbent amount: 10.0 mg, shaking time: 30 min, n=3).

At the studied conditions (10.0 mL of 500.0 μgL^{-1} solution, sorbent amount: 10.0 mg), even silica and sol-gel silica showed a high sorption of Hg^{2+}/CH_3Hg^+ at high pH's whereas the sorption percentage was lower than 45% at low pH's. Nevertheless, all of the –SH or $–NH_2$ modified silica-based sorbents demonstrated almost quantitative (>98%) sorption and this property was a big advantage of surface functionalization of silica gel with these groups. However, it is known that Hg binds strongly to thiol groups (soft base) as it is a soft acid. Due to the high selectivity and binding affinity exhibited by thiol groups towards mercury ions, thiol-modified sorbent is generally preferred for the removal of mercury species from aqueous media. Hence, 3-MPTMS-silica was used for further studies because of its simple preparation and ease of operation.

3.3.1.2. Effect of Sorbent Amount (Solid/Liquid Ratio)

As explained in section 2.7.1.2, the optimum amount of the sorbent for maximum take up was determined by increasing the amount of 3-MPTMS-silica added into 10.0 mL of 500.0 μgL^{-1} Hg^{2+} and 500.0 μgL^{-1} CH_3Hg^+. Figure 3.27 and Figure 3.28 demonstrate the sorption behavior of the two mercury species with changing amount of the sorbent. As can be seen from the figures, quantitative sorption is achievable for both Hg^{2+} and CH_3Hg^+ even with 5.0 mg sorbent for 10.0 mL solution. Still, a sorbent amount of 10.0 mg was chosen to guarantee the quantitative sorption.
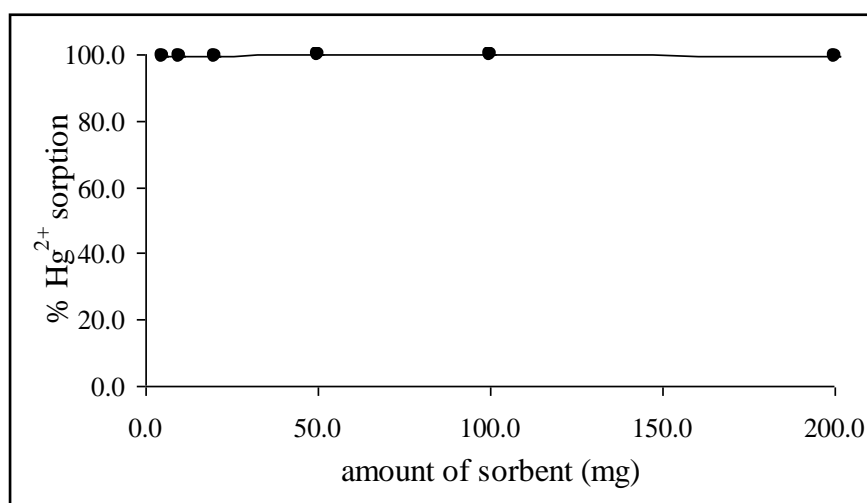
Figure 3.27. Effect of sorbent amount on Hg^{2+} sorption at pH 7.0 in 10.0 mL of 500.0 μgL^{-1} solution, shaking time: 30 min, (n=3).
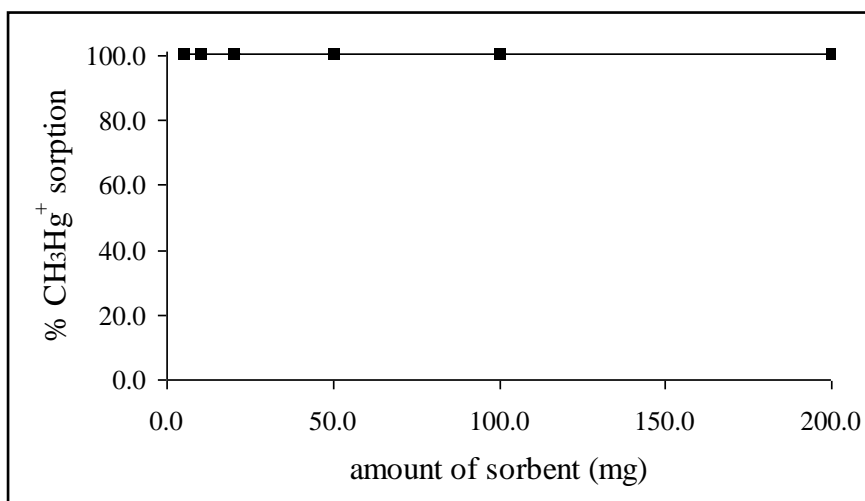
Figure 3.28. Effect of sorbent amount on CH_3Hg^+ sorption at pH 7.0 in 10.0 mL of 500.0 μgL^{-1} solution, shaking time: 30 min, (n=3).

3.3.1.3. Effect of Shaking Time

The sorption of Hg^{2+} and CH_3Hg^+ by 3-MPTMS-silica against time was studied keeping the other parameters constant in order to find out the time necessary to reach the sorption equilibrium. The percentage of sorption was determined at different time intervals ranging from 1 to 90 min as explained in section 2.7.1.3. Figure 3.29 represents the percent sorption of Hg^{2+} versus shaking time. According to the figure, the sorption of Hg^{2+} on 3-MPTMS-silica was very fast and quantitative sorption (>99%) was obtained even in 1 min. This graph also implies that the active donor atom S on the modified silica gel surface is so oriented that its accessibility is so easy and it causes a fast interaction with Hg^{2+}. However, 30 min shaking time was chosen in order to be on the safe side to have quantitative sorption.

A similar trend was also observed for CH_3Hg^+ and Figure 3.30 indicates the effect of shaking time on CH_3Hg^+ sorption. In the figure, it was demonstrated that the binding of CH_3Hg^+ on the sorbent was rapid and ~99% of CH_3Hg^+ was removed from the solution even in 1 min. Still, a contact time of 30 min was used for all subsequent experiments to guarantee the quantitative sorption.
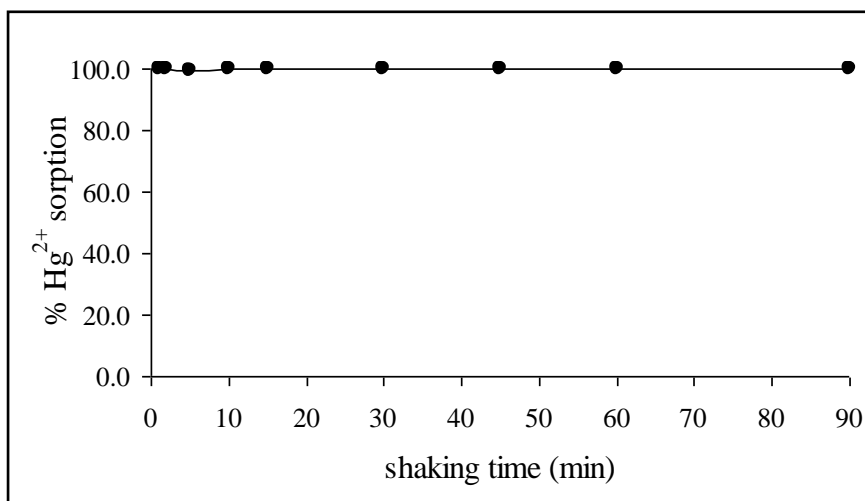
Figure 3.29. Effect of shaking time on Hg^{2+} sorption at pH 7.0 in 10.0 mL of 500.0 μgL^{-1} solution, sorbent amount: 10.0 mg, (n=3).
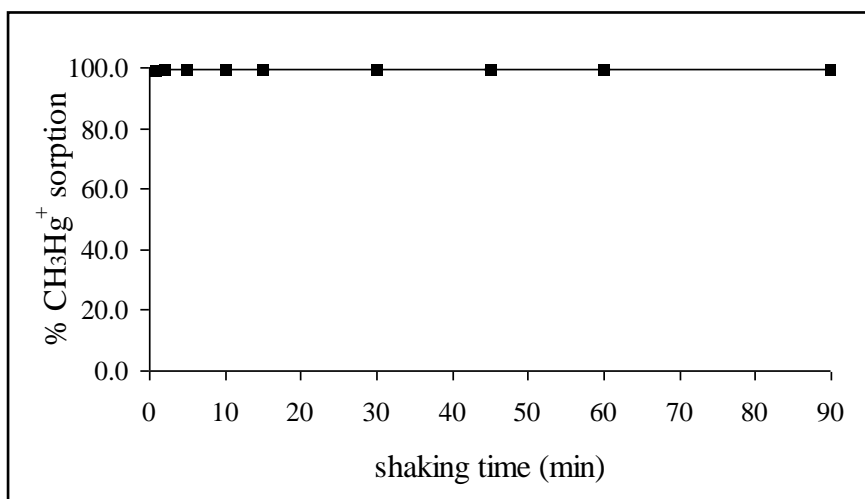
Figure 3.30. Effect of shaking time on CH_3Hg^+ sorption at pH 7.0 in 10.0 mL of 500.0 μgL^{-1} solution, sorbent amount: 10.0 mg, (n=3).

3.3.1.4. Effect of Temperature

The sorption behavior of 3-MPTMS-silica as a function of temperature is shown in Figure 3.31 and 3.32. The results indicated that there is no significant change in sorption with increasing temperature.
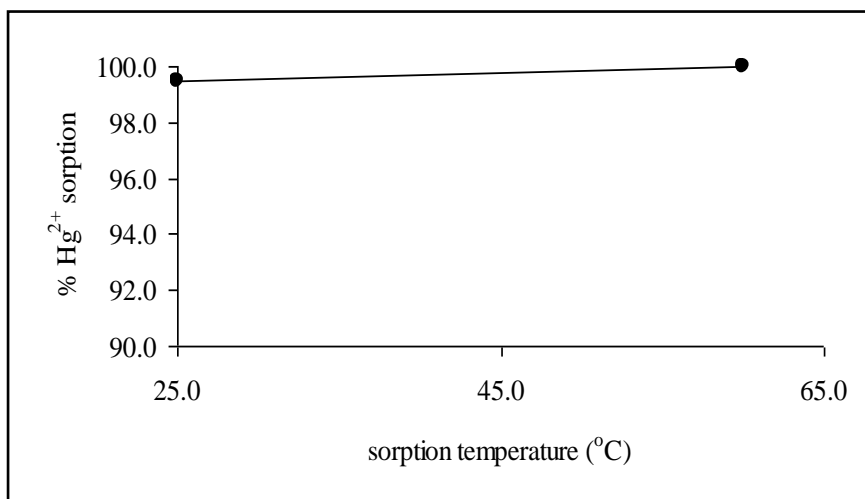
Figure 3.31. Effect of temperature on Hg^{2+} sorption at pH 7.0 in 10.0 mL of 500.0 μgL^{-1} solution, sorbent amount: 10.0 mg, shaking time: 30 min, (n=3).
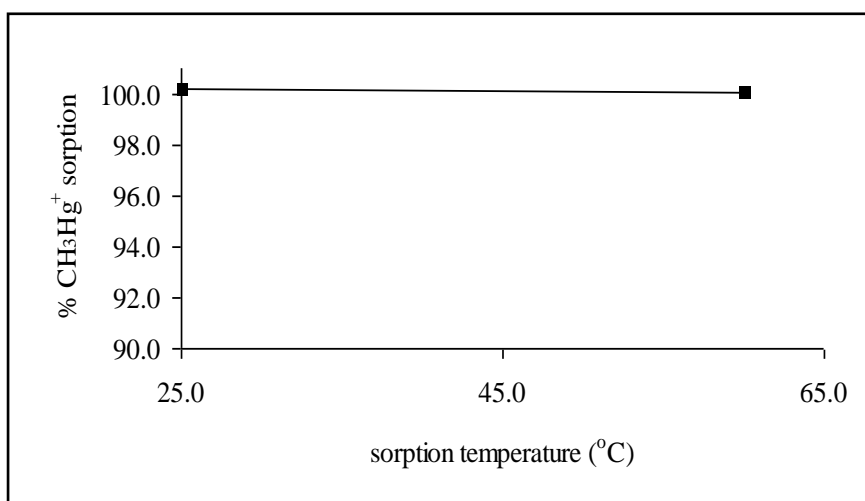
Figure 3.32. Effect of temperature on CH_3Hg^+ sorption at pH 7.0 in 10.0 mL of 500.0 μgL^{-1} solution, sorbent amount: 10.0 mg, shaking time: 30 min, (n=3).

3.3.1.5. Desorption from 3-MPTMS-Silica

In order to take the mercury species retained on the sorbent back into solution, desorption experiments were performed. The eluents were chosen by considering the affinity to form mercury complexes with sulfur or nitrogen atoms. For this purpose, L-cysteine, sodium sulfide (Na_2S), thiourea and potassium thiocyanate (KSCN) were tried. Besides these eluents, mineral acids (HNO_3, HCl, H_2SO_4, H_3PO_4), a strong base (KOH), a weak base (NH_3), organic acids (tartaric acid, formic acid, thioglycolic acid (TGA), citric acid), potassium iodide (KI), and EDTA were also investigated. After the

usual sorption process, the mixture was filtered through filter paper and the sorbent was taken into the eluent. The mixture was shaken for another 30.0 min and at the end of this period, the contents were filtered and the filtrate was analyzed by CVAAS. The eluent concentrations and the corresponding recoveries are given in Table 3.10. Blank solutions were also prepared by the same procedure.

As seen from the table, 2.0 M TGA and 5.0 M KOH offered the best results for Hg^{2+} desorption and ~95% recovery was obtained for inorganic mercury while <25% and 5% recovery was achieved for CH_3Hg^+ with TGA and KOH, respectively. Unfortunately, CH_3Hg^+ could not be eluted efficiently by any of the eluents investigated. However, this finding may enable a speciation opportunity if an efficient eluent for CH_3Hg^+ can be found in further studies. That is, both species can be sorbed and then eluted sequentially; first with 2.0 M TGA and then with a possible eluent for CH_3Hg^+.

The effect of TGA and KOH on Hg^{2+} signals was also investigated. It was observed that a signal suppression was obtained when 5.0 M KOH was applied which may be due to the formation of mercury hydroxide species. To the contrary, TGA has no effect on Hg^{2+} signals. A negative aspect of TGA, however, was that, it was contaminated with Hg which had an undesired contribution to the blank signal in the eluates. This signal is negligible when working with relatively high Hg^{2+} concentrations; but it has to be considered for low (μgL^{-1}) Hg^{2+} concentrations. Several procedures were tried to clean the TGA solutions before elution; none of them was successful. The contamination problem in the eluent precluded a detailed enrichment study.

Table 3.10. Desorption of Hg^{2+} and CH_3Hg^+ from 3-MPTMS-silica (500.0 μgL^{-1} Hg^{2+} or CH_3Hg^+ solution, sample volume: 10.0 mL, sorbent amount: 10.0 mg, pH=7.0, shaking time: 30 min and temperature: 25 ^oC).

Eluent	% Recovery	
	Hg^{2+}	CH_3Hg^+
1 M TGA	62.9±1.0	11.7±3.9
2 M TGA	92.0±4.5	21.3±0.2
3 M KOH	60.5±2.1	<5
5 M KOH	94.6±5.1	<5
3 M HNO_3	<5	<5
3 M HCl	<5	<5
3 M H_2SO_4	<5	<5
3 M H_3PO_4	<5	<5
conc. HCl	16.2±3.1	<5
3 M NH_3	<5	7.1±2.0
0.5 M KI	<5	<5
1 M Na_2S	<5	<5
2 M KSCN	<5	<5
0.1430 M EDTA	<5	<5
1 M tartaric acid	<5	<5
1 M citric acid	<5	<5
1 M formic acid	<5	<5
1% L-cysteine	<5	<5
10% thiourea	<5	<5

3.3.1.6. Sorption Capacity of 3-MPTMS-Silica

Sorption capacity of 3-MPTMS-silica was tested by varying the concentration of Hg^{2+} between 50.0 and 1000.0 mgL^{-1} at pH 7.0. The change in the percent sorption of 3-MPTMS-silica as a function of concentration is demonstrated in Figure 3.33, which shows a decreased sorption with an increase in the concentration. Finally, the sorption capacity of 3-MPTMS-silica for Hg^{2+} was calculated as 0.94 mmol g^{-1}.
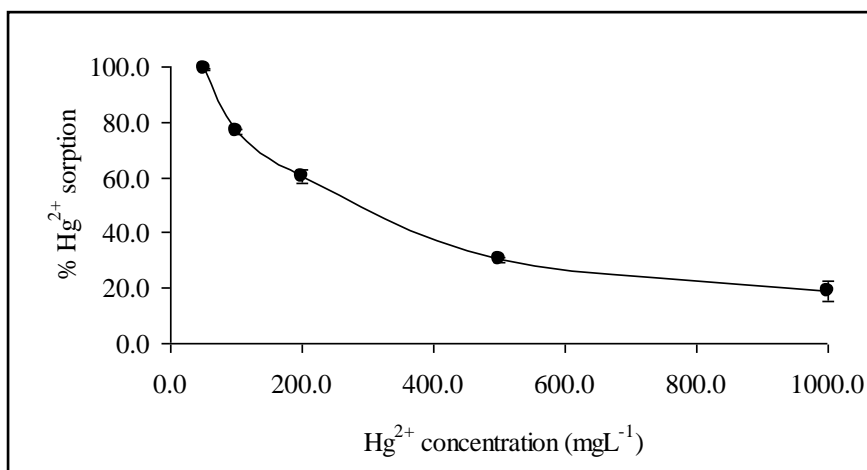
Figure 3.33. Effect of concentration on Hg^{2+} sorption at pH 7.0 in 5.0 mL sample volume, sorbent amount: 5.0 mg, shaking time: 30 min, (n=3).

The Hg^{2+} sorption by 3-MPTMS-silica in the presence of Cu^{2+}, Ni^{2+} and Pb^{2+} was also examined. It was observed that these ions had no effect on the sorption of Hg^{2+} and >98% sorption was observed at the studied conditions.

3.3.1.7. Application to Real Samples

As mentioned in Section 2.7.1.7, 3-MPTMS-silica and unmodified silica were applied to the spiked samples of ultrapure, bottled drinking, tap, sea and geothermal water. The sorption performance of the sorbents was checked. The results are summarized in Table 3.11 for Hg^{2+} and CH_3Hg^+, respectively. As can be seen from the tables, 3-MPTMS-silica displayed very efficient performances towards mercury species at pH 7.0; the sorption percentages were above 95% in all cases. A relatively high sorption was obtained for also sea water demonstrating the efficiency of 3-MPTMS-silica even in a heavy matrix sample. However, in the case of silica, quantitative sorption results were not achieved and unmodified silica did not work properly in all samples. Hence, the modification of silica with 3-MPTMS increased the removal efficiency even in sea water.

Table 3.11. Percent sorption of spiked (1.0 mgL^{-1}) Hg^{2+} or CH$_3$Hg$^+$ with ultrapure, bottled drinking, tap, sea and geothermal water samples from 3-MPTMS-silica (sample volume: 10.0 mL, sorbent amount: 10.0 mg, pH=7.0, shaking time: 30 min and temperature: 25 ^{o}C, n=3).

Sample	%Hg^{2+} sorption		%CH$_3$Hg$^+$ sorption	
	silica	3-MPTMS-silica	3-MPTMS-silica	3-MPTMS-silica
Ultrapure Water	81.6 ± 4.2	99.7 ± 0.0	silica	99.3 ± 0.8
Bottled Drinking Water	72.7 ± 3.0	99.8 ± 0.0	61.5 ± 0.0	99.5 ± 0.1
Alsancak Tap Water	46.9 ± 5.5	99.6 ± 0.2	63.7 ± 2.4	99.4 ± 0.5
Gülbahçe Tap Water	61.0 ± 2.5	99.8 ± 0.0	64.1 ± 1.1	97.5 ± 0.1
Sea Water	29.4 ± 4.2	99.6 ± 0.1	41.6 ± 2.4	95.1 ± 0.5
Geothermal Water	55.7 ± 2.8	99.3 ± 0.8	*ND	*ND

*ND: not detected

3.3.2. Sorption with nZVI and ZVI-Modified/Unmodified Sorbents

As it is known that nZVI dissolves at acidic pH values, it is necessary to present the partial dissolution of ZVI from the resin surface in acidic pHs. For this purpose, the initial experiments focused on the investigation of this effect. The pHs of the solutions were adjusted between 1.0 and 6.0 and iron release as a function of pH was followed by FAAS. Afterwards, the related sorption experiments were performed. The effect of solution pH was also examined for ZVI alone.

3.3.2.1. Effect of Solution pH on the Dissolution of nZVI

The effect of pH on nZVI is demonstrated in Figure 3.34. As can be seen from the figure, dissolution of nZVI increases with a decrease in the solution pH, as expected. In a pH of 1.0, iron ion concentration in the solution was around 400 mgL^{-1}. These results might be considered from two different perspectives; firstly, it is a disadvantage since it precludes the use of the sorbent at pHs below 4.0. Secondly, the complete solubility of nZVI in 0.1 M HCl or HNO_3 can be used in an advantageous way in a way that the retained species can be desorbed from the sorbent very easily with the use of acids.
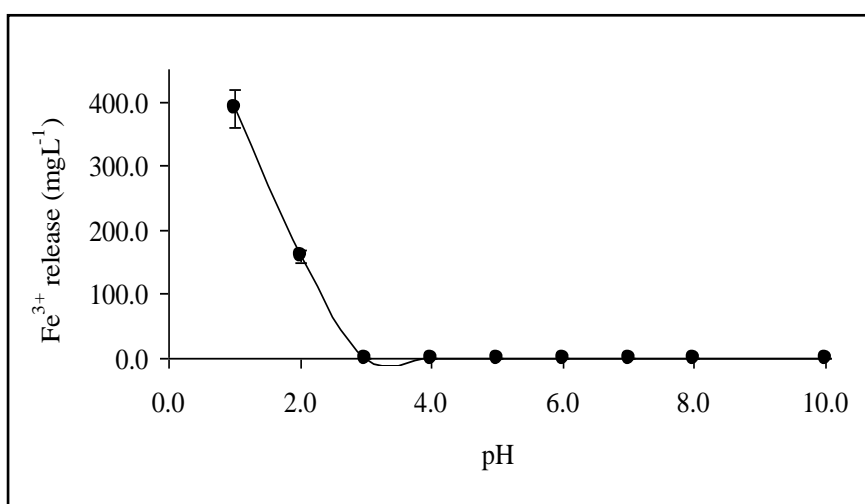
Figure 3.34. Fe^{3+} released from nZVI as a function of solution pH (10.0 mL ultrapure water, sorbent amount: 10.0 mg, shaking time: 30 min, n=3).

3.3.2.2. Effect of Solution pH on the Dissolution of ZVI-Modified Diaion SK116/Amberlite IRC50

Diaion SK116 is a strong cation exchanger that has positively charged sulfonic acid groups whereas Amberlite IRC50 is a weak cation exchanger that contains carboxylic acid functional groups on the surface. Figure 3.35 indicates the iron release as a function of pH. According to the figure, iron concentration was low compared to nZVI alone at the pH value of 1.0 due to the replacement of surface-bound Fe^{3+} ions with H^+ ions. This could be attributed to the successful fixation of the ZVI into the pores of the polymeric resin.
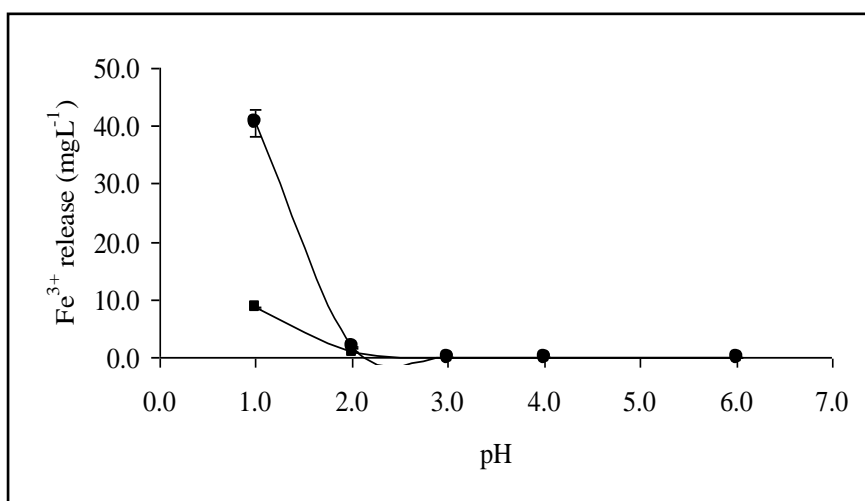
Figure 3.35. Fe^{3+} released from (●) ZVI-modified Diaion SK116 and (■) ZVI-modified Amberlite IRC50 as a function of solution pH (10.0 mL ultrapure water, sorbent amount: 10.0 mg, shaking time: 30 min, n=3).

3.3.2.3. Effect of Solution pH on the Dissolution of ZVI-Modified Amberlite IRA400/Amberlite IRA458/Amberlite IRA67

Amberlite IRA 400 and Amberlite IRA458 are strong anion exchangers that have quaternary ammonium functional groups whereas Amberlite IRA 67 is a weak anion exchanger that has polyamine functional groups on the resin surface. Iron release as a function of pH is shown in Figure 3.36. The iron concentration was ~0.8 mgL^{-1} in strong anion exchangers and this provides an advantage for sorption studies in order to

study at low pH values. Nonetheless, higher amounts of iron (~4 mgL^{-1}) were released compared to other anion exchangers but again the iron concentration was low in contrast to nZVI alone.
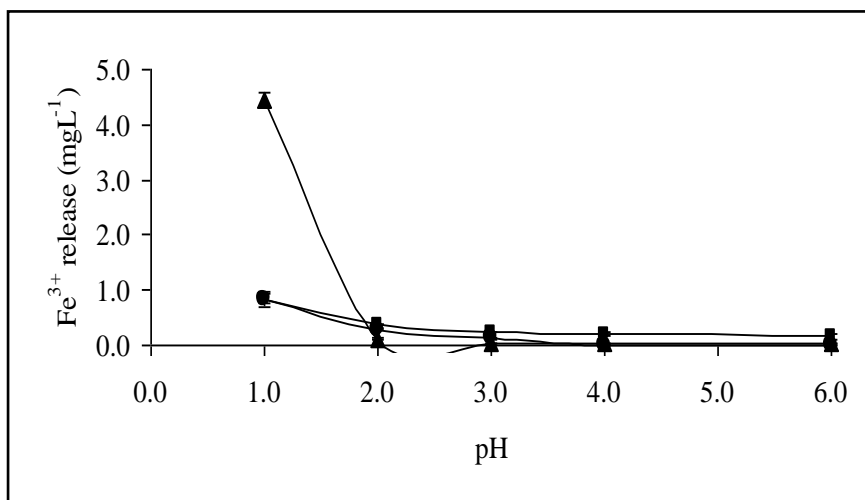
Figure 3.36. Fe^{3+} released from (●) ZVI-modified Amberlite IRA400, (■) ZVI-modified Amberlite IRA458 and (▲) ZVI-modified Amberlite IRA67 as a function of solution pH (10.0 mL ultrapure water, sorbent amount: 10.0 mg, shaking time: 30 min, n=3).

After dissolution experiments at the studied conditions (10.0 mL ultra pure water, sorbent amount: 10.0 mg) with nZVI alone and unmodified/modified resins, it can be concluded that ZVI-modified resins demonstrated a lower iron release compared to nZVI alone during shaking. Cation and anion exchangers always exhibited lower iron release compared to nZVI alone, anion exchangers releasing even lower iron to the solution. This phenomenon, that is a relatively higher release/dissolution of iron from the cation exchange resins than anion exchangers, can be attributed to the replacement of surface-bound Fe^{3+} ions with H^{+} ions in acidic solutions. The lower extent of dissolution of ZVI from the modified resins may enable to use these types of sorbents due to their higher resistance to acidic conditions.

As a result of the dissolution experiments, the effect of pH on nZVI and ZVI-modified sorbents towards mercury species were investigated.

3.3.2.4. Effect of Solution pH

3.3.2.4.1. Effect of pH with nZVI

The effect of pH on sorption was studied for nZVI and the percent sorption versus pH solution is demonstrated in Figure 3.37. As seen from the figure, nZVI offered significant sorption for Hg^{2+} and CH_3Hg^+ at the studied pH range. The percent sorption of Hg^{2+} and CH_3Hg^+ were ~97% and ~90%, respectively, for pH range 5.0-7.0. Nevertheless, sorption of both Hg species was lowered at pH 10.0. By considering the speciation graph (Figure 3.18) it can be said that Hg^{2+} ion is in the form of $Hg(OH)_2$ and nZVI shows strong affinity for this species. The core-shell structure of iron nanoparticles allows two uptake mechanisms towards metals. The core is the zero-valent iron and used as an electron source. It might reduce ions having higher standard reduction potentials than iron. In contrast, the shell has hydroxyl groups at the interface with the solution which causes surface complexation with the adsorbate. The sorption mechanism for Hg^{2+} is probably due to the reduction of Hg^{2+} into Hg^0 since the reduction potential of Fe^{2+} (E^0= -0.41 V) is lower compared to Hg^{2+} (E^0= +0.85 V). nZVI also adsorbs CH_3Hg^+ (Figure 3.37.) but it is not very easy to speculate about the sorption mechanism since no speciation diagram is available for CH_3Hg^+ in literature. Lower pH values were not tried in the sorption studies since nZVI dissolves below pH 3.5.

Figure 3.38 indicates Fe^{3+} release from nZVI as a function of pH after Hg^{2+} and CH_3Hg^+ sorption. According to the figure, ~0.5 mgL^{-1} iron was measured in solution after sorption when the pH was adjusted to 5.0 and 7.0 whereas ~1.5 mgL^{-1} of iron was released at pH 10.0.
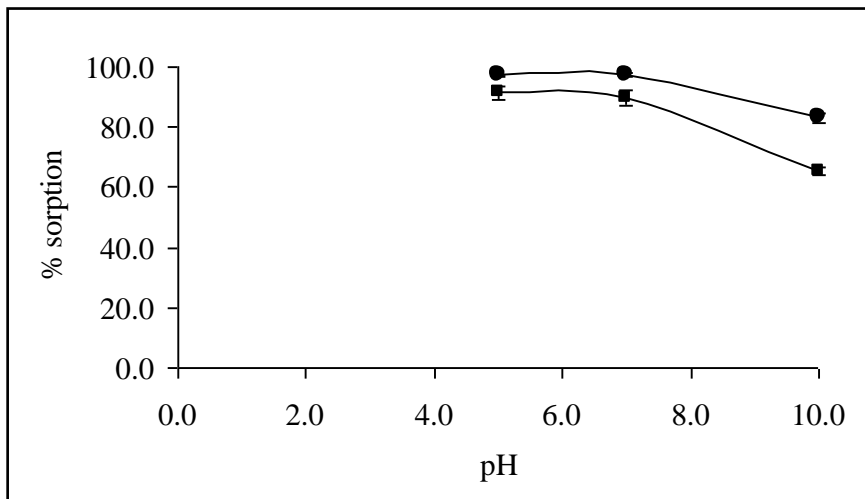
Figure 3.37. (●) Hg^{2+} and (■) CH_3Hg^+ sorption as a function of pH for nZVI (10.0 mL of 1.0 mgL^{-1} solution, sorbent amount: 10.0 mg, shaking time: 30 min, n=3).
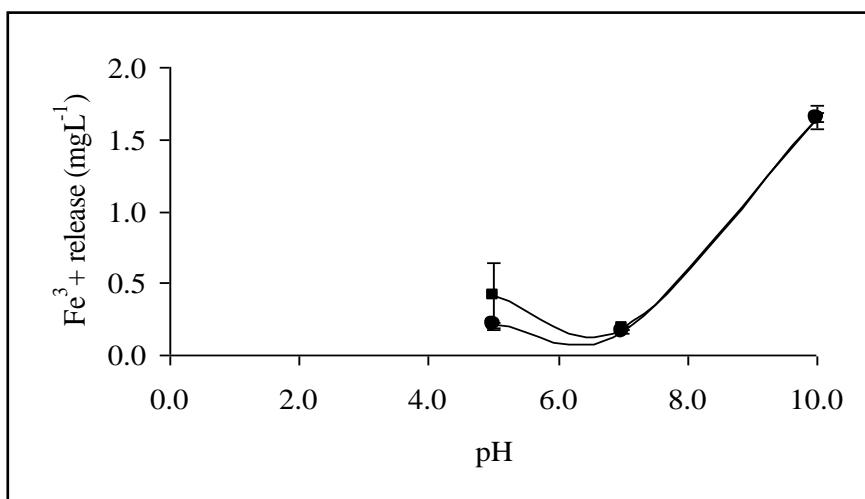
Figure 3.38. Fe^{3+} released from nZVI as a function of pH (10.0 mL of 1.0 mgL^{-1} (●) Hg^{2+} and 1.0 mgL^{-1} (■) CH_3Hg^+ solution, sorbent amount: 10.0 mg, shaking time: 30 min, n=3).

3.3.2.4.2. Effect of pH with ZVI-Modified/Unmodified Diaion SK116

The sorption of Hg^{2+} on ZVI-modified/unmodified Diaion SK116 is demonstrated in Figure 3.39. As can be seen, ZVI-modified Diaion SK116 exhibited a low affinity to Hg^{2+} at pH 1.0; only about 20% of Hg^{2+} was retained by the sorbent due to high concentration of H^+. This is thought to be originating from the dissolution of

surface-bound ZVI and therefore leaving reduced functionality on the surface. To the contrary, a quantitative adsorption (>85%) was found for Hg^{2+} at pH's greater than 3.0.

A similar trend was also observed for Diaion SK116. At low pH values Hg^{2+} accumulation on the sorbent was again low but sorption increased to ~90% when the pH of the solution was greater than 3.0. It can be concluded from the results that modification process has no effect on Hg^{2+} sorption.
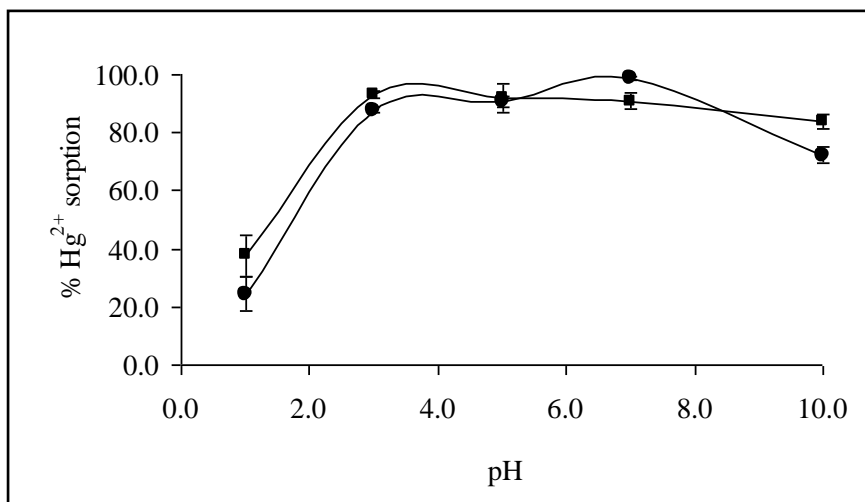
Figure 3.39. Hg^{2+} sorption as a function of pH on (●) ZVI-modified Diaion SK116 and (■) unmodified Diaion SK116 (10.0 mL of 1.0 mgL^{-1} solution, sorbent amount: 10.0 mg, shaking time: 30 min, n=3).

The retention of CH_3Hg^+ on ZVI modified/unmodified Diaion SK116 is presented in Figure 3.40. According to the figure, the efficiency of CH_3Hg^+ sorption was low at pH values 1.0, 3.0 and 5.0 when ZVI-modified Diaion SK116 was applied as sorbent for removal. However, the removal of CH_3Hg^+ on the sorbent was higher than 85% at pH values 7.0 and 10.0.

The sorption percentage of CH_3Hg^+ on Diaion SK116 was greater than 70% at all pH values. As seen from the graph, the sorption of CH_3Hg^+ decreased when the sorbent was modified with ZVI for pH values 1.0, 3.0 and 5.0.
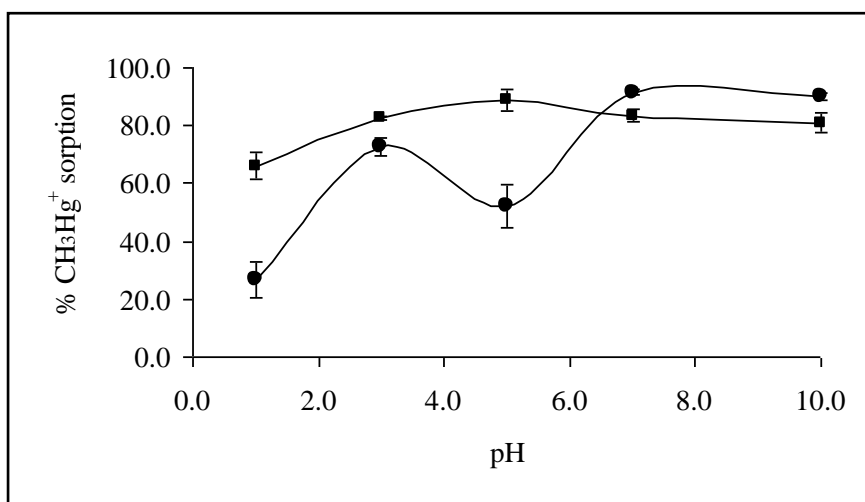
Figure 3.40. CH_3Hg^+ sorption as a function of pH on (●) ZVI-modified Diaion SK116 and (■) unmodified Diaion SK116 (10.0 mL of 1.0 mgL^{-1} solution, sorbent amount: 10.0 mg, shaking time: 30 min, n=3).

Figure 3.41 indicates the effect of pH on ZVI-modified Diaion SK116 after Hg^{2+}/CH_3Hg^+ sorption. Similar results obtained with ultrapure water were also achieved for the solutions containing Hg^{2+}/CH_3Hg^+. Higher amounts of iron (but not greater than nZVI only) were released into the solution at pH 1.0.
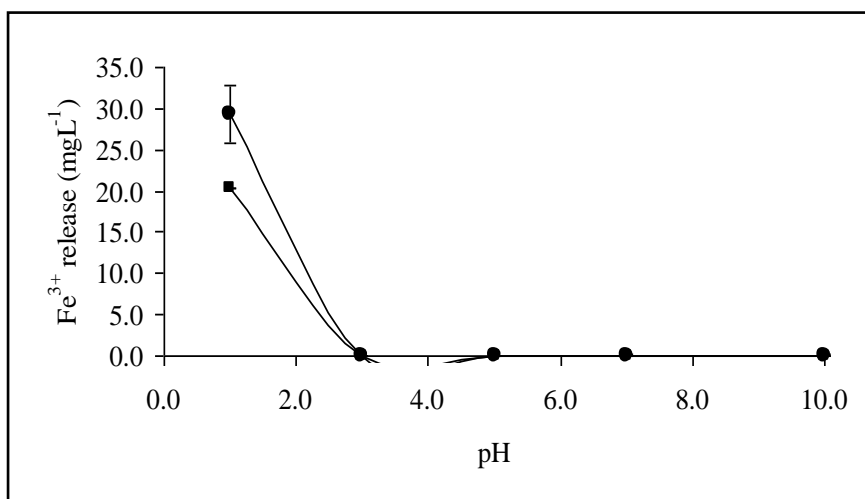
Figure 3.41. Fe^{3+} released from ZVI-modified Diaion SK116 as a function of pH (10.0 mL of 1.0 mgL^{-1} (●) Hg^{2+} and 1.0 mgL^{-1} (■) CH_3Hg^+ solution, sorbent amount: 10.0 mg, shaking time: 30 min, n=3).

3.3.2.4.3. Effect of pH with ZVI-Modified/Unmodified Amberlite IRC50

The effect of pH on sorption was also studied with ZVI-modified Amberlite IRC50 and the percent sorption versus pH graph is depicted in Figure 3.42. As seen from the figure, Hg^{2+} removal from the resin was again less at low pH's but it increased to ~80% at higher pH values.

The sorption behavior of Amberlite IRC50 towards Hg^{2+} represented a similar performance with ZVI-modified Amberlite IRC50. The sorption capacity of the resin was increased with pH from 1.0 to 3.0. At high pH values, the sorption was ~80% since IRC50 could utilize all of the carboxylic acid groups in strong alkaline media.

Figure 3.42. Hg^{2+} sorption as a function of pH on (●) ZVI-modified Amberlite IRC50 and (■) unmodified Amberlite IRC50 (10.0 mL of 1.0 mgL^{-1} solution, sorbent amount: 10.0 mg, shaking time: 30 min, n=3).

The sorption percentage of CH_3Hg^+ on ZVI-modified/unmodified Amberlite IRC50 is illustrated in Figure 3.43 It was observed that sorption was high at all pH values for both sorbents and ~95% sorption was obtained when the pH was adjusted to 10.0. It was observed that CH_3Hg^+ accumulation on ZVI-modified Amberlite IRC50 was quantitative (>95%) and independent of pH. As a result, ZVI-modified Amberlite IRC50 offered best results for CH_3Hg^+ removal and ~95% sorption was obtained for organic mercury while <10% sorption was achieved for Hg^{2+}. This finding may be used for the speciation of inorganic and organic mercury in further studies.
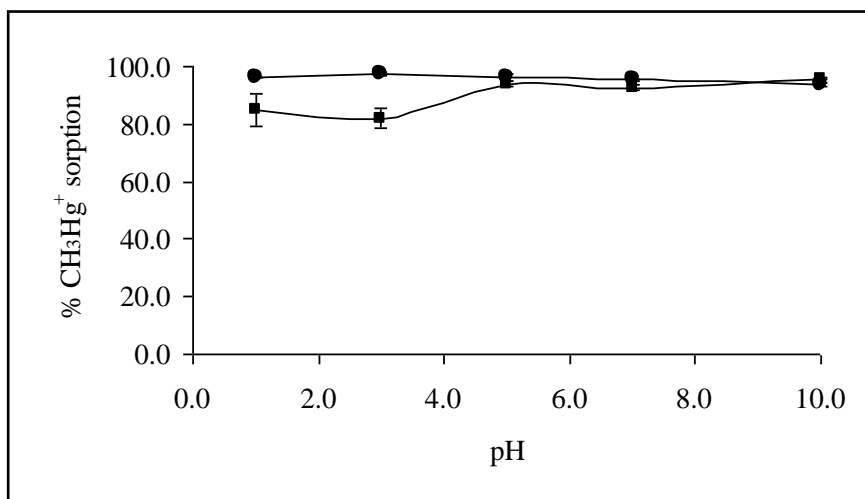
Figure 3.43. CH_3Hg^+ sorption as a function of pH on ($\bullet$) ZVI-modified Amberlite IRC50 and ($\blacksquare$) unmodified Amberlite IRC50 (10.0 mL of 1.0 mgL^{-1} solution, sorbent amount: 10.0 mg, shaking time: 30 min, n=3).

Figure 3.44 presents the effect of pH on ZVI-modified Amberlite IRC50 after Hg^{2+}/CH_3Hg^+ sorption. The results showed similarity with the results obtained with ultra pure water. Higher amounts of iron were released into the solution at pH 1.0 but in contrast to nZVI alone, iron concentration was very low.
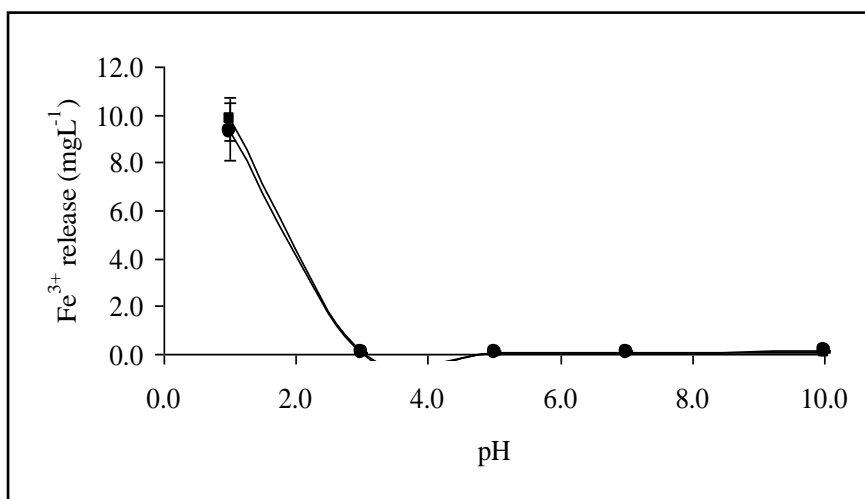
Figure 3.44. Fe^{3+} released from ZVI-modified Amberlite IRC50 as a function of pH (10.0 mL of 1.0 mgL^{-1} ($\bullet$) Hg^{2+} and 1.0 mgL^{-1} ($\blacksquare$) CH_3Hg^+ solution, sorbent amount: 10.0 mg, shaking time: 30 min, n=3).

3.3.2.4.4. Effect of pH with ZVI-Modified/Unmodified Amberlite IRA400

The retention of Hg^{2+} on ZVI-modified/unmodified Amberlite IRA400 is demonstrated in Figure 3.45. According to the figure, the efficiency of Hg^{2+} sorption was quantitative (>99%) at all pH values when the sorbent surface was modified with ZVI.

As seen from Figure 3.45, Hg^{2+} retention on Amberlite IRA400 was again less at low pH's but it increased to ~70% at higher pH values. It can be concluded that the sorption increases in the case of modification process.
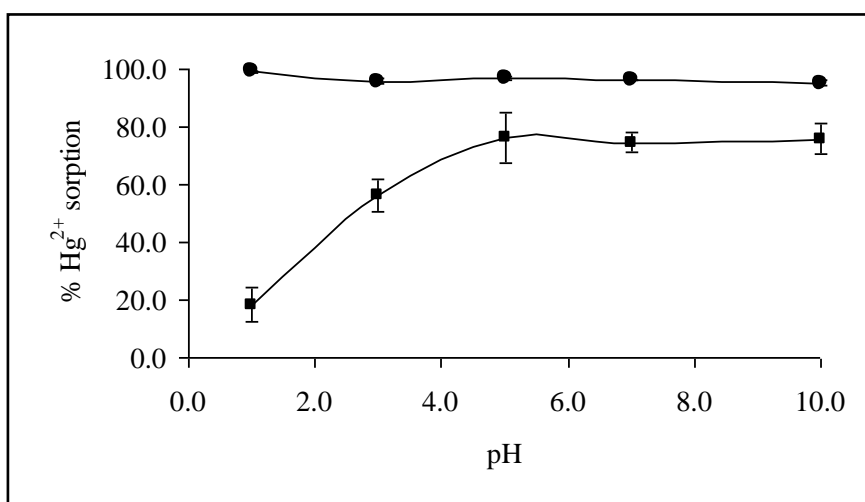
Figure 3.45. Hg^{2+} sorption as a function of pH on (●) ZVI-modified Amberlite IRA400 and (■) unmodified Amberlite IRA400 (10.0 mL of 1.0 mgL^{-1} solution, sorbent amount: 10.0 mg, shaking time: 30 min, n=3).

A similar trend was also observed for CH_3Hg^+. As shown in Figure 3.46, when ZVI-modified Amberlite IRA400 was used as a sorbent, the removal of CH_3Hg^+ was again independent of pH and quantitative at all values (~98) except at pH 1.0. Nevertheless, the removal of CH_3Hg^+ on Amberlite IRA400 was ~65% at pH up to 3.0 whereas it increased to ~80% after pH 3.0. Thus, by comparing the modified and unmodified sorbents, the results were improved with the modification process.
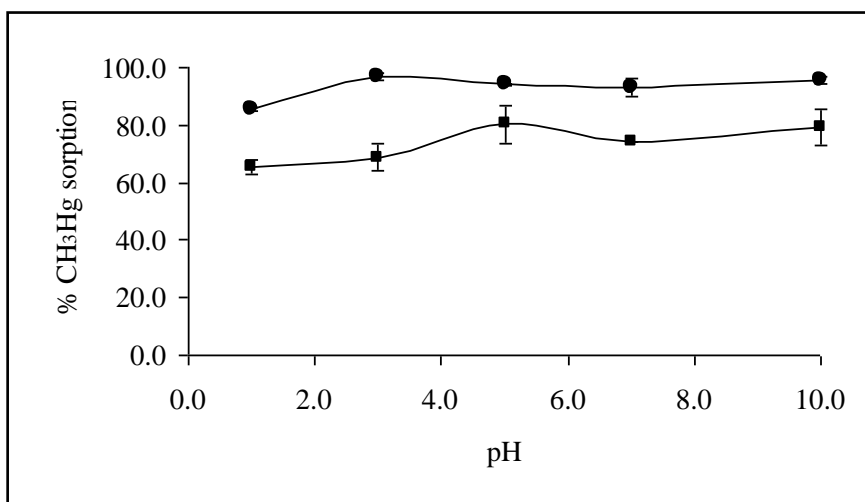
Figure 3.46. CH$_3$Hg$^+$ sorption as a function of pH on (●) ZVI-modified Amberlite IRA400 and (■) unmodified Amberlite IRA400 (10.0 mL of 1.0 mgL^{-1} solution, sorbent amount: 10.0 mg, shaking time: 30 min, n=3).

Iron release as a function of pH after Hg^{2+}/CH$_3$Hg$^+$ sorption is displayed in Figure 3.47. As can be observed from the graph, the iron concentration was ~2-3 mgL^{-1} after sorption when the pH was adjusted to 1.0. The results were also nearly the same with the results obtained with ultrapure water.
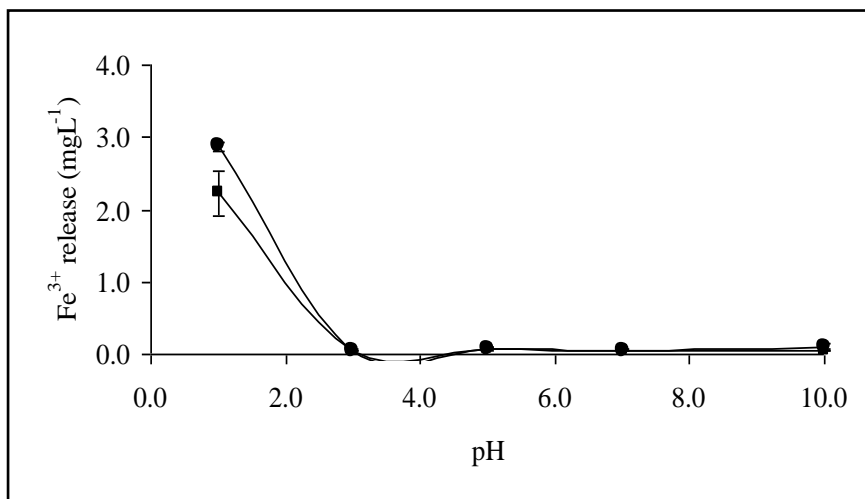
Figure 3.47. Fe^{3+} released from ZVI-modified Amberlite IRA400 as a function of pH (10.0 mL of 1.0 mgL^{-1} (●) Hg^{2+} and 1.0 mgL^{-1} (■) CH$_3$Hg$^+$ solution, sorbent amount: 10.0 mg, shaking time: 30 min, n=3).

3.3.2.4.5. Effect of pH with ZVI-Modified/Unmodified Amberlite IRA458

The removal of Hg^{2+} from ZVI-modified Amberlite IRA458 is demonstrated in Figure 3.48. As can be seen from the figure, quantitative sorption is achievable for Hg^{2+} at all pH values. Nonetheless, the retention of Hg^{2+} from Amberlite IRA458 was again low at pH 1.0 while the retention was greater than 40% after pH 3.0.
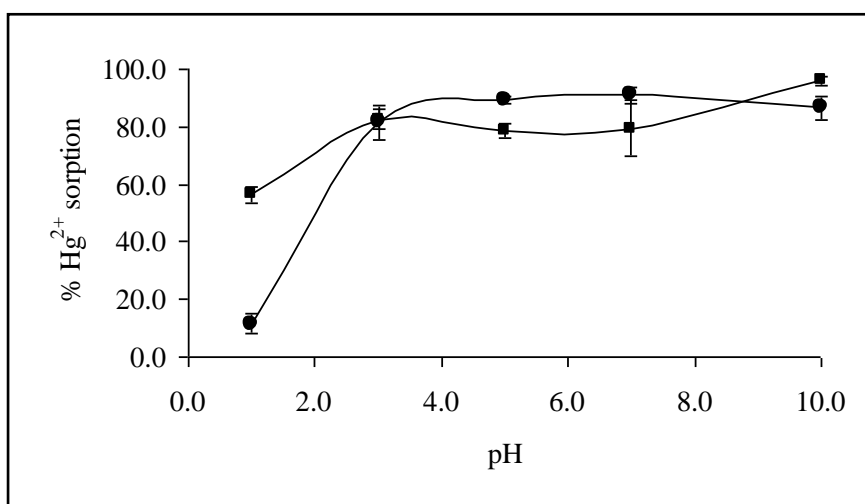

Figure 3.48. Hg^{2+} sorption as a function of pH on (●) ZVI-modified Amberlite IRA458 and (■) unmodified Amberlite IRA458 (10.0 mL of 1.0 mgL^{-1} solution, sorbent amount: 10.0 mg, shaking time: 30 min, n=3).

The sorption of CH_3Hg^+ by ZVI-modified Amberlite IRA458 is displayed in Figure 3.49. According to the figure, the removal of CH_3Hg^+ on the modified sorbent was ~90% at pH greater than 3.0. However, Amberlite IRA458 showed also the same sorption results at pH greater than 7.0. It can be concluded that modification process has no effect on the removal of CH_3Hg^+.

The effect of pH on ZVI-modified Amberlite IRA 458 after Hg^{2+}/CH_3Hg^+ sorption was shown in Figure 3.50. The iron concentration after sorption was changing between ~3 and 4 mgL^{-1} at pH 1.0 and the results were consistent with the ones obtained with ultrapure water.
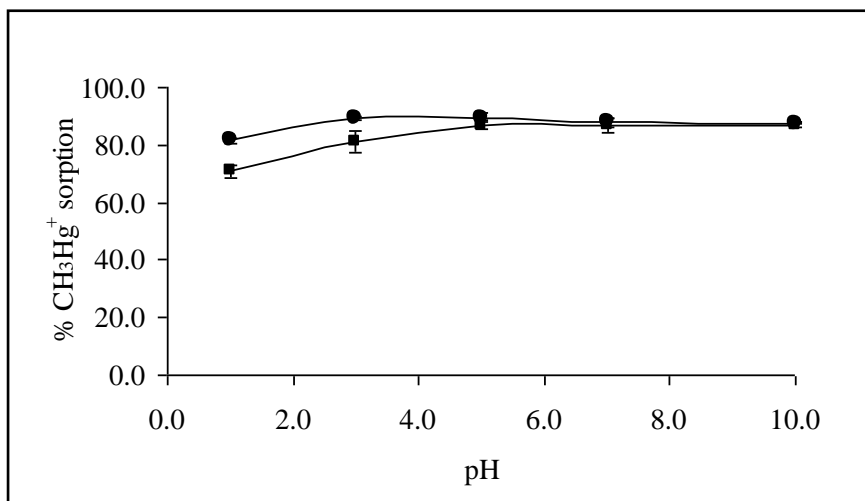
Figure 3.49. CH_3Hg^+ sorption as a function of pH on ($\bullet$) ZVI-modified Amberlite IRA458 and ($\blacksquare$) unmodified Amberlite IRA458 (10.0 mL of 1.0 mgL^{-1} solution, sorbent amount: 10.0 mg, shaking time: 30 min, n=3).

Figure 3.50. Fe^{3+} released from ZVI-modified Amberlite IRA458 as a function of pH (10.0 mL of 1.0 mgL^{-1} ($\bullet$) Hg^{2+} and 1.0 mgL^{-1} ($\blacksquare$) CH_3Hg^+ solution, sorbent amount: 10.0 mg, shaking time: 30 min, n=3).

3.3.2.4.6. Effect of pH with ZVI-Modified/Unmodified Amberlite IRA67

The effect of pH on the sorption of Hg^{2+} is demonstrated in Figure 3.51. As can be seen from the figure, ZVI-modified Amberlite IRA67 did not exhibit a very good affinity towards Hg^{2+}, only about 60% of Hg^{2+} was retained onto the sorbent surface

after pH 3.0. However, ~80% sorption was obtained at pH 1.0 due to the competition between H^+ and Fe^{3+} ions.

A similar trend was also observed for Amberlite IRA67. Hg^{2+} accumulation on the sorbent was low due to the protonation of amine functional groups on the surface but sorption increased to ~60% when the pH of the solution was greater than 3.0. It can be concluded from the results that modification process has no effect on Hg^{2+} sorption.

Figure 3.52 depicts the removal of CH_3Hg^+ on ZVI-modified/unmodified Amberlite IRA67. According to the figure, ZVI-modified Amberlite IRA67 exhibited a high sorption efficiency towards CH_3Hg^+ and the sorption was quantitative (~90%) at all pH values.

Similar results on CH_3Hg^+ sorption were also obtained for Amberlite IRA67. In the figure, the removal of CH_3Hg^+ was ~80% and independent of pH. At neutral pH values, the amino groups of weakly basic exchanger are sufficiently protonated to allow the accumulation of CH_3Hg^+. Thus, the modification process has little effect on the CH_3Hg^+ retention.

Figure 3.51. Hg^{2+} sorption as a function of pH on (●) ZVI-modified Amberlite IRA67 and (■) unmodified Amberlite IRA67 (10.0 mL of 1.0 mgL^{-1} solution, sorbent amount: 10.0 mg, shaking time: 30 min, n=3).

Iron release as a function of pH after Hg^{2+}/CH_3Hg^+ sorption is represented in Figure 3.53. As can be seen from the graph, ~3 mgL^{-1} Fe^{3+} was released in solution after sorption for both species when the pH was adjusted to 1.0. The results were consisted with the ones obtained with ultrapure water.
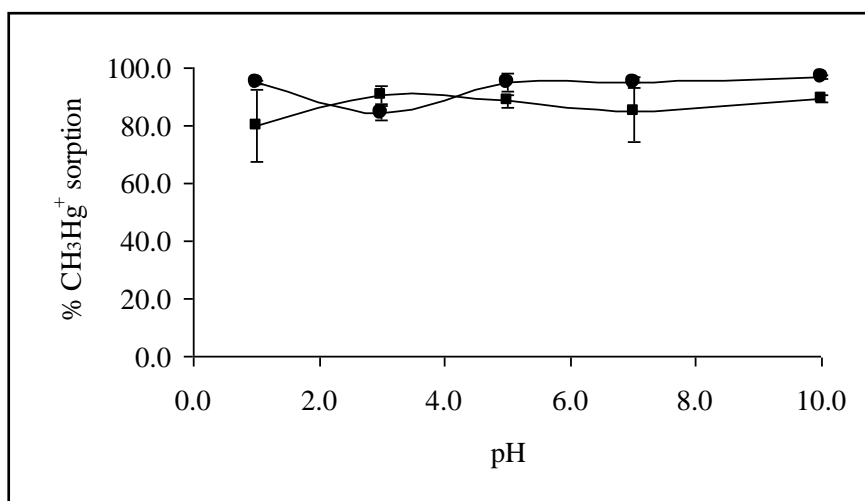
Figure 3.52. CH_3Hg^+ sorption as a function of pH on ($\bullet$) ZVI-modified Amberlite IRA67 and ($\blacksquare$) unmodified Amberlite IRA67 (10.0 mL of 1.0 mgL^{-1} solution, sorbent amount: 10.0 mg, shaking time: 30 min, n=3).


Figure 3.53. Fe^{3+} released from ZVI-modified Amberlite IRA458 as a function of pH (10.0 mL of 1.0 mgL^{-1} ($\bullet$) Hg^{2+} and 1.0 mgL^{-1} ($\blacksquare$) CH_3Hg^+ solution, sorbent amount: 10.0 mg, shaking time: 30 min, n=3).

3.3.2.4.7. Effect of pH with ZVI-Modified/Unmodified Silica

Figure 3.54 indicates the sorption behavior of ZVI-modified/unmodified silica towards Hg^{2+} as a function of pH. According to the figure, Hg^{2+} sorption was greater than 90% for pHs > 3.0 for ZVI-modified silica. The low affinity of the sorbent to Hg^{2+} at pH 1.0 can be attributed to the dissolution of surface-bound ZVI and therefore leaving reduced functionality on the surface. Silica also exhibited a low affinity in

96

acidic conditions; only ~30% of Hg^{2+} was retained onto silica. To the contrary, higher sorption (>85%) was found for Hg^{2+} at pHs 5.0, 7.0 and 10.0. Only appreciable difference in the sorption of ZVI-modified and unmodified silica was observed at pH 3.0 where percent sorption for ZVI-modified silica was greater than 80%. Still, this difference is not considered to be too meaningful to base the sorption studies at this pH.
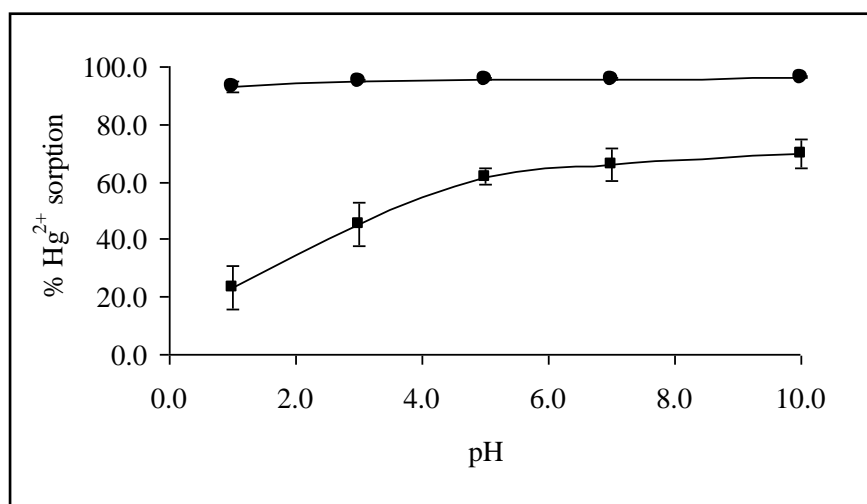

Figure 3.54. Hg^{2+} sorption as a function of pH on (●) ZVI-modified silica and (■) unmodified silica (10.0 mL of 1.0 mgL^{-1} solution, sorbent amount: 10.0 mg, shaking time: 30 min, n=3).

The retention of CH_3Hg^+ on ZVI-modified/unmodified silica is demonstrated in Figure 3.55. According to the figure, the efficiency of CH_3Hg^+ sorption was low at pH values 1.0, 3.0 and 5.0 and about 80% at pH's 7.0 and 10.0 for ZVI-modified silica. Nevertheless, CH_3Hg^+ sorption on unmodified silica was between 70-85% in the indicated pH range. It can be concluded from the results that modification process did not enhance the sorption efficiency of silica towards CH_3Hg^+; instead, it deteriorated the sorption.

Figure 3.56 represents the effect of pH on the release of Fe^{3+} from ZVI-modified silica after Hg^{2+}/CH_3Hg^+ sorption. Higher amounts of iron were released into the solution at pH 1.0 while it showed a decrease after pH 3.0 due to low solubility.

Figure 3.55. CH_3Hg^+ sorption as a function of pH on (●) ZVI-modified silica and (■) unmodified silica (10.0 mL of 1.0 mgL^{-1} solution, sorbent amount: 10.0 mg, shaking time: 30 min, n=3).
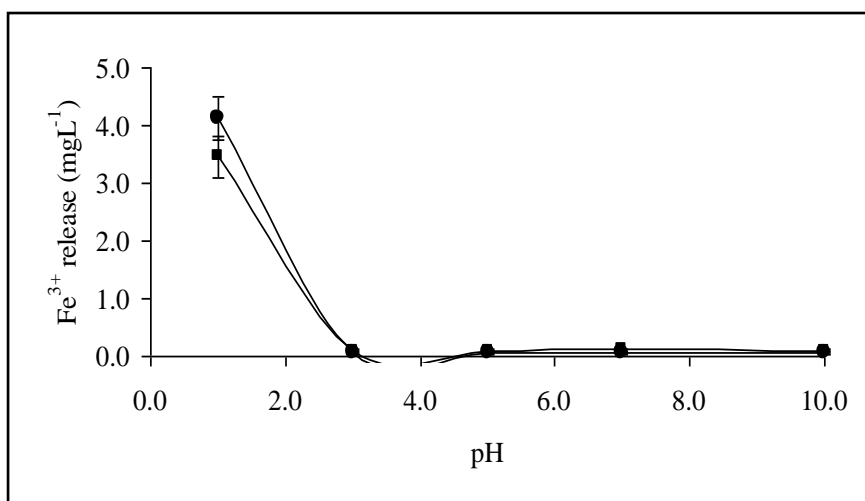

Figure 3.56. Fe^{3+} released from ZVI-modified silica as a function of pH (10.0 mL of 1.0 mgL^{-1} (●) Hg^{2+} and 1.0 mgL^{-1} (■) CH_3Hg^+ solution, sorbent amount: 10.0 mg, shaking time: 30 min, n=3).

3.3.2.4.8. Effect of pH with ZVI-Modified/Unmodified Alumina

The sorption percentage of Hg^{2+} on ZVI-modified/unmodified alumina is illustrated in Figure 3.57. As seen from the figure, Hg^{2+} removal by both ZVI-modified and unmodified alumina was again less at low pHs but increased to ~80% at pH values higher than 5.0. Hence, the ZVI modification process seemed to bring no advantage on the removal of Hg^{2+}.
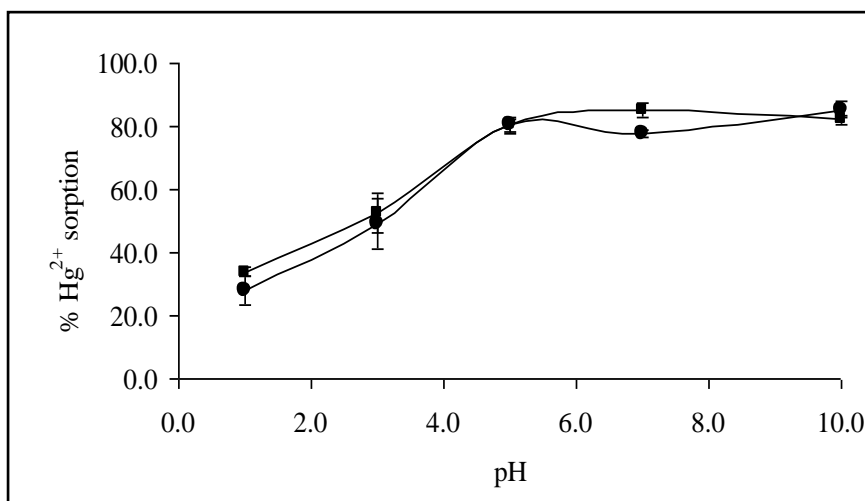
Figure 3.57. Hg^{2+} sorption as a function of pH on ($\bullet$) ZVI-modified alumina and ($\blacksquare$) unmodified alumina (10.0 mL of 1.0 mgL^{-1} solution, sorbent amount: 10.0 mg, shaking time: 30 min, n=3).

The retention of CH_3Hg^+ on ZVI-modified/unmodified alumina is demonstrated in Figure 3.58. As can be seen from the figure, the efficiency of CH_3Hg^+ sorption was quantitative (>80%) for ZVI-modified alumina at all pH values tried.

As seen from Figure 3.58, CH_3Hg^+ retention on unmodified alumina displayed very similar results with ZVI-modified alumina. The removal of CH_3Hg^+ on alumina was ~80% at all pH values except pH 3.0. It can be concluded from the results that the modification of alumina surface with ZVI did not bring any advantage over unmodified alumina; the sorption of CH_3Hg^+ did not change significantly.

Figure 3.59 indicates the iron release from ZVI-modified alumina as a function of pH after Hg^{2+}/CH_3Hg^+ sorption. According to the figure, ~4 and ~7 mgL^{-1} iron was measured in solution after sorption when the pH was 1.0 for Hg^{2+}/CH_3Hg^+, respectively. This amount was very low compared to nZVI alone. This could be due to insufficient modification of alumina with ZVI which was also proved with EDX results.
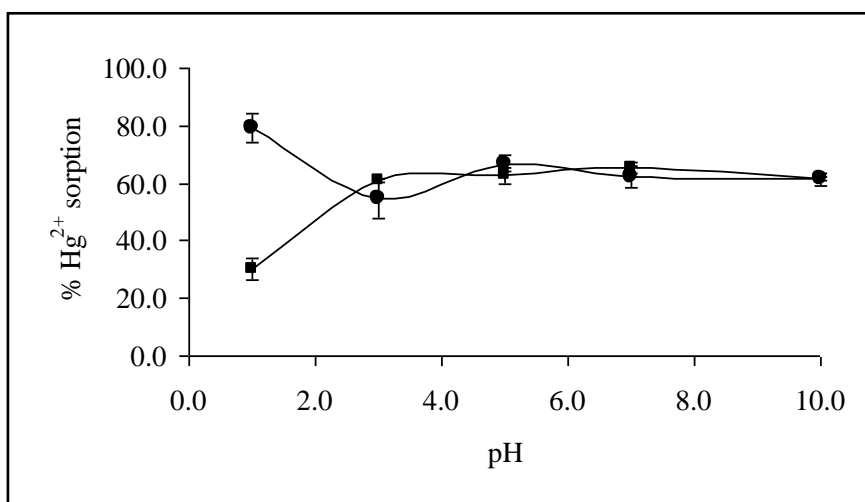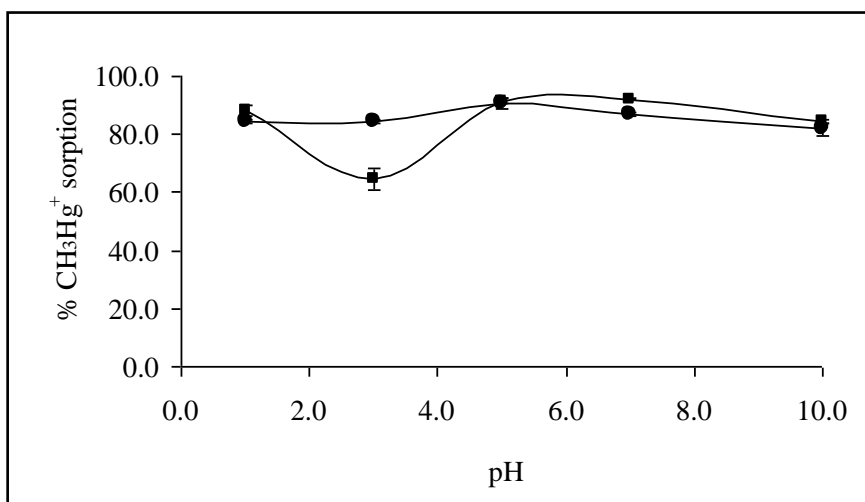
Figure 3.58. CH_3Hg^+ sorption as a function of pH on (●) ZVI-modified alumina and (■) unmodified alumina (10.0 mL of 1.0 mgL^{-1} solution, sorbent amount: 10.0 mg, shaking time: 30 min, n=3).
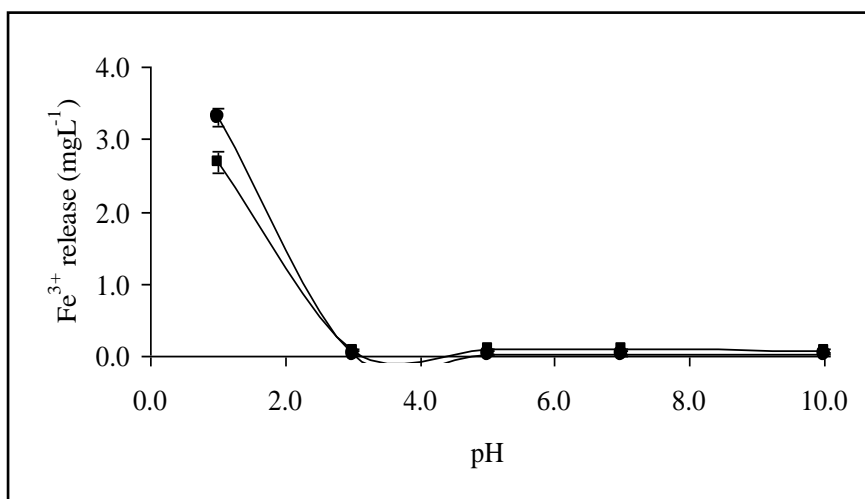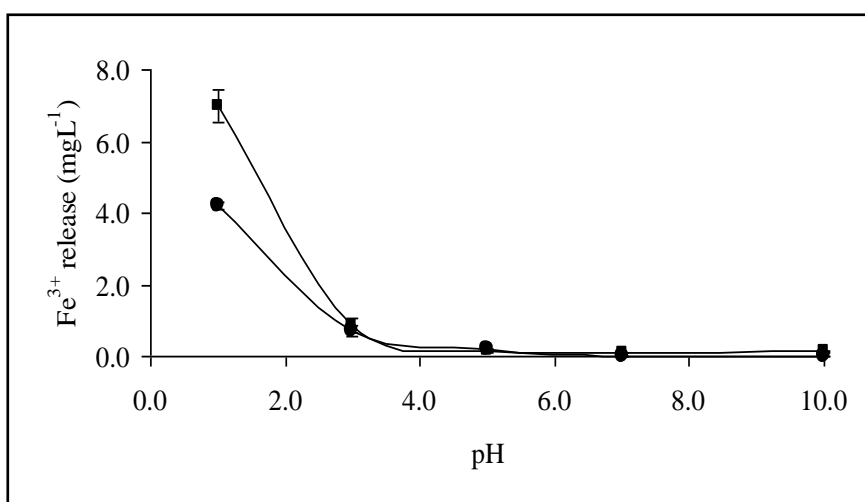

Figure 3.59. Fe^{3+} released from ZVI-modified alumina as a function of pH (10.0 mL of 1.0 mgL^{-1} (●) Hg^{2+} and 1.0 mgL^{-1} (■) CH_3Hg^+ solution, sorbent amount: 10.0 mg, shaking time: 30 min, n=3).

3.3.2.4.9. Effect of pH with ZVI-Modified/Unmodified Titania

Figure 3.60 compares the removal efficiency for ZVI-modified/unmodified titania at different initial pHs. The sorption of Hg^{2+} was comparable for both sorbents and only about 20% of Hg^{2+} was retained by the sorbent at pH 1.0, then, the sorption increased to ~80% after pH 3.0. Nevertheless, a higher adsorption (>80%) was observed

at pH's greater than 1.0. Thus, the modification had a poor effect on Hg^{2+} sorption under the selected experimental conditions.
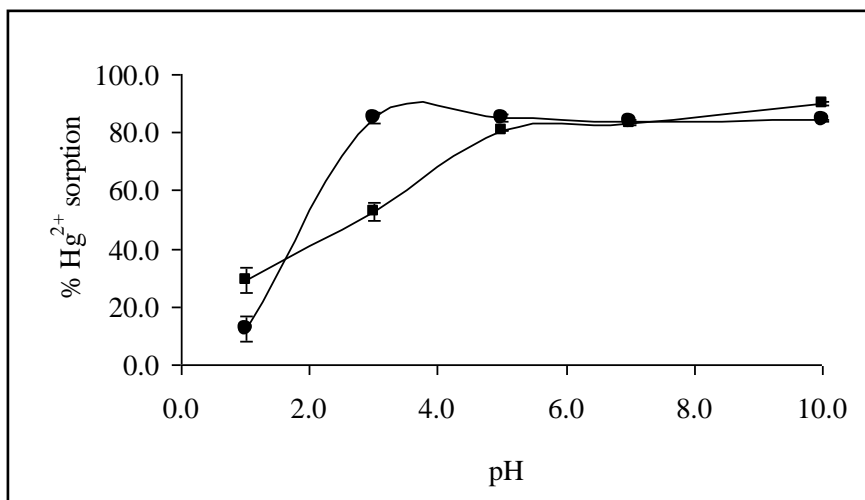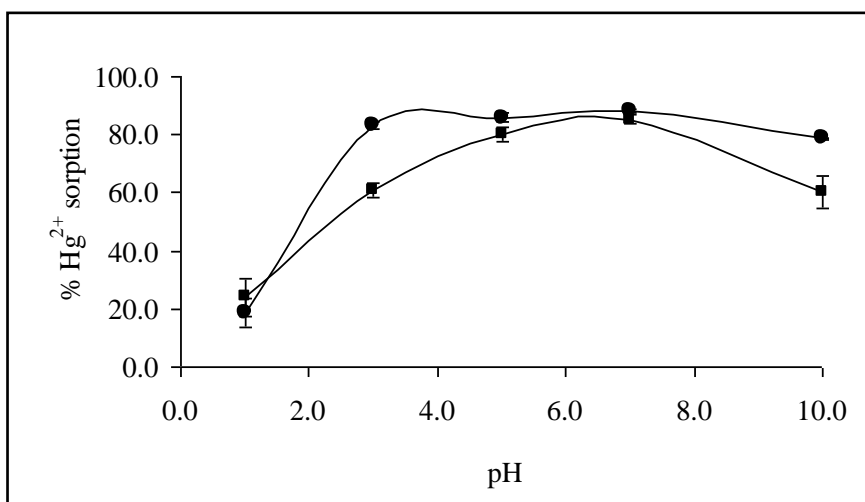

Figure 3.60. Hg^{2+} sorption as a function of pH on (●) ZVI-modified titania and (■) unmodified titania (10.0 mL of 1.0 mgL^{-1} solution, sorbent amount: 10.0 mg, shaking time: 30 min, n=3).

The removal of CH_3Hg^+ from ZVI-modified/unmodified titania is shown in Figure 3.61. As seen from the figure, CH_3Hg^+ removal from ZVI-modified titania was ~70% at low pH's but it increased to ~90% at higher pH values. Nonetheless, the sorption capacity of titania towards CH_3Hg^+ was again less at low pH values but an increase in sorption (~30%) was noticed after pH 3.0 and the sorption was ~60% at high pH values. It can be concluded from the results that the modification process seemed to be successful in CH_3Hg^+ sorption.

Iron release as a function of pH after Hg^{2+}/CH_3Hg^+ sorption is monitored in Figure 3.62. As can be observed from the graph, iron concentration was high but it was again low compared to nZVI alone after sorption when the pH was adjusted to 1.0.

At the studied conditions (10.0 mL of 1.0 mgL^{-1} solution, sorbent amount: 10 mg), even ZVI-modified ion exchange resins or inorganic substrates showed a high sorption of Hg^{2+} at high pHs whereas the sorption percentage was lower than 40% at low pH's due to the replacement of H^+ ions with Fe^{3+} ions. The surface becomes positively charged at low pH values which decrease the attraction between metal ions and the functional groups (nZVI) on the resin surface causing to decrease Hg^{2+} sorption, whereas the surface becomes negatively charged at high pH values, having an increase in Hg^{2+} sorption since the predominant specie of inorganic mercury is $Hg(OH)_2$ after pH

101

3.0. A similar trend was also observed for the accumulation of CH_3Hg^+ on ZVI-modified sorbents. Sorption was again low at low pH values due to the replacement of H^+ ions with Fe^{3+} ions while an increase was observed when the solution pH was adjusted to higher values.
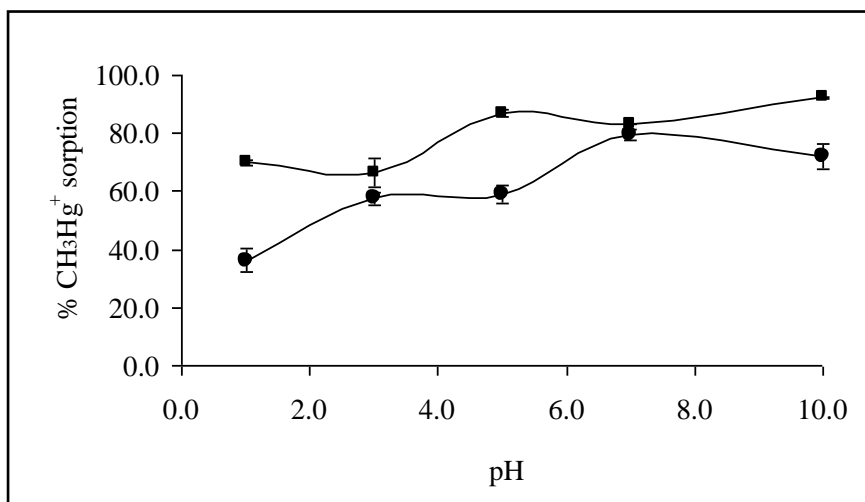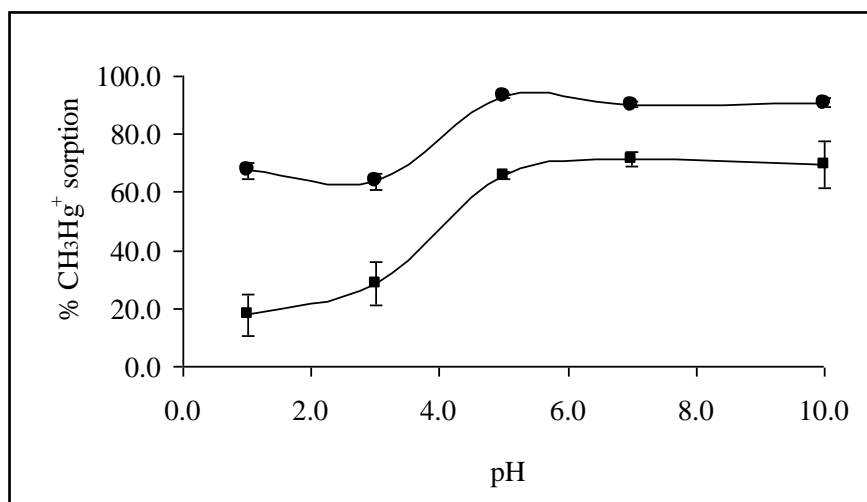

Figure 3.61. CH_3Hg^+ sorption as a function of pH on (●) ZVI-modified titania and (■) unmodified titania (10.0 mL of 1.0 mgL^{-1} solution, sorbent amount: 10.0 mg, shaking time: 30 min, n=3).
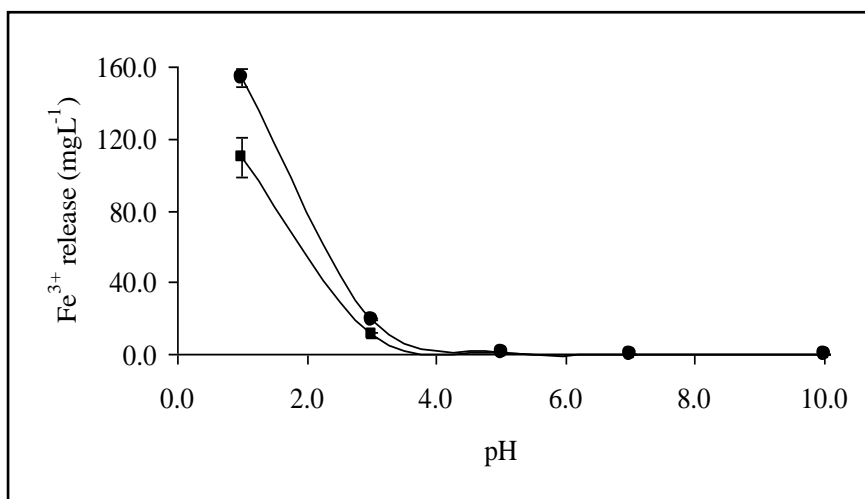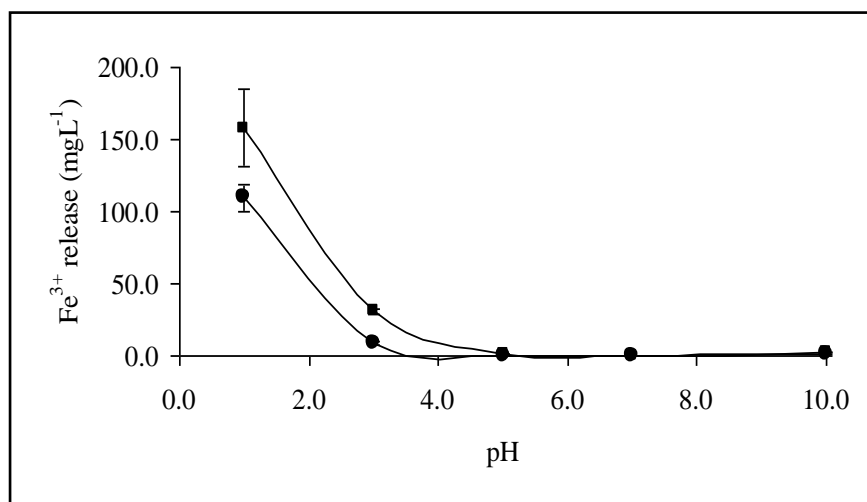

Figure 3.62. Fe^{3+} released from ZVI-modified titania as a function of pH (10.0 mL of 1.0 mgL^{-1} (●) Hg^{2+} and 1.0 mgL^{-1} (■) CH_3Hg^+ solution, sorbent amount: 10.0 mg, shaking time: 30 min, n=3).

Although the functionalization of ion exchange resins or inorganic substrates with nZVI seemed to have little effect on the removal of mercury species, it was decided to increase the initial concentration of Hg^{2+} in order to demonstrate the

efficiency of the modification on sorption. For this purpose, 5.0 mL of 100.0, 200.0, 500.0 and 1000.0 mgL^{-1} Hg^{2+} solutions at pH=7 were prepared and 5.0 mg of ZVI-modified/unmodified silica was added to each of them. Then, the mixtures were shaken for 30 minutes on the shaker at 25 ^{o}C. After filtration, the filtrates were analyzed with CVAAS for mercury content. The variation in the percent sorption of ZVI-modified/unmodified silica for different concentrations of Hg^{2+} was demonstrated in Figure 3.63. As can be seen from the figure, Hg^{2+} is not quantitatively absorbed by silica. When the case of ZVI-modified silica is considered, it is seen that the sorption percentage does not decrease under 93.9($\pm$1.9) % at the studied concentration range. Hence, the capacity of silica was exceeded and the success of modification process was observed when the concentration of Hg^{2+} increased. However, further studies are not performed since these concentrations are so toxic.
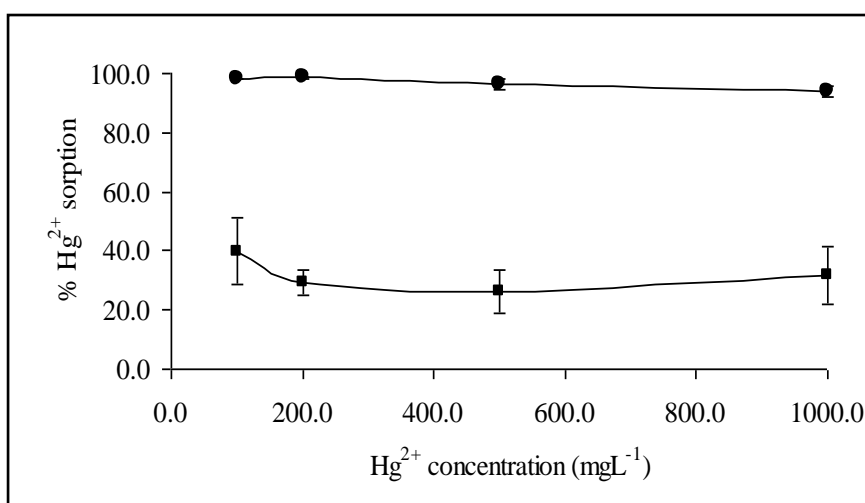
Figure 3.63. Hg^{2+} sorption as a function of concentration on ($\bullet$) ZVI-modified silica and ($\blacksquare$) unmodified silica (5.0 mL of solution, sorbent amount: 5.0 mg, shaking time: 30 min, n=3).

As the modification process had little effect on the removal of both mercury species at low concentrations, nZVI alone was used for further studies because of its simple preparation and ease of operation.

3.3.2.5. Effect of Sorbent Amount (Solid/Liquid Ratio)

Several experiments were made to determine the required amount of nZVI for the maximum sorption of mercury species. Figure 3.64 and Figure 3.65 demonstrate the results for the two mercury species at pH 7.0. As can be seen from the figures, quantitative sorption is achievable for both Hg^{2+} and CH_3Hg^+ with 10.0 mg nZVI for 10.0 mL solution.
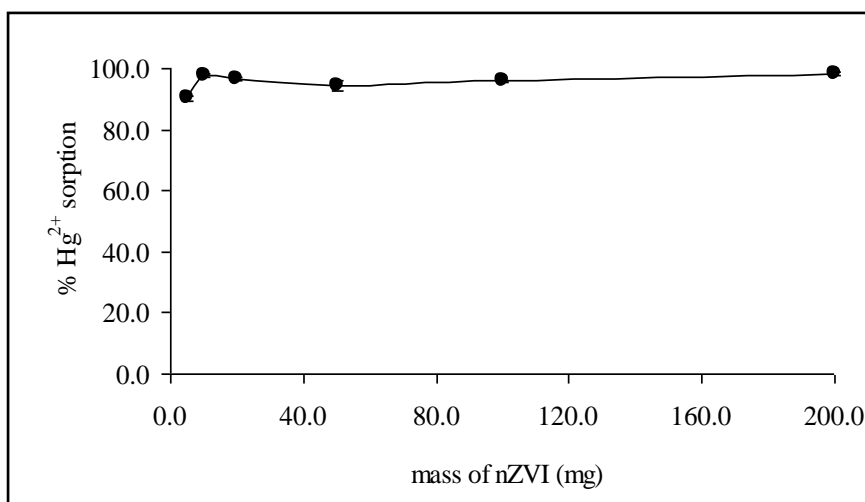
Figure 3.64. Effect of nZVI amount on Hg^{2+} sorption at pH 7.0 in 10.0 mL of 1.0 mgL^{-1} solution, shaking time: 30 min, (n=3).

Iron release as a function of nZVI mass after sorption was demonstrated in Figure 3.66 for both mercury species. As seen from the graph, iron concentration reached a maximum as the amount of nZVI increased up to 100.0 mg, and then it showed a small decrease at 200.0 mg for Hg^{2+} whereas it remained nearly constant for CH_3Hg^+. This small change in iron concentration for Hg^{2+} could be due to the oxidation of nZVI particles.
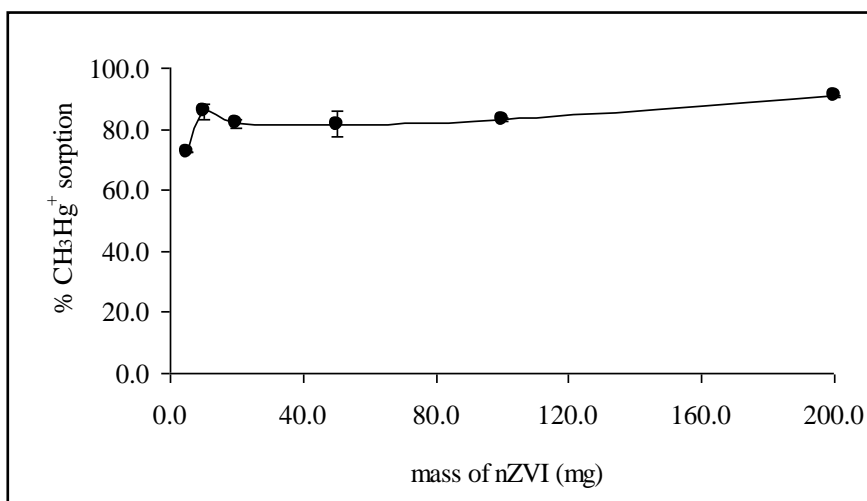
Figure 3.65. Effect of nZVI amount on CH_3Hg^+ sorption at pH 7.0 in 10.0 mL of 1.0 mgL^{-1} solution, shaking time: 30 min, (n=3).
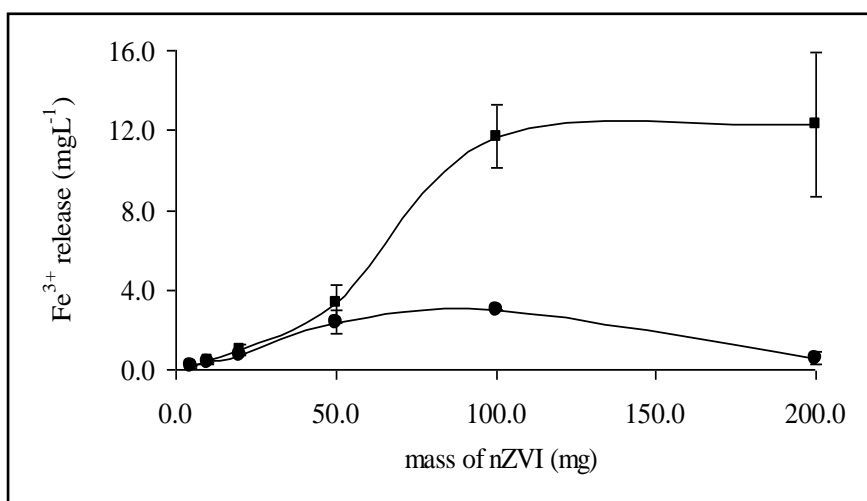
Figure 3.66. Fe^{3+} released as a function of mass of nZVI at pH 7.0 in 10.0 mL of (●) 1.0 mgL^{-1} Hg^{2+} and (■) 1.0 mgL^{-1} CH_3Hg^+ solution, shaking time: 30 min, n=3).

3.3.2.6. Effect of Shaking Time

The effect of shaking time on the extraction of Hg^{2+} and CH_3Hg^+ by nZVI was investigated as explained in Section 2.7.2.3. Ten milliliters of 1.0 mgL^{-1} Hg^{2+}/CH_3Hg^+ solution was shaken with 10.0 mg sorbent for different time intervals and the percentage of sorption results were presented in Figure 3.67 and 3.68. As in the case of Hg^{2+}, there is an appreciable sorption (~80%) even in 5 min, but the maximum sorption is obtained

in 30 min. In further experiments, a shaking time of 30 min was employed for Hg^{2+} to make sure obtaining high efficiency in sorption.

The optimization of shaking time on CH_3Hg^+ sorption was also studied. According to Figure 3.68, the binding of CH_3Hg^+ on nZVI was slow and ~30% of CH_3Hg^+ was removed from the solution in 1 min. The equilibrium was reached after 30 min for CH_3Hg^+. Hence, a contact time of 30 min was used for all subsequent experiments to guarantee the quantitative sorption.
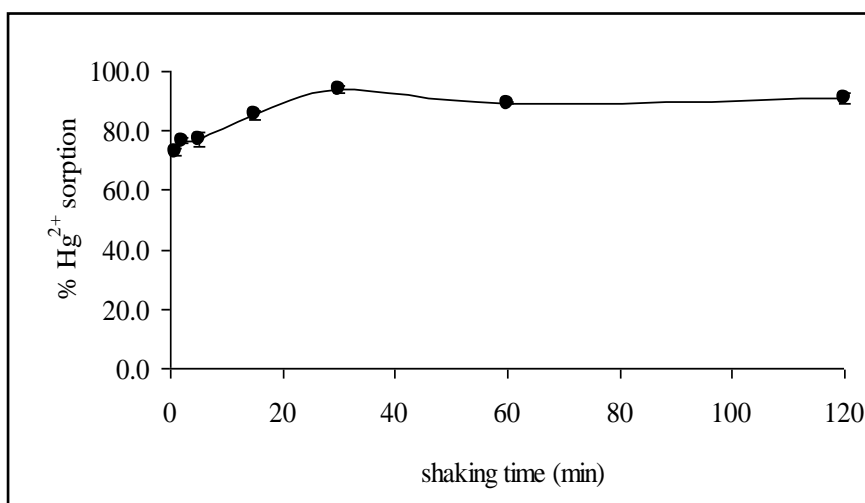
Figure 3.67. Effect of shaking time on Hg^{2+} sorption by nZVI at pH 7.0 in 10.0 mL of 1.0 mgL^{-1} solution, sorbent amount: 10.0 mg, (n=3).
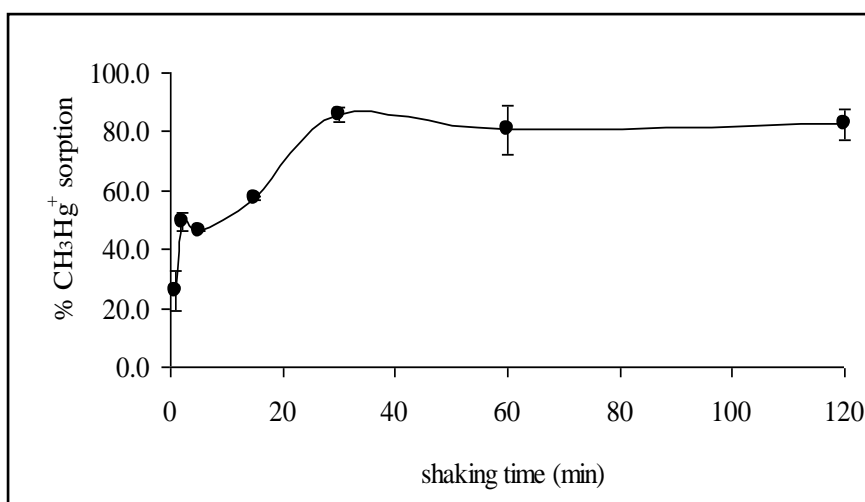
Figure 3.68. Effect of shaking time on CH_3Hg^+ sorption by nZVI at pH 7.0 in 10.0 mL of 1.0 mgL^{-1} solution, sorbent amount: 10.0 mg, (n=3).

The concentration of iron in the supernatant solution was also determined after sorption. Figure 3.69 depicts the iron release as a function of shaking time. As seen

from the figure, the amount of iron was nearly the same for all studied time intervals and ~2.5 mgL^{-1} iron was measured in solution for both mercury species at 30 min.
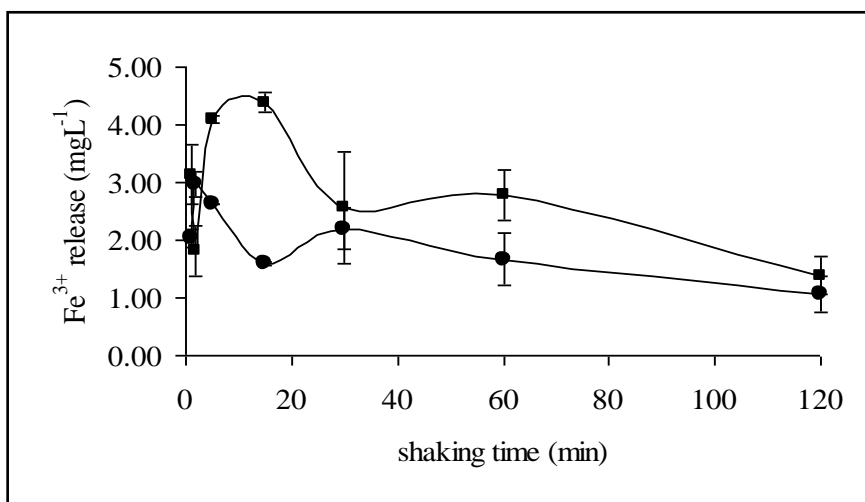
Figure 3.69. Fe^{3+} released from nZVI as a function of shaking time at pH 7.0 in 10.0 mL of (●) 1.0 mgL^{-1} Hg^{2+} and (■) 1.0 mgL^{-1} CH$_3$Hg$^+$ solution, sorbent amount: 10.0 mg, n=3).

3.3.2.7. Effect of Temperature

To identify the temperature effect on Hg^{2+}/CH$_3$Hg$^+$ removal, the temperature was adjusted between 25 ^{o}C and 75 ^{o}C with nZVI and the results are presented in Figure 3.70 and 3.71. According to Figure 3.70, the results indicated that there is no significant change in sorption with increasing temperature for Hg^{2+} removal. Nonetheless, in Figure 3.71, an obvious decrease was observed in the uptake efficiency of CH$_3$Hg$^+$ as the sorption temperature was increased.

Figure 3.72 illustrates the temperature effect on the iron release after the sorption of both mercury species. As seen from the figure, the iron concentration decreased as the temperature increased which could be due to the oxidation of iron nanoparticles at higher temperatures.
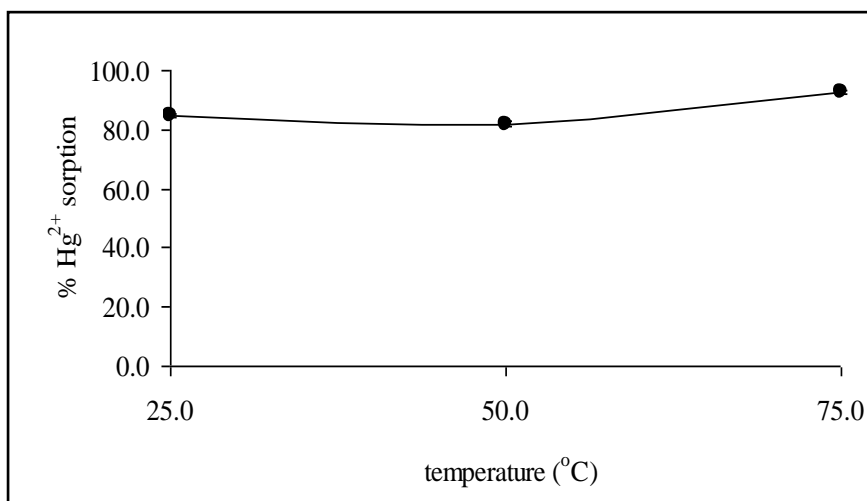
Figure 3.70. Effect of temperature on Hg^{2+} sorption from nZVI at pH 7.0 in 10.0 mL of 1.0 mgL^{-1} solution, sorbent amount: 10.0 mg, shaking time: 30 min, (n=3).
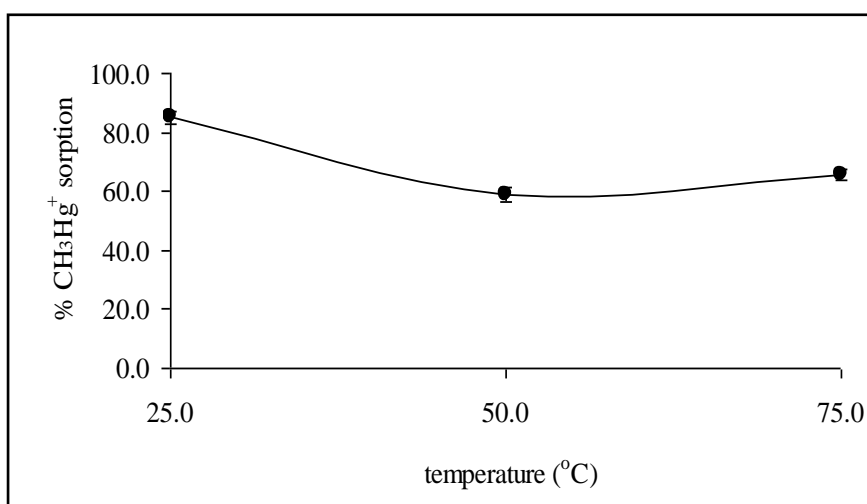
Figure 3.71. Effect of temperature on CH_3Hg^+ sorption from nZVI at pH 7.0 in 10.0 mL of 1.0 mgL^{-1} solution, sorbent amount: 10.0 mg, shaking time: 30 min, (n=3).
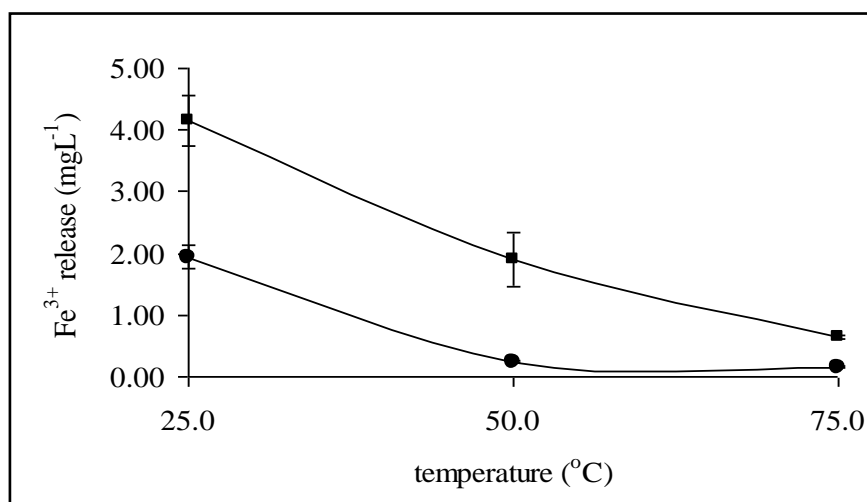
Figure 3.72. Fe^{3+} released from nZVI as a function of temperature at pH 7.0 in 10.0 mL of (●) 1.0 mgL^{-1} Hg^{2+} and (■) 1.0 mgL^{-1} CH_3Hg^+ solution, sorbent amount: 10.0 mg, shaking time: 30 min, n=3).

3.3.2.8. Desorption from nZVI

The efficiency of various eluents for the desorption of Hg^{2+}/CH_3Hg^+ was investigated as explained in Section 2.7.2.5. The eluent concentrations and the corresponding recoveries are given in Table 3.12. As seen from the tables, 2.0 M TGA offered the best results for Hg^{2+} desorption and ~89% recovery was obtained for Hg^{2+} while ~12% recovery was achieved for CH_3Hg^+ with 2.0 M TGA and 1.0 M HNO_3, respectively. Unfortunately, CH_3Hg^+ could not be eluted efficiently by any of the eluents investigated. A negative aspect of TGA, however, was that, it was contaminated with Hg and Hg signal was increased. This signal was negligible when higher Hg^{2+} concentrations was tried to be eluted. Further studies will be performed in order to avoid this problem.

The iron content of the filtrates was also analyzed by FAAS in order to see the dissolved iron after elution. As can be observed from the tables, iron concentration was varying between 250 and 700 mgL^{-1} for both mercury species when mineral acids were used as an eluent. This high concentration could be due to dissolution of iron in these acids.

Table 3.12. Desorption of Hg^{2+} or CH_3Hg^+ from nZVI (1.0 mgL^{-1} Hg^{2+}, sample volume: 10.0 mL, sorbent amount: 10.0 mg, pH=7.0, shaking time: 30 min and temperature: 25 ^oC).

Eluent		% Recovery	Release (mgL^{-1})	% Recovery	Release (mgL^{-1})
		Hg^{2+}	Fe^{3+}	CH_3Hg^+	Fe^{3+}
1 M HNO_3	at 25 ^oC	33.2 ± 4.2	294.0 ± 31.1	12.7 ± 2.8	428.0 ± 14.1
2 M HNO_3	at 25 ^oC	31.8 ± 2.3	335.0 ± 56.6	<5	375.0 ± 23.6
5 M HNO_3	at 25 ^oC	27.8 ± 2.8	390.0 ± 67.2	<5	383.2 ± 22.3
14.3 M HNO_3	at 25 ^oC	32.5 ± 3.5	521.3 ± 26.5	<5	567.3 ± 17.8
1 M HCl	at 25 ^oC	29.0 ± 1.4	345.0 ± 41.0	<5	557.0 ± 41.0
2 M TGA	at 25 ^oC	84.7 ± 7.1	621.0 ± 60.8	<5	550.0 ± 45.8
1% (m/v) L-cysteine in 2% HCl	at 25 ^oC	5.2 ± 0.7	414.5 ± 37.5	<5	448.0 ± 54.6
5% (m/v) thiourea	at 25 ^oC	<5	0.6 ± 0.2	<5	0.6 ± 0.2
10% (v/v) methanol	at 25 ^oC	<5	0.3 ± 0.1	<5	0.3 ± 0.1
1 M HNO_3	at 50 ^oC	26.2 ± 0.0	348.8 ± 30.1	<5	328.8 ± 12.9
2 M HNO_3	at 50 ^oC	24.2 ± 0.7	268.8 ± 83.1	<5	225.8 ± 13.1
5 M HNO_3	at 50 ^oC	26.0 ± 4.6	481.3 ± 58.3	<5	481.3 ± 58.3
14.3 M HNO_3	at 50 ^oC	34.0±4.2	468.8±47.8	<5	472.8 ± 23.4
1 M HCl	at 50 ^oC	54.3±11.0	391.0±58.0	<5	369.2 ± 38.0
2 M TGA	at 50 ^oC	89.4±2.8	671.0±60.8	<5	571.0 ± 30.9

3.3.2.9. Sorption Capacity of nZVI

Sorption capacity of nZVI was performed by changing the concentration of Hg^{2+} between 50.0 and 1000.0 mgL^{-1} at pH 7.0. The variation in the percent sorption of nZVI as a function of concentration is demonstrated in Figure 3.73 which shows a slight decrease in sorption with an increase in the concentration. Finally, the sorption capacity of nZVI for Hg^{2+} was calculated as 4.0 mmol g^{-1} and it can be concluded that nZVI has a very high sorption capacity for Hg^{2+}.
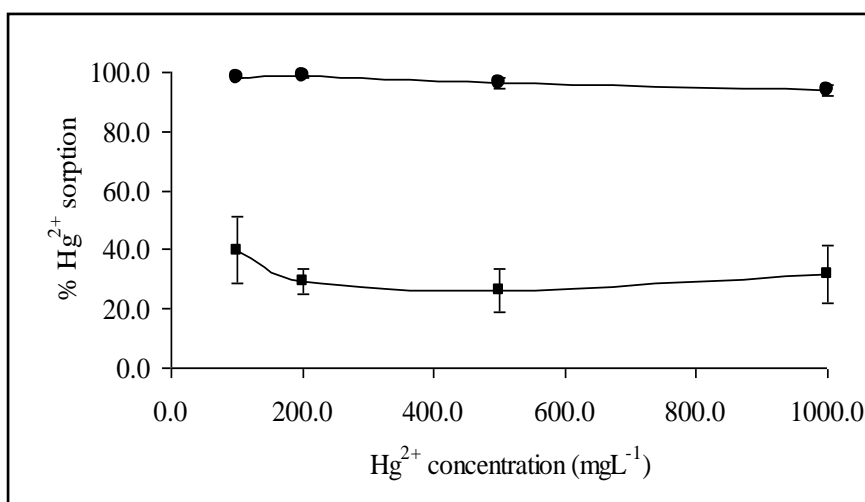
Figure 3.73. Effect of concentration on Hg^{2+} sorption from nZVI at pH 7.0 in 5.0 mL sample volume, sorbent amount: 5.0 mg, shaking time: 30 min, (n=3).

Inorganic mercury (Hg^{2+}) removal trend with respect to (volume of metal solution)/(mass of sorbent) was also studied to reveal the capacity of nZVI by the help V/m ratio. For this purpose, different amounts of nZVI (10.0, 50.0, 100.0, 250.0 and 1000.0 mg) was weighed and added into 1.0 L of 1.0 mgL^{-1} Hg^{2+} solutions at pH 7.0. The resulting V/m ratios are 1, 4, 10, 20 and 100 (mLg^{-1}), respectively. The mixtures were shaken for 30 min, then filtered and analyzed by CVAAS for mercury content. The results regarding Hg^{2+} uptake at various V/m ratios are given in Table 3.13. According to the table, as the V/m ratio increased the removal efficiency of nZVI decreased and quantitative result (>95%) was achieved for the ratio of 1.

Table 3.13. %Hg^{2+} sorption results on nZVI obtained for different V/m ratios at pH=7.0, (Hg^{2+} concentration: 1.0 mgL^{-1}, shaking time: 30 min and temperature: 25 ^{o}C, n=3).

Volume (mL)	Mass of nZVI (mg)	V/m ratio (mLg^{-1})	%Hg^{2+} sorption	Fe^{3+} release (mgL^{-1})
	1000.0	1	97.5 ± 0.1	<0.05
	250.0	4	87.6 ± 2.5	<0.05
1000.0	100.0	10	79.2 ± 3.6	<0.05
	50.0	20	66.2 ± 1.5	<0.05
	10.0	100	51.3 ± 10.2	<0.05

The sorption behavior of nZVI towards Hg^{2+} in the presence of Cu^{2+}, Ni^{2+}, Pb^{2+} was also investigated. For this purpose, 1.0 mgL^{-1} solution of the selected metal ions was prepared and spiked with 1 mgL^{-1} Hg^{2+}. Subsequently, the mixture was shaken for 30 min, and then filtered. The filtrate was analyzed with CVAAS/FAAS for the determination of percentage sorption. The percent sorption values of the chosen ions by nZVI at the optimized conditions for Hg^{2+} are demonstrated in Table 3.14. According to the table, these ions had no interference effect on the sorption of Hg^{2+}, at least under the experimental conditions employed, and quantitative sorption results (>95%) were obtained for mercury at the studied conditions.

Table 3.14. Percent sorption of Hg^{2+} by nZVI in the presence of 1.0 mgL^{-1} Cu^{2+}, Ni^{2+}, Pb^{2+} at the optimized conditions (Hg^{2+} concentration: 1.0 mgL^{-1}, shaking time: 30 min and temperature: 25 ^{o}C, n=3).

sorbent	% Hg^{2+} sorption	% Cu^{2+} sorption	% Ni^{2+} sorption	% Pb^{2+} sorption
nZVI	97.2 ± 0.2	99.0 ± 0.1	61.0 ± 1.7	99.0 ± 0.2

3.3.2.10. Application to Real Samples

The proposed method was validated via spiked samples due to the unavailability of a proper certified reference material for mercury. Spiking was applied to four different types of water; namely, ultrapure, bottled drinking, tap and sea water. The sorption performance of sorbents (nZVI and ZVI-modified/unmodified silica) was

checked and the results are summarized in Table 3.15 for Hg^{2+} and CH_3Hg^+, respectively. As can be seen from the tables, nZVI alone offered very efficient results towards mercury species at pH 7.0; the sorption percentages were above 92% in all cases. The proposed methodology worked also efficiently when ZVI-modified silica was applied as a sorbent and quantitative sorption results (>93%) were achieved for Hg^{2+}. The uptake of CH_3Hg^+ in ZVI-modified silica was again >80% except Gülbahçe tap water. However, in the case of silica, quantitative sorption results were not achieved and unmodified silica did not work properly in all samples. Thus, by the help of modification process the removal efficiency of mercury species increases.

Table 3.15. Percent sorption of spiked (1.0 mgL-1) Hg^{2+} or CH_3Hg^+ with ultrapure, bottled drinking, tap and sea water samples (sample volume: 10.0 mL, sorbent amount: 10.0 mg, pH=7.0, shaking time: 30 min and temperature: 25 $^{\circ}$C, n=3).

Sample	%Hg^{2+} sorption			%CH_3Hg^+ sorption		
	silica	ZVI-silica	nZVI	silica	ZVI-silica	nZVI
Ultrapure Water	81.6 ± 4.2	97.7 ± 0.2	98.0 ± 0.0	61.5 ± 0.0	87.6 ± 4.3	96.0 ± 0.8
Bottled Drinking Water	72.7 ± 3.0	97.3 ± 0.1	98.1 ± 0.1	63.7 ± 2.4	83.2 ± 4.1	92.2 ± 2.9
Alsancak Tap Water	46.9 ± 5.5	98.2 ± 0.1	98.0 ± 0.5	64.1 ± 1.1	95.3 ± 2.2	99.4 ± 0.4
Gülbahçe Tap Water	61.0 ± 2.5	97.2 ± 0.2	97.7 ± 0.1	41.6 ± 2.4	72.2 ± 3.3	96.0 ± 2.0
Sea Water	29.4 ± 4.2	93.0 ± 1.5	96.0 ± 0.7	26.3 ± 6.1	84.8 ± 3.8	100.0 ± 0.0

3.3.3. Sorption with ZVC and ZVC-Modified/Unmodified Sorbents

As it is known that ZVC dissolves at acidic pH values, it is necessary to demonstrate the partial dissolution of ZVC from the resin surface in acidic pHs. For this purpose, the initial experiments focused on the investigation of this effect. The pHs of the solutions were adjusted between 1.0 and 10.0 and copper release as a function of pH was followed by FAAS. Afterwards, the related sorption experiments were done. The effect of solution pH was also examined for ZVC alone.

3.3.3.1. Effect of Solution pH on the Dissolution of ZVC

The pH effect on ZVC is presented in Figure 3.74. According to the figure, the concentration of copper increased as the pH decreased, as expected. In a pH of 1.0, copper ion concentration in the solution was around 700 mgL^{-1} whereas ~480 mgL^{-1} copper was detected at pH 10.0 due to complex formation of $Cu(NH_3)_2^+$. These results might be looked at from two different perspectives; firstly, it is a disadvantage since it precludes the use of the sorbent at pHs below 4.0. Secondly, the complete solubility of ZVC in 0.1 M HCl or HNO_3 can be used in an advantageous way in a way that the retained species can be desorbed from the sorbent very easily with the use of acids.

Figure 3.74. Cu^{2+} released from ZVC as a function of solution pH (10.0 mL ultrapure water, sorbent amount: 10.0 mg, shaking time: 30 min, n=3).

3.3.3.2. Effect of Solution pH on the Dissolution of ZVC-Modified Diaion SK116/Amberlite IRC50

Figure 3.75 represents the copper release as a function of pH. As can be seen, copper concentration was low compared to ZVC alone at the pH value of 1.0 due to the replacement of surface-bound Cu^{2+} ions with H^+ ions. This could be attributed to the successful fixation of the ZVC into the pores of the polymeric resin. The copper dissolution of ZVC-modified Diaion SK116 was less against ZVC-modified Amberlite IRC50 since the former is a strong cation exchanger and the binding of copper onto Diaion SK116 could be more strongly.
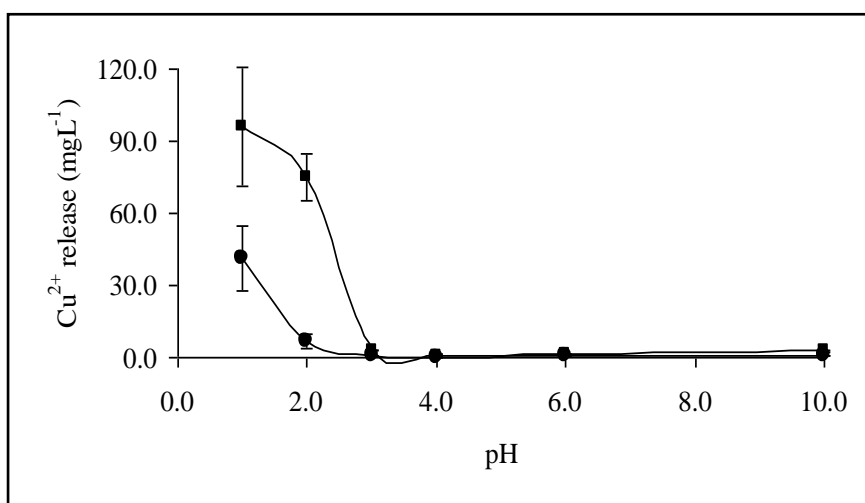
Figure 3.75. Cu^{2+} released from (●) ZVC-modified Diaion SK116 and (■) ZVC-modified Amberlite IRC50 as a function of solution pH (10.0 mL ultrapure water, sorbent amount: 10.0 mg, shaking time: 30 min, n=3).

3.3.3.3. Effect of Solution pH on the Dissolution of ZVC-Modified Amberlite IRA458/Amberlite IRA67

The dissolution of copper on ZVC-modified Amberlite IRA458/Amberlite IRA67 is demonstrated in Figure 3.76. As can be seen, the copper concentration was ~60 mgL^{-1} in ZVC-modified Amberlite IRA458 while ~80 mgL^{-1} was detected in ZVC-modified Amberlite IRA67 and this provides an advantage for sorption studies in order

to study at low pH values. However, the copper release was again low in contrast to ZVC alone.
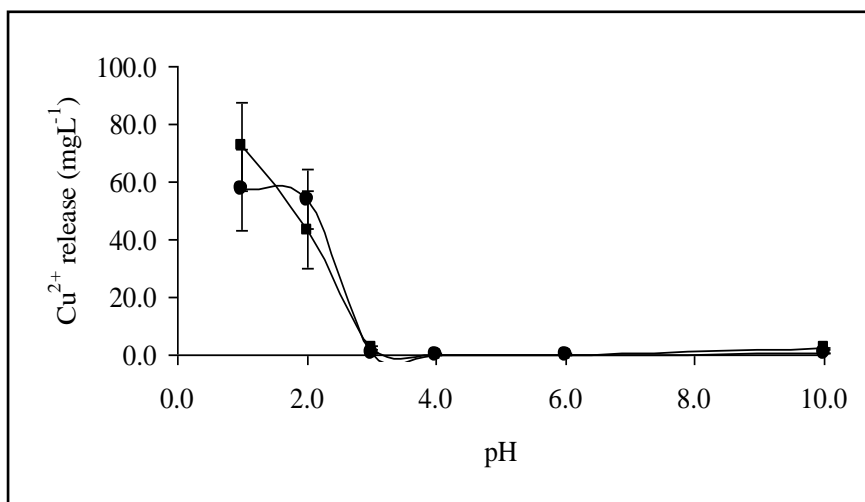
Figure 3.76. Cu^{2+} released from (●) ZVC-modified Amberlite IRA458 and (■) ZVC-modified Amberlite 67 as a function of solution pH (10.0 mL ultrapure water, sorbent amount: 10.0 mg, shaking time: 30 min, n=3).

3.3.3.4. Effect of Solution pH on the Dissolution of ZVC-Modified Alumina

Figure 3.77 indicates the effect of pH on ZVC-modified alumina. Higher amounts of copper were released into the solution but again the copper concentration was low in contrast to ZVC alone.

After dissolution experiments at the studied conditions (10.0 mL ultra pure water, sorbent amount: 10.0 mg) with ZVC alone and unmodified/modified resins, the results demonstrate that the copper release as a function of pH was less in ZVC-modified resins compared to nZVC alone during shaking. The lower extent of dissolution of ZVC from the modified resins may enable to use these types of sorbents at acidic pH range due to their higher resistance to acidic conditions.

As a result of the dissolution experiments, the effect of pH on ZVC and ZVC-modified sorbents towards mercury species were investigated.
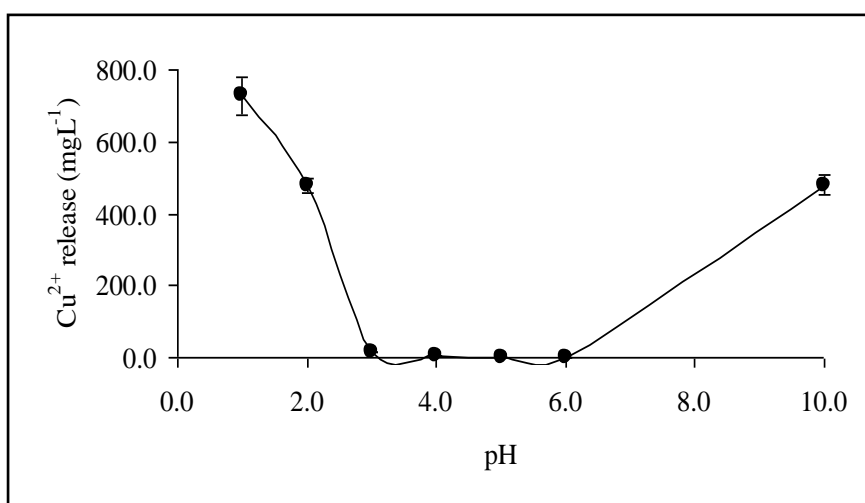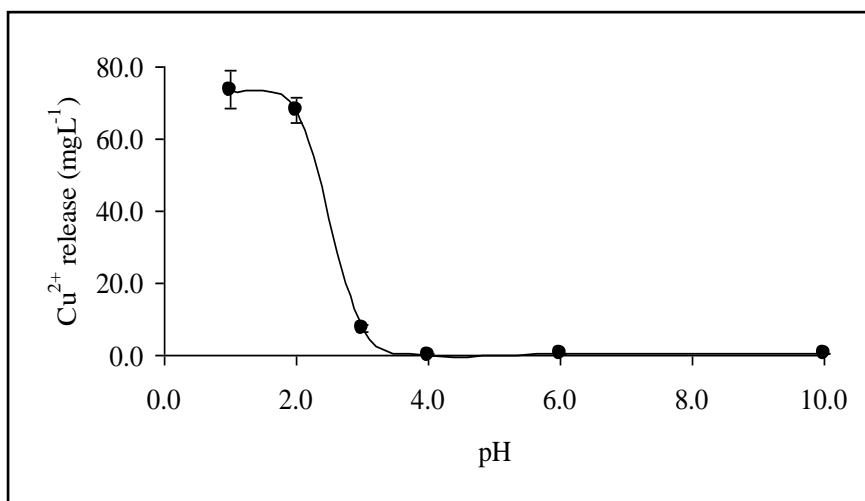
Figure 3.77. Cu^{2+} released from (●) ZVC-modified alumina as a function of solution pH (10.0 mL ultrapure water, sorbent amount: 10.0 mg, shaking time: 30 min, n=3).

3.3.3.5. Effect of Solution pH

3.3.3.5.1. Effect of pH with ZVC

The effect of pH on the sorption of Hg^{2+}/CH_3Hg^+ was studied for ZVC and the percent sorption versus pH solution is monitored in Figure 3.78. As seen from the figure, ZVC offered significant sorption for Hg^{2+} and ~93% sorption was achieved at the studied pH range. On the other hand, quantitative results could not be obtained for CH_3Hg^+ and only ~65% sorption was observed at pH ranges 5.0 and 7.0. Lower pH values were not tried in the sorption studies since ZVC dissolves below pH 3.5.

Figure 3.79 indicates Cu^{2+} release from ZVC as a function of pH after Hg^{2+} and CH_3Hg^+ sorption. According to the figure, ~2 mgL^{-1} copper was measured in solution after sorption when the pH was adjusted to 5.0 and 7.0 whereas it showed an increase when the solution pH was adjusted to 10.0 due to the formation of $Cu(NH_3)_2^+$.
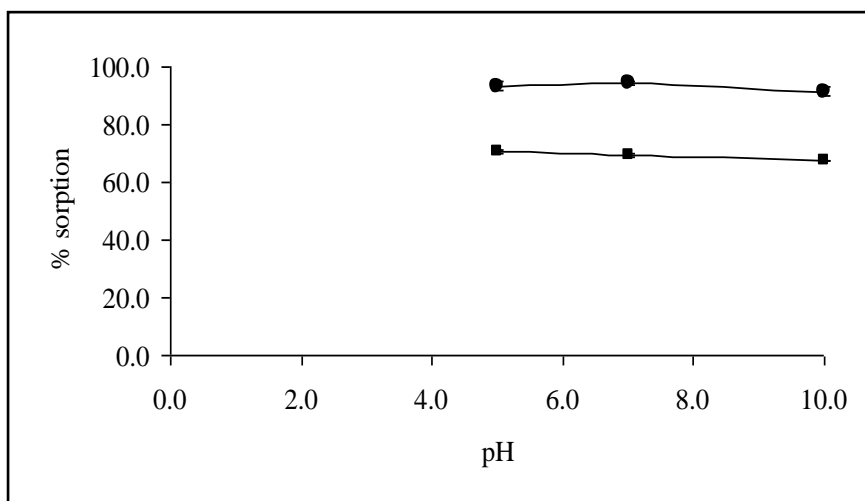
Figure 3.78. (●) Hg^{2+} and (■) CH_3Hg^+ sorption as a function of pH for ZVC (10.0 mL of 1.0 mgL^{-1} solution, sorbent amount: 10.0 mg, shaking time: 30 min, n=3).
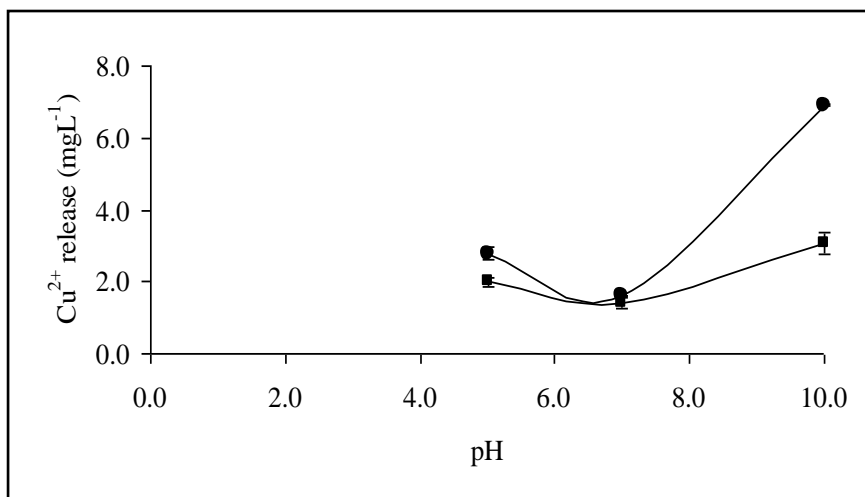
Figure 3.79. Cu^{2+} released from ZVC as a function of pH (10.0 mL of 1.0 mgL^{-1} (●) Hg^{2+} and 1.0 mgL^{-1} (■) CH_3Hg^+ solution, sorbent amount: 10.0 mg, shaking time: 30 min, n=3).

3.3.3.5.2. Effect of pH with ZVC-Modified/Unmodified Diaion SK116

The uptake of Hg^{2+} on ZVI-modified/unmodified Diaion SK116 as a function of pH is demonstrated in Figure 3.80. Obviously, the highest uptake value was obtained at pH 1.0 when ZVC-modified Diaion SK116 was applied as the sorbent. To the contrary, a slight decrease in sorption (~80%) was monitored at pH's greater than 3.0. However, when the results of ZVC-modified/unmodified were compared, the modification process

119

did not have a significant effect on the sorption of Hg^{2+}. Higher sorption results were achieved in the case of Diaion SK116 except pH 1.0. At low pH values Hg^{2+} accumulation on Diaion SK116 was less, but it increased to ~90% when the pH of the solution was higher than 3.0.
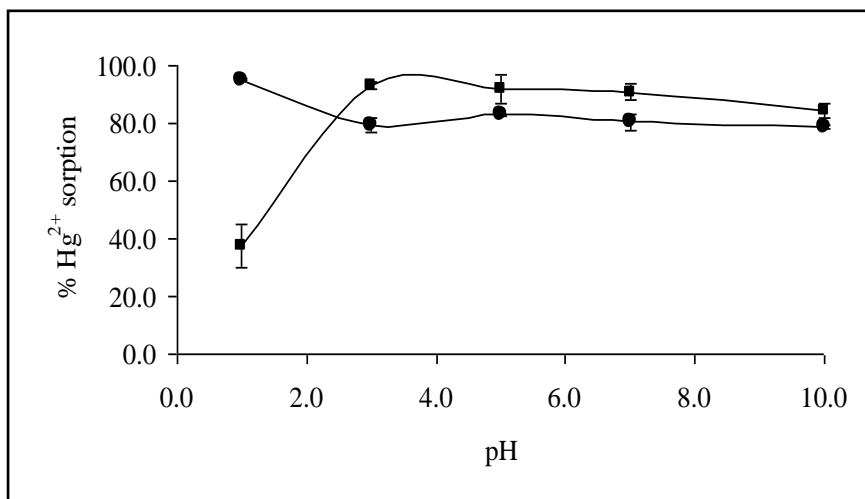
Figure 3.80. Hg^{2+} sorption as a function of pH on (●) ZVC-modified Diaion SK116 and (■) unmodified Diaion SK116 (10.0 mL of 1.0 mgL^{-1} solution, sorbent amount: 10.0 mg, shaking time: 30 min, n=3).

The effect of pH on the removal of CH_3Hg^+ is also investigated and the sorption results for ZVC-modified/unmodified Diaion SK116 are depicted in Figure 3.81. As can be seen, the removal efficiency of CH_3Hg^+ was nearly same for both sorbents except pH 1.0 and ~80% sorption was attained at pH values between 3.0 and 10.0. A difference in acidic pH range could be observed due to the dissolution of copper ions at pH 1.0 which enables a decline in sorption. It can be concluded that the functionalization process is not working well for CH_3Hg^+.

The dissolution of copper on ZVC-modified Diaion SK116 after Hg^{2+}/CH_3Hg^+ sorption is indicated in Figure 3.82. The copper concentration was around 450 and 30 mgL^{-1} for Hg^{2+} and CH_3Hg^+, respectively. Similar results obtained with ultrapure water were also achieved for CH_3Hg^+, but in the case of Hg^{2+}, the results showed similarity with ZVC alone.
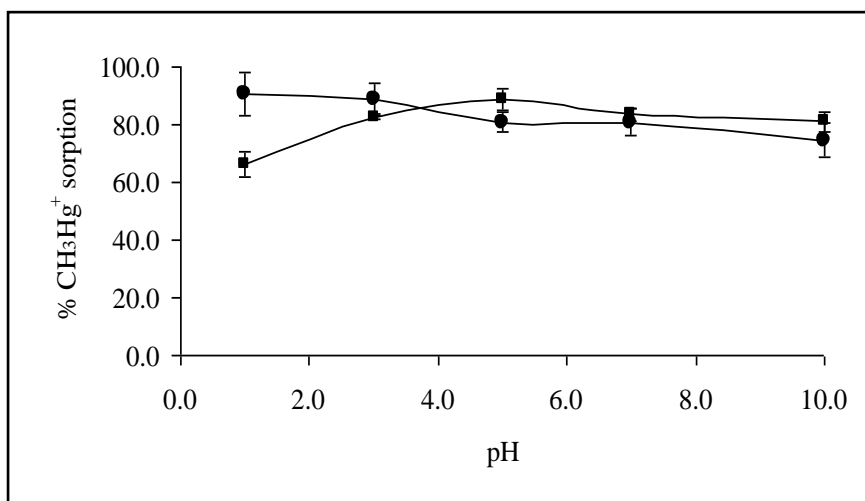
Figure 3.81. CH$_3$Hg$^+$ sorption as a function of pH on (●) ZVC-modified Diaion SK116 and (■) unmodified Diaion SK116 (10.0 mL of 1.0 mgL^{-1} solution, sorbent amount: 10.0 mg, shaking time: 30 min, n=3).
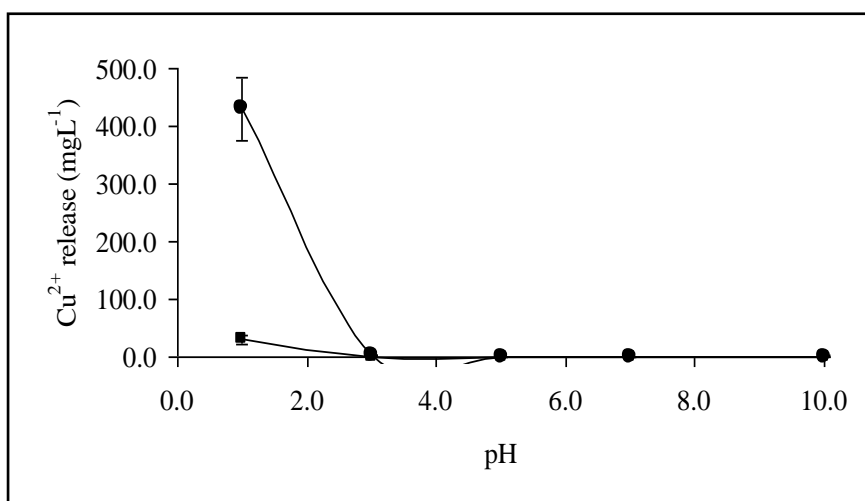
Figure 3.82. Cu^{2+} released from ZVC-modified Diaion SK116 as a function of pH (10.0 mL of 1.0 mgL^{-1} (●) Hg^{2+} and 1.0 mgL^{-1} (■) CH$_3$Hg$^+$ solution, sorbent amount: 10.0 mg, shaking time: 30 min, n=3).

3.3.3.5.3. Effect of pH with ZVC-Modified/Unmodified Amberlite IRC50

Figure 3.83 demonstrates the retention of Hg^{2+} on ZVC-modified/unmodified Amberlite IRC50 as a function of pH. Considering the figure, the sorption was quantitative (>93%) and independent of pH for Hg^{2+} with the use of ZVC-modified Amberlite IRC50 as a sorbent. To the contrary, the sorption behavior of Amberlite

IRC50 towards Hg^{2+} represented a similar performance with ZVC-modified Amberlite IRC50 except pH 1.0. Hence, it can be concluded that there is no difference in sorption upon modification.

Figure 3.83. Hg^{2+} sorption as a function of pH on (●) ZVC-modified Amberlite IRC50 and (■) unmodified Amberlite IRC50 (10.0 mL of 1.0 mgL^{-1} solution, sorbent amount: 10.0 mg, shaking time: 30 min, n=3).

The sorption percentage of CH_3Hg^+ on ZVC-modified/unmodified Amberlite IRC50 is illustrated in Figure 3.84. It was observed that CH_3Hg^+ sorption varied between 85-93% at pH values higher than 3.0 for both sorbents.

Figure 3.84. CH_3Hg^+ sorption as a function of pH on (●) ZVC-modified Amberlite IRC50 and (■) unmodified Amberlite IRC50 (10.0 mL of 1.0 mgL^{-1} solution, sorbent amount: 10.0 mg, shaking time: 30 min, n=3).

Figure 3.85 represents the effect of pH on ZVC-modified Amberlite IRC50 after Hg^{2+}/CH_3Hg^+ sorption. The results showed similarity with the results obtained with ultra pure water for CH_3Hg^+ whereas higher amounts of copper were released into the solution at pH 1.0 for Hg^{2+} as in the case of ZVC alone.
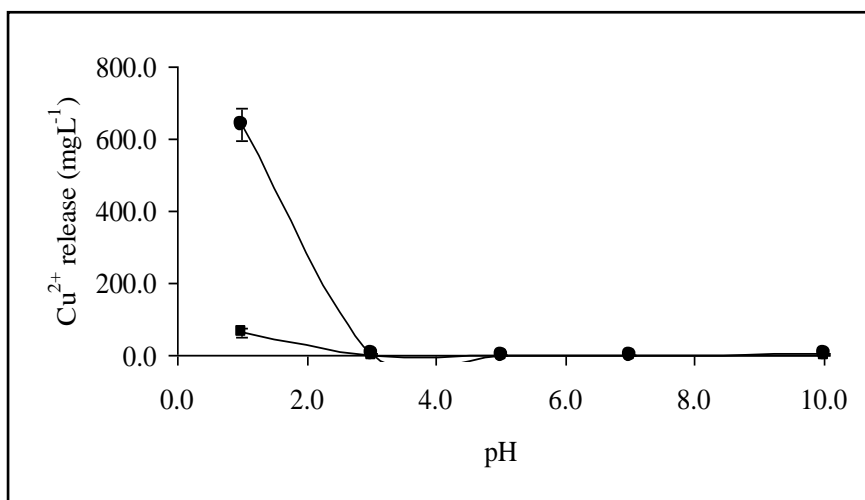
Figure 3.85. Cu^{2+} released from ZVC-modified Amberlite IRC50 as a function of pH (10.0 mL of 1.0 mgL^{-1} (●) Hg^{2+} and 1.0 mgL^{-1} (■) CH_3Hg^+ solution, sorbent amount: 10.0 mg, shaking time: 30 min, n=3).

3.3.3.5.4. Effect of pH with ZVC-Modified/Unmodified Amberlite IRA458

The sorption behavior of ZVC-modified/unmodified Amberlite IRA458 towards Hg^{2+} is demonstrated in Figure 3.86. As can be concluded from the figure, the retention of Hg^{2+} on ZVC-modified Amberlite IRA458 was ~91% at pH 1.0 and a slight decline was monitored after pH 3.0. Nevertheless, the uptake efficiency of Amberlite IRA458 on Hg^{2+} was low compared to the modified sorbent, but the sorption was nearly same at the pH value of 10.0. It can be concluded that the modification process has a little effect on the sorption of Hg^{2+}.

Figure 3.86. Hg^{2+} sorption as a function of pH on (●) ZVC-modified Amberlite IRA458 and (■) unmodified Amberlite IRA458 (10.0 mL of 1.0 mgL^{-1} solution, sorbent amount: 10.0 mg, shaking time: 30 min, n=3).

The uptake of CH_3Hg^+ by ZVC-modified Amberlite IRA458 is revealed in Figure 3.87. In terms of the figure, the removal of CH_3Hg^+ on the modified sorbent was ~95% at all pH values. However, the retention of CH_3Hg^+ on Amberlite IRA458 was low at pH 1.0, but an increase was achieved after pH 3.0 and nearly same sorption results were obtained for both sorbents in the case of CH_3Hg^+.

Figure 3.87. CH_3Hg^+ sorption as a function of pH on (●) ZVC-modified Amberlite IRA458 and (■) unmodified Amberlite IRA458 (10.0 mL of 1.0 mgL^{-1} solution, sorbent amount: 10.0 mg, shaking time: 30 min, n=3).

The effect of pH on ZVC-modified Amberlite IRA 458 after Hg^{2+}/CH_3Hg^+ sorption was shown in Figure 3.88. The copper concentration after sorption was ~380

and ~280 mgL^{-1} at pH 1.0 for Hg^{2+} and CH_3Hg^+, respectively. The results were a bit higher than obtained with ultrapure water.

Figure 3.88. Cu^{2+} released from ZVC-modified Amberlite IRA458 as a function of pH (10.0 mL of 1.0 mgL^{-1} (●) Hg^{2+} and 1.0 mgL^{-1} (■) CH_3Hg^+ solution, sorbent amount: 10.0 mg, shaking time: 30 min, n=3).

3.3.3.5.5. Effect of pH with ZVC-Modified/Unmodified Amberlite IRA67

Figure 3.89 demonstrates the change of the uptake of Hg^{2+} from aqueous solutions at different pH values. Considering the figure, ZVC-modified Amberlite IRA67 exhibited a good affinity towards Hg^{2+} and ~93% of Hg^{2+} was retained on the sorbent surface at all pH values. However, in the case of Amberlite IRA67, the uptake of Hg^{2+} found to be ~60% at pH values between 3.0 and 10.0, but a decrease in sorption was observed at pH 1.0. The decrease in the uptake of Hg^{2+} could be attributed to the protonation of the lone pair of nitrogen which hinder the approach of Hg^{2+}. It can be concluded from the results that the Hg^{2+} sorption increases with the modification process.
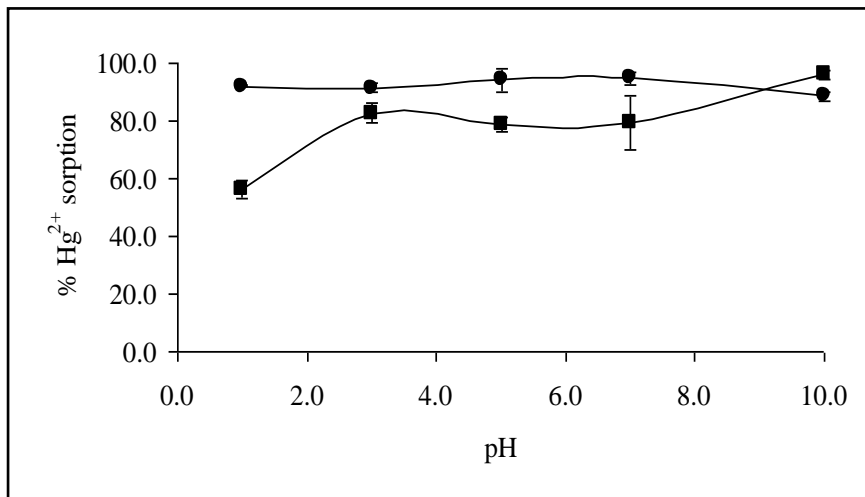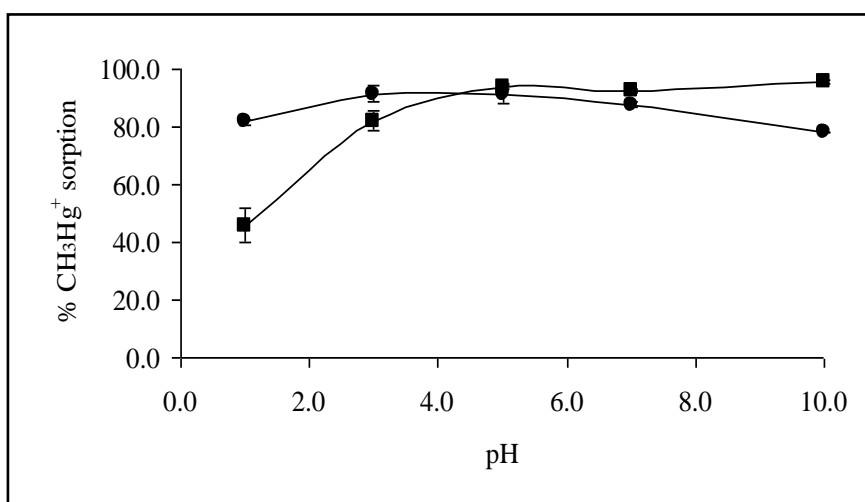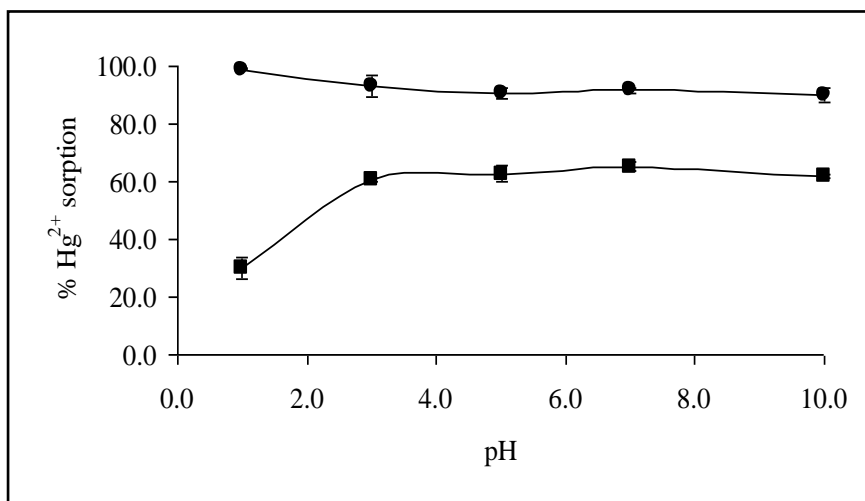
Figure 3.89. Hg^{2+} sorption as a function of pH on (●) ZVC-modified Amberlite IRA67 and (■) unmodified Amberlite IRA67 (10.0 mL of 1.0 mgL^{-1} solution, sorbent amount: 10.0 mg, shaking time: 30 min, n=3).

The effect of the acidity of the medium on the removal of CH_3Hg^+ using ZVC-modified/unmodified Amberlite IRA67 was also investigated. The removal data are presented in Figure 3.90. It is seen that the retention of CH_3Hg^+ on ZVC-modified/unmodified Amberlite IRA67 was nearly same and ~85% sorption was achieved at all pH values for both sorbents. Finally, it can be said that the modification process did not have a significant effect on CH_3Hg^+ removal.
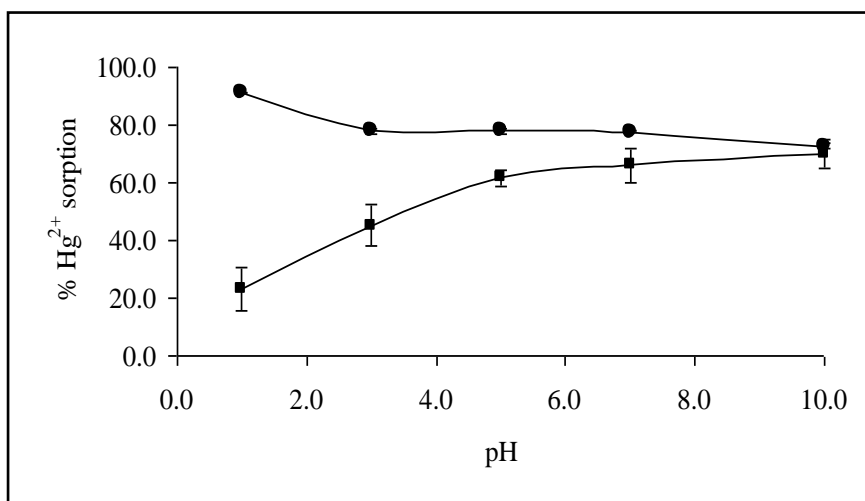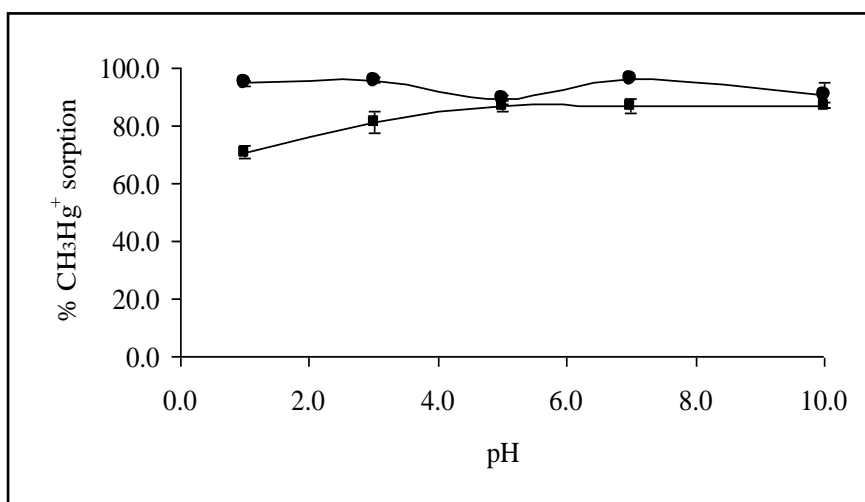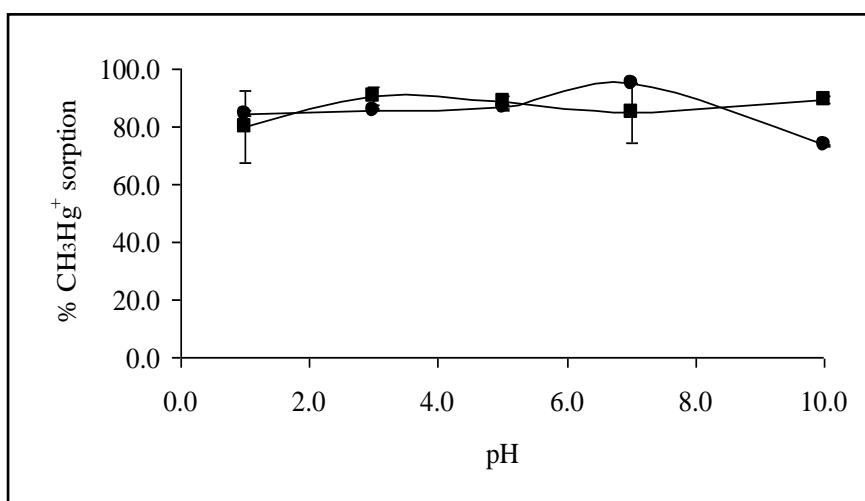

Figure 3.90. CH_3Hg^+ sorption as a function of pH on (●) ZVC-modified Amberlite IRA67 and (■) unmodified Amberlite IRA67 (10.0 mL of 1.0 mgL^{-1} solution, sorbent amount: 10.0 mg, shaking time: 30 min, n=3).

Copper release as a function of pH after Hg^{2+}/CH_3Hg^+ sorption is depicted in Figure 3.91. As can be seen, ~700 mgL^{-1} Cu^{2+} was released in solution after sorption for Hg^{2+} at pH 1.0 whereas the copper concentration was found to be ~400 mgL^{-1} at pH 10.0. Nevertheless, ~15 mgL^{-1} Cu^{2+} was measured after CH_3Hg^+ sorption at pH 1.0.
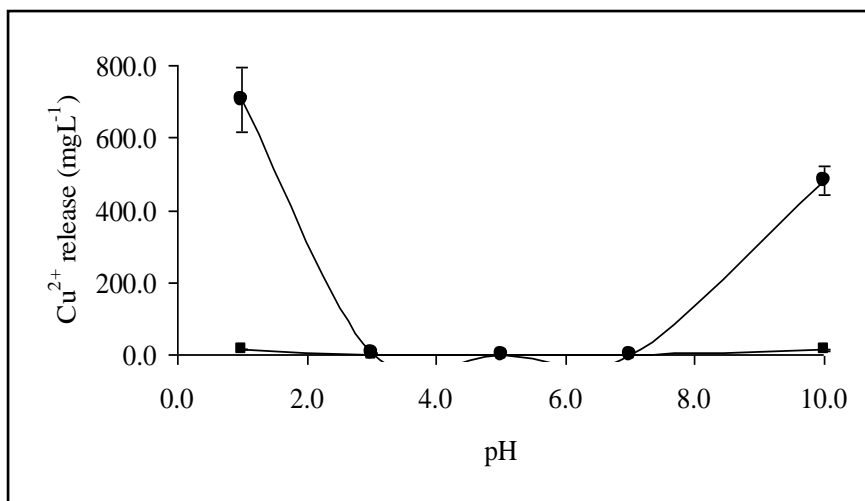
Figure 3.91. Cu^{2+} released from ZVC-modified Amberlite IRA458 as a function of pH (10.0 mL of 1.0 mgL^{-1} (●) Hg^{2+} and 1.0 mgL^{-1} (■) CH_3Hg^+ solution, sorbent amount: 10.0 mg, shaking time: 30 min, n=3).

3.3.3.5.6. Effect of pH with ZVC-Modified/Unmodified Alumina

The effect of pH on the extent of Hg^{2+} sorption by ZVC-modified/unmodified alumina is shown in Figure 3.92. It can be noticed that the removal of Hg^{2+} was ~77% and independent of pH for ZVC-modified alumina. To the contrary, the removal of Hg^{2+} on unmodified alumina increased with increasing pH and reached a maximum value (~80%) at pH 5.0. Thus, the modification process seemed to have a little effect on the removal of Hg^{2+}.
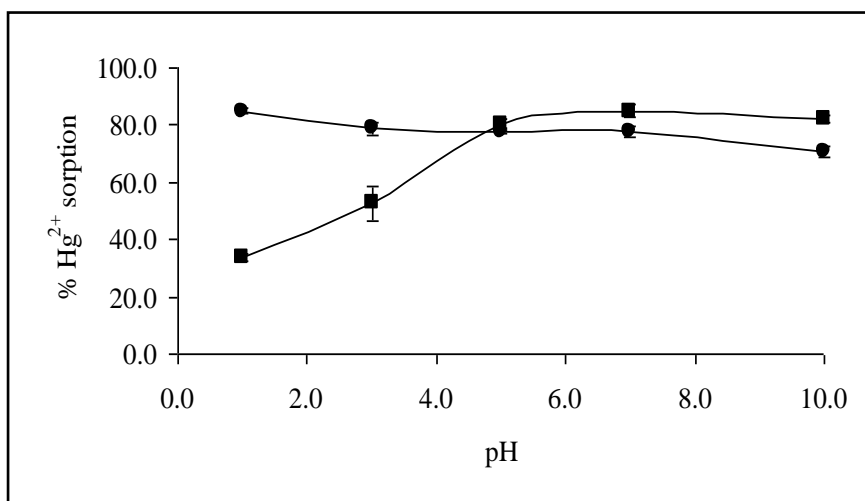
Figure 3.92. Hg^{2+} sorption as a function of pH on (●) ZVC-modified alumina and (■) unmodified alumina (10.0 mL of 1.0 mgL^{-1} solution, sorbent amount: 10.0 mg, shaking time: 30 min, n=3).

CH_3Hg^+ accumulation on ZVC-modified/unmodified alumina is represented in Figure 3.93. As seen from the figure, the removal efficiency of CH_3Hg^+ seemed to be the same for ZVC-modified/unmodified alumina at all pH values. This could be due to the insufficient coating of ZVC onto the alumina surface. It can be concluded from the results that the modification of alumina surface with ZVC did not bring any advantage over unmodified alumina; the sorption of CH_3Hg^+ did not change significantly.
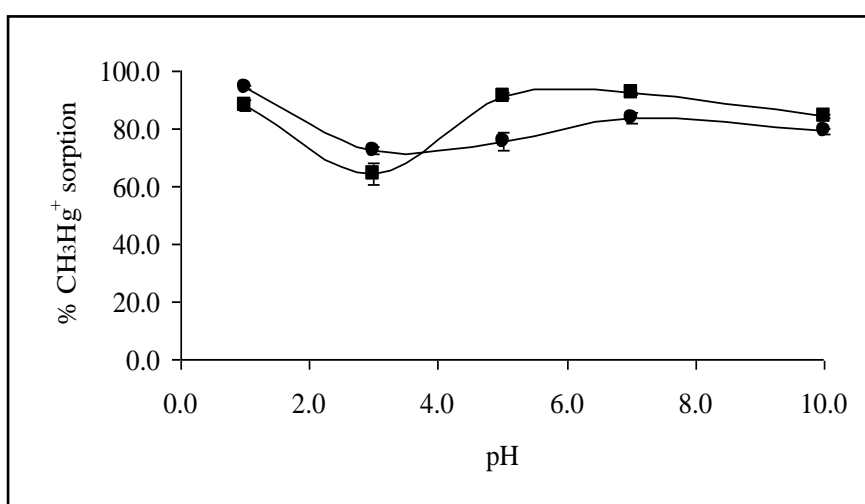
Figure 3.93. CH_3Hg^+ sorption as a function of pH on (●) ZVC-modified alumina and (■) unmodified alumina (10.0 mL of 1.0 mgL^{-1} solution, sorbent amount: 10.0 mg, shaking time: 30 min, n=3).

Figure 3.94 indicates the copper dissolution from ZVC-modified alumina as a function of pH after Hg^{2+}/CH_3Hg^+ sorption. According to the figure, ~650 and ~78

128

mgL^{-1} copper was detected in solution after sorption when the pH was 1.0 for Hg^{2+} and CH$_3$Hg$^+$, respectively. Higher amounts were released into the solution due to dissolution of surface bound Cu^{2+} ions into the solution.
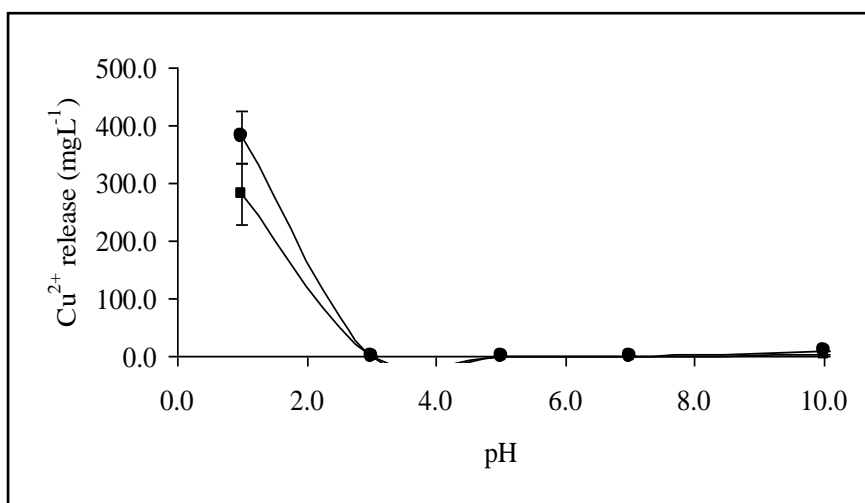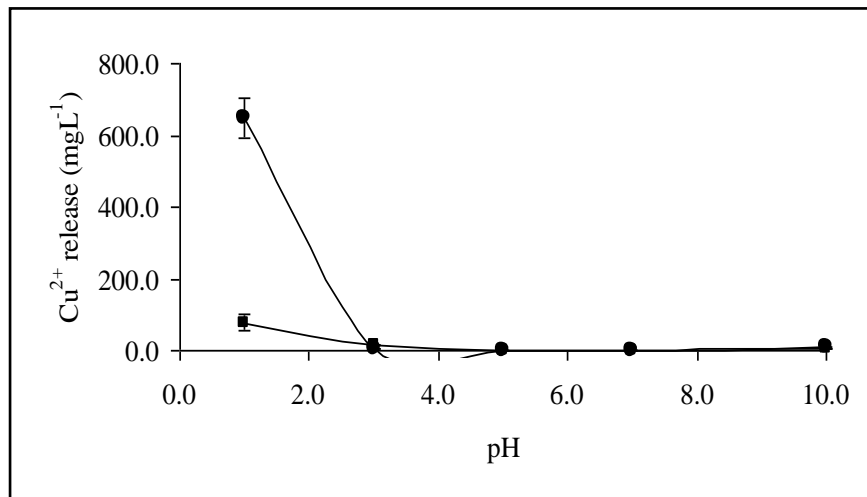

Figure 3.94. Cu^{2+} released from ZVC-modified alumina as a function of pH (10.0 mL of 1.0 mgL^{-1} (●) Hg^{2+} and 1.0 mgL^{-1} (■) CH$_3$Hg$^+$ solution, sorbent amount: 10.0 mg, shaking time: 30 min, n=3).

At the studied conditions (10.0 mL of 1.0 mgL^{-1} solution, sorbent amount: 10 mg), since the modification process seems to have little effect on the sorption of Hg^{2+}/CH$_3$Hg$^+$, the following experiments are carried out with only ZVC.

3.3.3.6. Effect of Sorbent Amount (Solid/Liquid Ratio)

Sorbent amount is an important parameter in sorption studies because it determines the capacity of sorbent for a given initial concentration of metal ion solution. The effect of ZVC amount on the sorption of Hg^{2+} is depicted in Figure 3.95. It was observed that the removal efficiency of ZVC was ~90% for Hg^{2+} even in 5.0 mg and quantitative sorption results (~98%) were achieved within 10.0 mg for 10.0 mL solution; further increasing had no effect on Hg^{2+} removal. Finally, a sorbent amount of 10.0 mg was chosen for further studies.
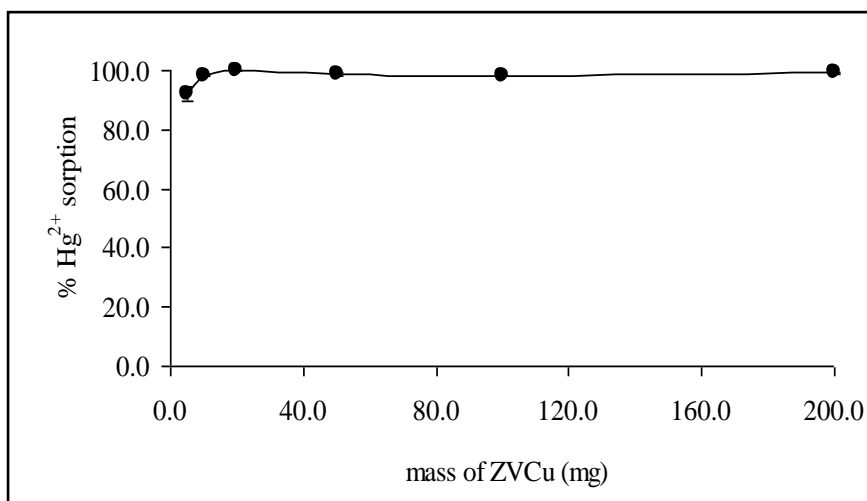
Figure 3.95. Effect of ZVC amount on Hg^{2+} sorption at pH 7.0 in 10.0 mL of 1.0 mgL^{-1} solution, shaking time: 30 min, (n=3).

The dissolution of copper after sorption is also investigated and the results are demonstrated in Figure 3.96. As can be seen, with the increasing amount of ZVC from 5.0 to 20.0 mg, the concentration of copper increased up to 1.5 mgL^{-1}. After 20.0 mg, a slight decrease in copper concentration was observed and this could be due to the increase in the amount of oxidized ZVC particles.
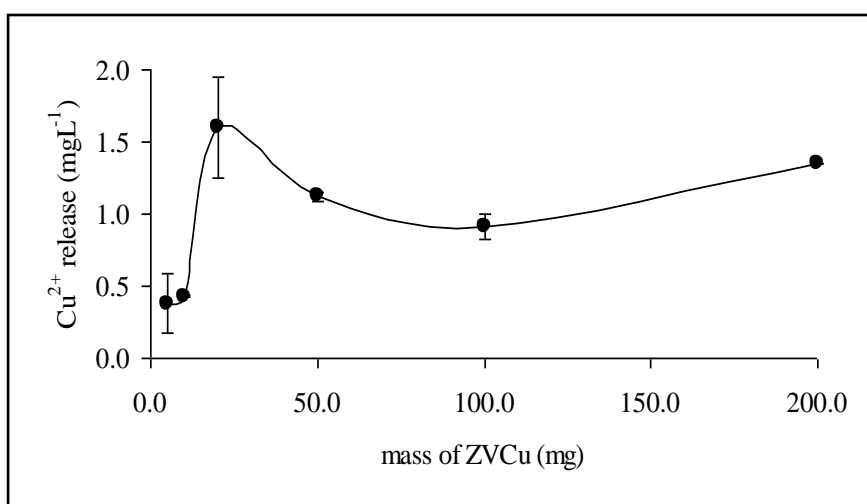
Figure 3.96. Cu^{2+} released as a function of mass of ZVC at pH 7.0 in 10.0 mL of 1.0 mgL^{-1} Hg^{2+} solution, shaking time: 30 min, n=3).

3.3.3.7. Effect of Shaking Time

The effect of shaking time on the extracted metal ion is considered as a key factor which must be studied and evaluated. The extraction of Hg^{2+} on ZVC as a function of shaking time is graphically demonstrated in Figure 3.97. The results indicated that the extraction percentage of Hg^{2+} reached above 96% within 1 min. Thus, the sorption of Hg^{2+} on ZVC is very fast. However, 30 min shaking time was chosen in order to be on the safe side to have quantitative sorption.
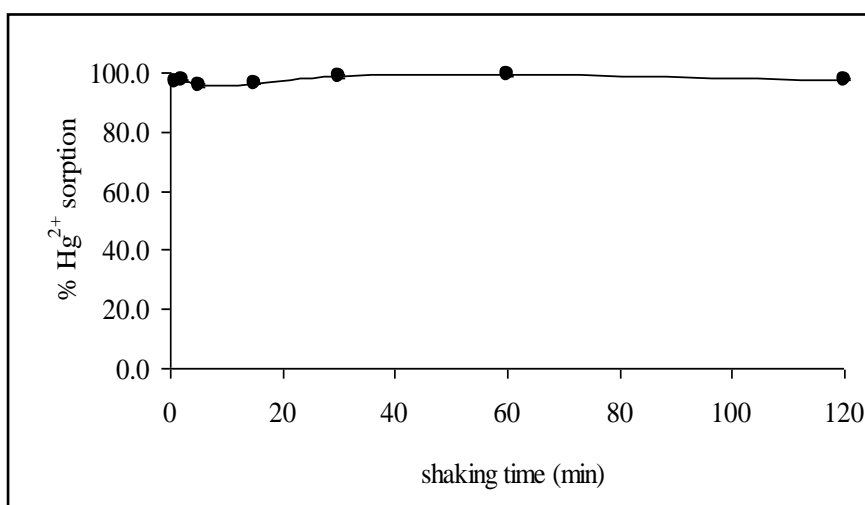
Figure 3.97. Effect of shaking time on Hg^{2+} sorption by ZVC at pH 7.0 in 10.0 mL of 1.0 mgL^{-1} solution, sorbent amount: 10.0 mg, (n=3).

The concentration of copper in the supernatant solution was also determined after Hg^{2+} sorption. Figure 3.98 indicates the copper release as a function of shaking time. As can be seen, the copper dissolves ~1.7 mgL^{-1} in early times (1-2 min) and then it showed a decrease as the time passed. This could be due to the increase of the interaction of ZVC with Hg^{2+}.
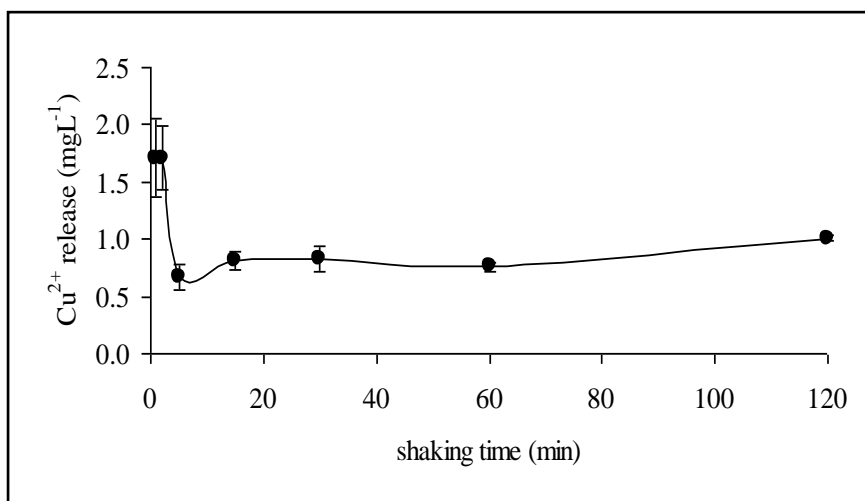
Figure 3.98. Cu^{2+} released from ZVC as a function of shaking time at pH 7.0 in 10.0 mL of 1.0 mgL^{-1} Hg^{2+} solution, sorbent amount: 10.0 mg, n=3).

3.3.3.8. Effect of Temperature

Figure 3.99 shows the variation of Hg^{2+} concentration at different sorption temperatures of 25.0, 50.0 and 75.0 ^{o}C. The experimental data represents that the uptake efficiency of ZVC on Hg^{2+} removal did not change with increasing temperature and quantitative sorption results were achieved in the sorption of Hg^{2+}.
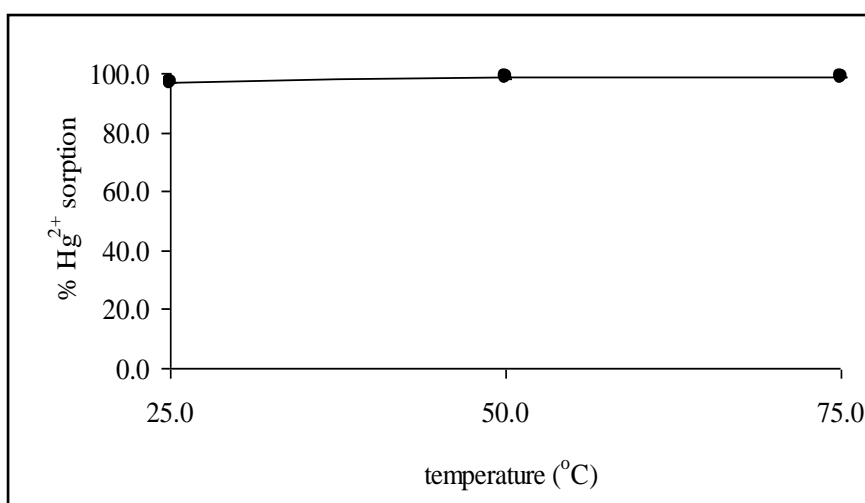
Figure 3.99. Effect of temperature on Hg^{2+} sorption from ZVC at pH 7.0 in 10.0 mL of 1.0 mgL^{-1} solution, sorbent amount: 10.0 mg, shaking time: 30 min, (n=3).

Figure 3.100 depicts the temperature effect on ZVC after the sorption. According to the figure, the concentration of copper increased as the temperature

132

increased and it stayed constant after 50 ^{o}C. The increase in concentration may be due the oxidation of copper nanoparticles at high temperatures.
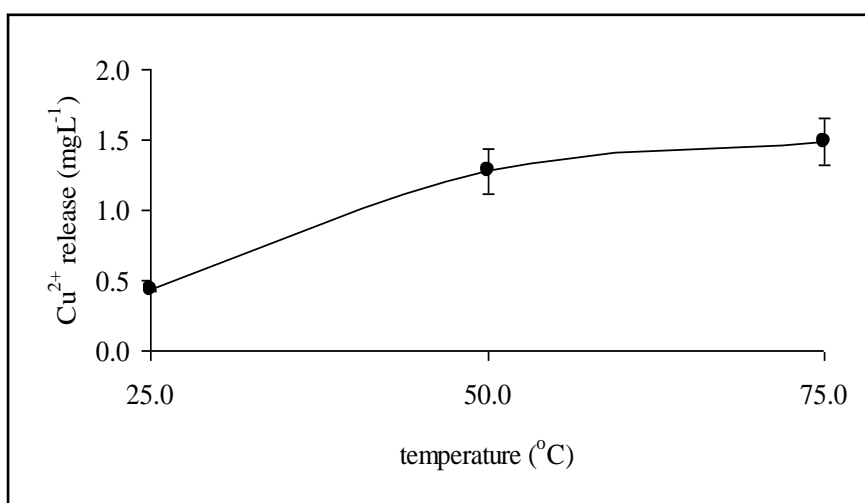
Figure 3.100. Cu^{2+} released from ZVC as a function of temperature at pH 7.0 in 10.0 mL of (●) 1.0 mgL^{-1} Hg^{2+}, sorbent amount: 10.0 mg, shaking time: 30 min, n=3).

3.3.3.9. Desorption from ZVC

A series of eluents have been tested for mercury recovery from ZVC. The selection of these eluents was based on acid-base properties or complexation reactions. Table 3.16 reports the eluent concentrations and the corresponding recoveries for Hg^{2+}. As can be seen from the table, all of the eluents tested except HCl was not sufficient to desorp Hg^{2+}. Nonetheless, ~53% desorption efficiency was obtained with the use of 1 M HCl. Further studies will be performed in order to elute the mercury species from ZVC.

The copper content in the supernatant was also analyzed with FAAS in order to observe the copper release after elution. It is demonstrated in the table that copper release varied between 95 and 860 mgL^{-1} for Hg^{2+} when mineral acids/bases were used as an eluent. The higher amounts were released into the solution due to the dissolution of copper in acidic or basic media.

Table 3.16. Desorption of Hg^{2+} from ZVC (1.0 mgL^{-1} Hg^{2+}, sample volume: 10.0 mL, sorbent amount: 10.0 mg, pH=7.0, shaking time: 30 min and temperature: 25 ^{o}C).

Eluent	% Recovery	Release (mgL^{-1})
	Hg^{2+}	Cu^{2+}
1 M HNO_3	<5	616.5 ± 7.8
1 M HCl	53.2 ± 2.6	861.0 ± 73.4
1 M NH_3	<5	95.5 ± 9.2
2% (m/v) KIO_3 in 1 M HCl	<5	747.0 ± 56.6
2% (m/v) urea	<5	3.5 ± 0.0

3.3.3.10. Application to Real Samples

The proposed method was applied to four different types of water samples from İzmir. Table 3.17 summarizes the sorption performance of ZVC and ZVC-modified alumina towards Hg^{2+} in ultrapure, bottled drinking, tap and sea water. According to the table, ZVC alone worked efficiently towards Hg^{2+} for all water samples except sea water at pH 7.0; the sorption percentages were above 85% in all cases. Although not quantitative, a relatively high uptake (>75%) obtained for sea water could also be considered as indication of the efficiency of the proposed methodology even in a heavy matrix sample. The performance of ZVC-modified alumina towards Hg^{2+} was also checked in water samples. Higher sorption results (>94%) were also achieved for Hg^{2+} at pH 7.0 except sea water but they were not as good as ZVC alone and a slight decrease was observed when compared. This could be due to the inefficiency of the modification process.

Table 3.17. Percent sorption of spiked (1.0 mgL^{-1}) Hg^{2+} with ultrapure, bottled drinking, tap and sea water samples (sample volume: 10.0 mL, sorbent amount: 10.0 mg, pH=7.0, shaking time: 30 min and temperature: 25 ^{o}C, n=3).

Sample	%Hg^{2+} sorption	
	ZVC	ZVC-alumina
Ultrapure Water	97.9 ± 0.3	95.3 ± 1.7
Bottled Drinking Water	97.0 ± 0.1	94.2 ± 0.6
Alsancak Tap Water	85.4 ± 5.1	78.1 ± 1.1
Gülbahçe Tap Water	96.6 ± 0.4	94.5 ± 0.0
Sea Water	76.0 ± 0.8	33.0 ± 1.0

CHAPTER 4

CONCLUSIONS

Determination of mercury species in environmental samples is usually performed by CVAAS. Although these techniques enable very sensitive determinations for mercury, it may still be necessary to apply a preconcentration step due to their low concentrations in certain samples. In addition, the presence of heavy matrix in some matrices may necessitate an efficient separation/matrix removal step to be employed prior to instrumental measurements.

In this thesis, a new method was proposed for the preconcentration of mercury in environmental samples prior to their determination by CVAAS. For this purpose, three novel sorbents, namely, 3-MPTMS-modified silica, nZVI and ZVC have been developed and used for the sorption of mercury from waters. Initial studies were concentrated on the synthesis and characterization of the sorbents. The results have demonstrated the success of synthesis procedure and surface modification with the functional groups. Characterization of the sorbents was performed with SEM/EDX, TGA, BET surface analysis, XRD, particle size measurement and elemental analysis and the successful attachment of the functional groups on the surface of the substrate has been demonstrated. After characterization, the experiments were concentrated on the investigation of a proper sorbent for mercury species. In addition to the sorbents developed, sorption behavior of several commercial resins was also investigated for the same purpose. For each sorbent, sorption parameters were optimized and performance data were obtained by CVAAS.

In the case of 3-MPTMS-modified silica, it has been demonstrated that either Hg^{2+} or CH_3Hg^+ can be retained on the sorbent at all pH values varying between 1.0 and 10.0. Quantitative uptake (>98%) towards both mercury species occurred even in 1 min which showed the fast kinetics of sorption process. In addition, only 5.0 mg sorbent worked efficiently for mercury species and the removal efficiency did not change with increasing temperature.

In the second part of the study, the synthesis of nZVI was performed with liquid phase reduction method and apart from this; several inorganic substrates and ion

exchange resins were modified with nZVI. According to the sorption results, the modification process did not have a signification effect on the removal of both mercury species. Thus, the following experiments were carried out with only nZVI. Quantitative sorption results (>90%) were achieved at pH values 5.0 and 7.0. A decrease in the sorption of mercury was observed at pH 10.0 which could be due to precipitation of $Fe(OH)_3$ at basic pH range. Besides the pH experiments, the sorbent amount, the effect of shaking time and temperature on sorption were also investigated. 10.0 mg of nZVI and 30 min shaking time were sufficient for quantitative sorption and the temperature did not change significantly with increasing temperature.

In the third part, the synthesis and modification of ZVC were carried out. As in the case of nZVI, the removal of Hg^{2+} did not improve with the modification process and nearly the same sorption results were achieved. Hence, ZVC were used for further experiments. The removal of Hg^{2+} was >96% at studied pH range and independent of pH. The sorption kinetics of ZVC was also fast; even in 1 min higher sorption (>95%) was obtained. 10.0 mg sorbent amount was adequate for quantitative sorption and temperature did not have an effect on the removal of Hg^{2+}.

Finally, the analytical performance of the proposed method was tested on real samples. The results demonstrated that the methodology can be applied to these types of samples for mercury determination.

REFERENCES

Andac, M., Asan, A., Bekdemir, Y., Kutuk, H., Isıldak, I. 2003. Spectrophotometric Flow-Injection Analysis of Mercury(II) in Pharmaceuticals with P-Nitrobenzoxosulfamate. *Talanta* 60: 191.

Antochshuk, V., Jaroniec, M. 2002. 1-Allyl-3-propylthiourea modified mesoporous silica for mercury removal. *Chem. Commun*. 258-259.

Bailey, S.E., Olin, T.J., Bricka, R.M. and Adrian, D.D. 1999. A Review of Potentially Low-Cost Sorbents for Heavy Metals. *Wat. Res.* 33: 2469-2479.

Bendl, R.F., Madden, J.T., Regan, A.L., Fitzgerald, N. 2006. Merccury determination by cold vapor atomic absorption spectrometry utilizing UV photoreduction. *Talanta* 68: 1366-1370.

Bennun, L., Gillette, V.H., Greaves, E.D. 1999. Data Processing Technique for Mercury Determination by Total-Reflection X-Ray Fluorescence, Using Amalgamation with Gold. *Spectrochimica Acta Part B* 54: 1291-1301.

Bibby, A., Mercier, L. 2002. Mercury(II) ion adsorption behavior in thiol-functionalized mesoporous silica microspheres. *Chem. Mater.* 14: 1591-1597.

Blowes, D.W., Ptacek, C.J., Benner, S.G., McRae, C.W.T., Bennett, T.A., Puls, R.W. 2000. Treatment of inorganic contaminants using permeable reactive barriers. *Journal of Contaminant Hydrology* 45: 123-137.

Bloxham, M.J., Hill, S.J. and Worsfold, P.J. 1996. Determination of mercury in filtered sea-water by flow injection with on-line oxidation and atomic fluorescence spectrometric detection. *J. Anal. Atom. Spectrosc.* 11: 511-514.

Bramanti, E., Lomonte, C., Onor, M., Zamboni, R., D'Ulivo, A., Raspi, G. 2005. Mercury speciation by liquid chromatography coupled with on-line chemical vapour generation and atomic fluorescence spectrometric detection (LC–CVGAFS). *Talanta* 66: 762–768.

Brinker, Jeffey C. and George W. Scherer 1990. *Sol-Gel Scien*ce. San Diego: Academic Press.

Burguera, J.L., Quintana, I.A., Salager, J.L., Burguera, M., Rondon, C., Carrero, P., Anton de Salager, R. and Petit de Pena, Y. 1999. The use of emulsions for the determination of methylmercury and inorganic mercury in fish-eggs oil by cold vapor generation in a flow injection system with atomic absorption spectrometric detection. *Analyst* 124: 593-599.

Camel, V. 2003. Solid Phase Extraction of Trace Elements. *Spectrochimica Acta part B* 58: 1177-1233.

Castro-Gonzalez, M.I. and Mendez-Armenta, M. 2008. Heavy metals: Implications associated to fish consumption. *Environ. Toxicology and Pharmacology* 26: 263-271.

Choe, S., Chang, Y.Y., Hwang, K.Y., Khim, J. 2000. Kinetics of reductive denitrification by nanoscale zero-valent iron. *Chemosphere* 41: 1307-1311.

Cruz-Guzman, M., Celis, R., Hermosin, M.C., Koskinen, W.C., Nater, E.A., Cornejo, J. 2006. Heavy Metal Adsorption by Montmorillonites Modified with Natural Organic Cations. *Soil Sci. Soc. Am. J.* 70: 215-221.

Dabrowski, A., Hubicki, Z., Podkoscielny, P. and Robens, E. 2004. Selective removal of the heavy metal ions from waters and industrial wastewaters by ion-exchange method. *Chemosphere* 56: 91-106.

Ebdon, L., Evans, E.H., Fisher, A., Hill, S.J. 1998. *An Introduction to Analytical Atomic Spectrometry*, (John Wiley and Sons, Chichester), p. 151-152.

El-Nahhal, I.M., El-Ashgar, N.M. 2007. A review on polysiloxane-immobilized ligand systems: Synthesis, characterization and applications. *J Organomet Chem.* 692: 2861-2886.

Eroğlu, T. 1996. "Use of Sol-gel Beads in Preconcentration", M.Sc. Thesis, METU, Ankara.

Falter, R. and Schöler, H.F. 1994. Interfacing high-performance liquid chromatography and cold vapor atomic absorption spectrometry with on-line UV irradiation for the determination of organic mercury compounds *J Chromatogr A*. 675: 253-256.

Gavilan, K.C., Pestov, A.V., Garcia, H.M., Yatluk, Y., Roussy, J., Guibal, E. 2009. Mercury sorption on a thiocarbamoyl derivative of chitosan. *Journal of Hazardous Materials* 165: 415-426.

Goswami, A., Singh, A.K. 2002. Silica gel functionalized with resacetophenone: synthesis of a new chelating matrix and its application as metal ion collector for their flame atomic absorption spectrometric determination. *Analytica Chimica Acta* 454: 229-240.

Göktürk, G., Delzendeh, M., Volkan, M. 2000. Preconcentration of Germanium on Mercapto-modified Silica Gel. *Spectrochim Acta B* 55: 1063-1071.

Guo, Y., Guadalupe, A.R. 1999. Preconcentration and Voltammetry of Mercury on a Functionalized Sol-Gel Thin Film Modified Glassy Carbon Electrode. *Journal of Pharmaceutical and Biomedical Analysis* 19: 175.

Hinds, M.W. 1998. Determination of Mercury in Gold Bullion by Flame and Graphite Furnace Atomic Absorption Spectrometry. *Spectrochimica Acta B* 53: 1063-1068.

Hintelmann, H. and Wilken, R.D. 1993. The analysis of organic mercury compounds using liquid chromatography with on-line atomic fluorescence spectrometric detection. *Appl Organometr Chem* 7: 173-180.

Houserov, P., Mate, D., Kub, V., Komarek, J. 2006. Liquid chromatographic – cold vapour atomic fluorescence spectrometric determination of mercury species. *J. Sep. Sci*. 29: 248–255.

http://www.unece.org/env/lrtap/full%20text/1998.Heavy.Metals.e.pdf. (accessed February 20, 2011.

http://people.uwec.edu/piercech/Hg/mercury_water/sources.htm (accessed March 1, 2011)

http://www.mercury.utah.gov/atmospheric_transport.htm (accessed March 1, 2011)

http://people.uwec.edu/piercech/Hg/mercury_water/drinkingwater.htm (accessed March 1, 2011)

http://en.wikipedia.org/wiki/Mercury_poisoning (accessed March 1, 2011)

Kanel, S.R., Manning, B., Charlet, L., Choi, H. 2005. Removal of arsenic(III) from groundwater by nanoscale zero-valent iron. *Environ. Sci. Technol.* 39: 1291-1298.

Keating, M.H., Mahaffey, K.R., Schoeny, R., Rice, G.E., Bullock, O.R., Ambrose, R.B., Swartout, J., Nichols, J.W. 1997. Mercury Study Report to Congress-Volume I: Executive Summary. Office of Air Quality Planning and Standards and Office of Research Development, (December 1997), *U.S. Environmental Protection Agency* 1: 1-95.

Krishna, M.V., Karunasagar, D., Rao, S.V. and Arunachalam, J. 2005. Preconcentration and speciation of inorganic and methyl mercury in waters using polyaniline and gold trap-CVAAS. *Talanta* 68: 329-335.

Kuban, P., Pelcova, P., Margetinova, J., Kuban, V. 2009. Mercury speciation by CE: An update. *Electrophoresis* 30: 92–99.

Kvitek, R.J., Evans, J.F., Carr, P.W. 1982. Diamine/Silane-Modified controlled pore glass: The covalent attachment reaction from aqueous solution and the mechanism of reaction of bound diamine with copper(II). *Anal Chim Acta* 144: 93-106.

Lawes, G., 1998. *SEM Instrumentation in Scanning Electron Microscopy and X-Ray Microanalysis*, (John Wiley&Sons, London), pp. 1-20, 78-79. [p.3, 6, 11]

Leermakers, M., Baeyens, W., Quevauviller, P., Horvat, M. 2005. Mercury in environmental samples: Speciation, artifacts and validation. *Trends in Analytical Chemistry* 24(5): 383-393.

Lev, O., M. Tsionsky, L. Rabinovich, V. Glezer, S. Sampath, I. Pankratov, J. Gun. 1995. Organically modified sol-gel sensors. *Analytical Chemistry* 67: 22A-30A.

Li, X., Brown, D.G., Zhang, W. 2007. Stabilization of biosolids with nanoscale zero-valent iron (nZVI). *Journal of Nanoparticle Research* 9: 233-243.

Li, L., Fan, M., Brown, R.C., van Leeuwen, L. 2006a. Synthesis, Properties, and Environmental Applications of Nanoscale Iron-Based Materials: A Review. *Critical Reviews in Environmental Science and Technology* 36: 405-431.

Li, X. and Zhang, W. 2006b. Iron Nanoparticles: the Core-Shell Structure and Unique Properties for Ni(II) Sequestration. *Langmuir* 22: 4638-4642.

Li, X. and Zhang, W. 2007. Sequestration of Metal Cations with Zerovalent Iron NanoparticlessA Study with High Resolution X-ray Photoelectron Spectroscopy (HR-XPS). *Journal of Physical Chemistry C* 111(19): 6939-6946.

Liu, Y., Choi, H., Dionysiou, D., Lowry, G.V. 2005a. Trichloroethene Hydrodechlorination in Water by Highly Disordered Monometallic Nanoiron. *Chemistry of Materials* 17: 5315-5322.

Liu, Y., Majetich, S.A., Tilton, R.D., Sholl, D.S., Lowry, G.V. 2005b. TCE Dechlorination Rates, Pathways, and Efficiency of Nanoscale Iron Particles with Different Properties. *Environmental Science & Technology* 39: 1338-1345.

Ma, X., Huang, B., Cheng, M. 2007. Analysis of trace mercury in water by solid phase extraction using dithizone modified nanometer titanium dioxide and cold vapor atomic absorption spectrometry. *Rare Metals* 26(6): 541-546.

Madden, J.T., Fitzgerald, N. 2009. Investigation of ultraviolet photolysis vapor generation with in-atomizer trapping graphite furnace atomic absorption spectrometry for the determination of mercury. *Spectrochimica Acta Part B: Atomic Spectroscopy* 64(9): 925-927.

Mahmoud, M.E., Osman, M.M., Mohamed, E., Amer, M.E. 2000. "Selective Preconcentration and Solid Phase Extraction of Mercury(II) from Natural Water by Silica Gel-Loaded Dithizone phases", *Anal Chim Acta*, 415: 33–40.

Mercier, L., Pinnavaia, T.J. 1998. Heavy metal ion adsorbents formed by the grafting of a thiol functionality to mesoporous silica molecular sieves: Factors affecting Hg(II) uptake. *Environ. Sci. Technol.* 32: 2749-2754.

Neto, J.A.G., Zara, L.F., Rocha, J.C., Santos, A., Dakuzaku, C.S., Nobrega, J.A. 2000. Determination of Mercury in Agroindustrial Samples by Flow-Injection Cold Vapor Atomic Absorption Spectrometry Using Ion Exchange and Reductive Elution. *Talanta* 51: 587-594.

Nevado, J.J.B., Martin-Doimeadios, R.C.R., Bernardo, F.J.G. and Moreno, M.J. 2005. Determination of Mercury Species in Fish Reference Materials by Gas Chromatography-Atomic Fluorescence Detection after Closed-Vessel Microwave-Assisted Extraction. *Journal of Chromatography A* 1093: 21-28.

Nurmi, J.T., Tratnyek, P.G., Sarathy, G., Baer, D.R., Amonette, J.E., Pecher, K., Wang, C., Linehan, J.C., Matson, M.W., Penn, R.L., Driessen, M.D. 2005. Characterization and Properties of Metallic Iron Nanoparticles: Spectroscopy, Electrochemistry, and Kinetics. *Environmental Science & Technology* 39: 1221- 1230.

Perez-Quintanilla, D., Hierro-del, I., Fajardo, M., Sierra, I. 2006. 2-Mercaptothiazoline modified mesoporous silica for mercury removal from aqueous media. *Journal of Hazardous Materials* B 134: 245-256.

Puanngam, M., Unob. 2008. Preparation and use of chemically modified MCM-41 and silica gel as selective adsorbents for Hg(II) ions. *Journal of Hazardous Materials* 154: 578-587.

Ponder, S.M., Darab, J.G., Bucher, J., Caulder, D., Craig, I., Davis, L., Edelstein, N., Lukens, W., Nitsche, H., Rao, L., Shuh, D.K., Mallouk, T.E. 2001. Surface Chemistry and Electrochemistry of Supported Zerovalent Iron Nanoparticles in the Remediation of Aqueous Metal Contaminants. *Chem. Mater.* 13: 479-486.

Pourreza, N., Ghanemi, K. 2009. Determination of mercury in water and fish samples by cold vapor atomic absorption spectrometry after solid phase extraction on agar modified with 2-mercaptobenzimidazole. *Journal of Hazardous Materials* 161(2-3): 982-987.

Ramalhosa, E., Rio Segade, S., Pereira, E., Vale, C. and Duarte, A. 2001. Simple methodology for methyl mercury and inorganic mercury determinations by high-performance liquid chromatography- cold vapor atomic fluorescence spectrometry. *Anal Chim Acta* 448: 135-143.

Rispoli, F., Angelov, A., Badia, D., Kumar, A., Seal, S., Shah, V. 2010. Understanding the toxicity of aggregated zero valent copper nanoparticles against Escherichia coli. *Journal of Hazardous Materials* 180: 212-216.

Sandor, M., Geistmann, F., Schuster, M. 1999. An Anthracene-Substituted Benzoylthiourea for the Selective Determination of Hg(II) in Micellar Media. *Analytica Chimica Acta* 388: 19-26.

Scherer, M.M., Richter, S., Valentine, R.L., Alvarez, P.J.J. 2000. Chemistry and Microbiology of Permeable Reactive Barriers for *In Situ* Groundwater Clean up. *Critical Reviews in Environmental Science and Technology* 30(3): 363-411.

Shamsipur, M., Tashkhourian, J., Hemmateenejad, B., Sharghi, H. 2004. Application of artificial neural network to simultaneous potentiometric determination of silver(I), mercury(II) and copper(II) ions by an unmodified carbon paste electrode. *Talanta* 64(3): 590-596.

Skoog, D.A. and West, D.M., 1971. *Principles of Instrumental Analysis*, (Hardcover, New York, USA), p.549.

Skoog, D.A., Holler, F.J., Nieman, T.A., 1998. *Principles of Instrumental Analysis*, *Fifth Edition* (Harcourt Brace & Company, Florida, USA), p.844, 798-800.

Spivakov, B.Y., Malofeeva, G.I., Petrukhin, O.M. 2006. Solid-Phase Extraction on Alkyly-bonded Silica Gels in Inorganic Analysis. *Analytical Sciences* 22: 503-519.

Sun, Y., Li, X., Cao, J., Zhang, W., Wang, H.P. 2006. Characterization of zero-valent iron nanoparticles. *Advances in Colloid and Interface Science* 120: 47-56.

Üzüm, Ç., Shahwan, T., Eroğlu, A.E., Lieberwirth, I., Scott, T.B., Hallam, K.R. 2008. Application of zero-valent iron nanoparticles for the removal of aqueous Co^{2+} ions under various experimental conditions. *Chem Eng. J.* 144: 213-220.

Wang, Q., Kim, D., Dionysiou, D.D., Sorial, G.A., Timberlake, D. 2004. Sources and remediation for mercury contamination in aquatic systems- a literature review. *Environmental Pollution* 131: 323-336.

Welz, B. and Sperling, M. 1999. *Atomic Absorption Spectrometry*, (WILEY-VCH, Weinheim), p. 47-48, 222-223, 523-524.

Wuilloud, J.C.A., Wuilloud, R.G., Silva, M.F., Olsina, R.A., Martinez, L.D. 2002a. Sensitive Determination of Mercury in Tap Water by Cloud Point Extraction Preconcentration and Flow Injection-Cold Vapor-Inductively Coupled Plasma Optical Emission Spectrometry. *Spectrochimica Acta Part B.* 57: 365-374.

Wuilloud, J.C.A., Willoud, R.G., Olsina, R.A. and Martinez, L.D. 2002b. Separation and Preconcentration of Inorganic and Organomercury Species in Water Samples Using A Selective Reagent and an Anion Exchange Resin and Determination by Flow Injection-Cold Vapor Atomic Absorption Spectrometry. *J Anal Atom Spectrom* 17: 389-394.

Zhang, W., Su, Z., Yang, X. 2010. Evaluation of a new electrolytic cold vapor generation system for mercury determination by AFS. *Talanta* 80(5): 2106-2112.

Zizek, S., Horvat, M., Gibicar, D., Fajon, V., Toman, M. 2007. Bioaccumulation of mercury in benthic communities of a river ecosystem affected by mercury mining. *Science of the Total Environment* 377: 407-415.

VITA

PERSONAL INFORMATION

Surname, Name: ERDEM ARZU
Nationality: Turkish (TC)
Date and Place of Birth: 26.11.1979, İzmir
Marital Status: Single
Phone: +90 (232) 422 1369
E-mail: arzuerdem7@hotmail.com

EDUCATION

Degree	Institution	Year of Graduation
MS	İzmir Institute of Technology	2005
BS	Celal Bayar University	2001
High School	İzmir Özel Türk Anadolu Lisesi	1997

WORK EXPERIENCE

Year	Place	Enrollment
2002-2011	İzmir Institute of Technology	Research Assistant
2000	Tüpraş	Trainee
1999	Bak Ambalaj A.Ş.	Trainee

FOREIGN LANGUAGES

English (Advanced)